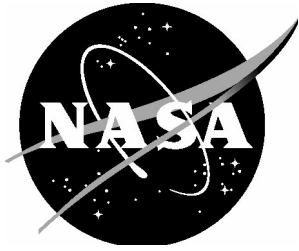


NASA/CR-20250011200



# Fitness-For-Service Assessments of Crack-Like Flaws Using NASGRO<sup>®</sup>

*Joseph W. Cardinal, Yi-Der Lee, and Laura D. Hunt  
Southwest Research Institute, San Antonio, Texas*

---

December 2025

## NASA STI Program . . . in Profile

Since its founding, NASA has been dedicated to the advancement of aeronautics and space science. The NASA scientific and technical information (STI) program plays a key part in helping NASA maintain this important role.

The NASA STI program operates under the auspices of the Agency Chief Information Officer. It collects, organizes, provides for archiving, and disseminates NASA's STI. The NASA STI program provides access to the NTRS Registered and its public interface, the NASA Technical Reports Server, thus providing one of the largest collections of aeronautical and space science STI in the world. Results are published in both non-NASA channels and by NASA in the NASA STI Report Series, which includes the following report types:

- **TECHNICAL PUBLICATION.** Reports of completed research or a major significant phase of research that present the results of NASA Programs and include extensive data or theoretical analysis. Includes compilations of significant scientific and technical data and information deemed to be of continuing reference value. NASA counter-part of peer-reviewed formal professional papers but has less stringent limitations on manuscript length and extent of graphic presentations.
- **TECHNICAL MEMORANDUM.** Scientific and technical findings that are preliminary or of specialized interest, e.g., quick release reports, working papers, and bibliographies that contain minimal annotation. Does not contain extensive analysis.
- **CONTRACTOR REPORT.** Scientific and technical findings by NASA-sponsored contractors and grantees.

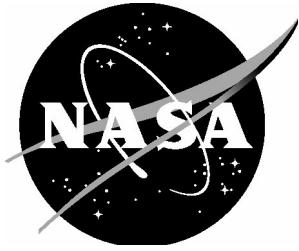
- **CONFERENCE PUBLICATION.** Collected papers from scientific and technical conferences, symposia, seminars, or other meetings sponsored or co-sponsored by NASA.
- **SPECIAL PUBLICATION.** Scientific, technical, or historical information from NASA programs, projects, and missions, often concerned with subjects having substantial public interest.
- **TECHNICAL TRANSLATION.** English-language translations of foreign scientific and technical material pertinent to NASA's mission.

Specialized services also include organizing and publishing research results, distributing specialized research announcements and feeds, providing information desk and personal search support, and enabling data exchange services.

For more information about the NASA STI program, see the following:

- Access the NASA STI program home page at <http://www.sti.nasa.gov>

NASA/CR-20250011200



# Fitness-For-Service Assessments of Crack-Like Flaws Using NASGRO<sup>®</sup>

*Joseph W. Cardinal, Yi-Der Lee, and Laura D. Hunt  
Southwest Research Institute, San Antonio, Texas*

National Aeronautics and  
Space Administration

Enter Ames Research Center  
Moffett Field, CA

Prepared for Ames Research Center  
under Contract/Task 80NSSC24PA995

December 2025

The use of trademarks or names of manufacturers in this report is for accurate reporting and does not constitute an official endorsement, either expressed or implied, of such products or manufacturers by the National Aeronautics and Space Administration.

Available from:

NASA STI Program / Mail Stop 050  
NASA Langley Research Center  
Hampton, VA 23681-2199

**Fitness-For-Service Assessments of Crack-Like  
Flaws Using NASGRO®**

**Revision 0**

**FINAL REPORT**

**by**

**Joseph W. Cardinal  
Yi-Der Lee  
Laura D. Hunt**

**SwRI Project No. 18.28758**

**NASA Ames Research Center**

**NASA-Ames Contract No. 80NSSC24PA995**

**July 2025**



**Southwest Research Institute®**  
6220 Culebra Road • Post Office Drawer 28510  
San Antonio, Texas 78228-0510

# Fitness-For-Service Assessments of Crack-Like Flaws Using NASGRO

Revision 0

**FINAL REPORT**

by

Joseph W. Cardinal  
Yi-Der Lee  
Laura D. Hunt

SwRI Project No. 18.28758

NASA Ames Research Center

NASA-Ames Contract No. 80NSSC24PA995

July 2025

**APPROVED:**

<b>Tim Fey</b>	<small>Digitally signed by: Tim Fey DN: CN = Tim Fey email = tim.fey@swri.org C = US O = Southwest Research Institute Date: 2025.07.30 15:09:10 -05'00'</small>
----------------	---

**Timothy A. Fey, Executive Director  
Structural Engineering Department**



Southwest Research Institute®  
6220 Culebra Road • Post Office Drawer 28510  
San Antonio, Texas 78228-0510

## ACKNOWLEDGEMENTS

The authors of this report would like to express their appreciation to Douglas Fraser, Pressure Systems Manager at NASA's Ames Research Center (ARC), for his helpful discussions and many years of technical and financial support to enhance the capabilities of the NASGRO software to perform fitness-for-service analyses of safety-critical, ground-based steel pressure vessels. Calogero Dirienzo, Pressure Systems Manager at NASA's Glenn Research Center (GRC) is also acknowledged. Clifton Arnold, Pressure Systems Program Executive within NASA's Office of Safety and Mission Assurance (OSMA), is acknowledged for his leadership within NASA to ensure the continued funding of these NASGRO development efforts from year to year.

Additionally, the activities and accomplishments of the NASA Layered Pressure Vessel (LPV) Working Group, run out of the NASA Marshall Space Flight Center, contributed to the success of this project, especially regarding the contribution of material property data for the LPV steel. Many helpful interactions with multiple MSFC engineers and LPV Working Group participants provided helpful background for NASGRO improvements.

Last, and by no means least, the GUI programming efforts of NASGRO Team members Randy Christian and Emilia Baldauf of the Amentum Clear Lake Group in Houston are especially acknowledged. Their programming and database efforts were invaluable for ensuring that the technical improvements to NASGRO are accessible and usable.

Finally, Deborah Gohmert of SwRI's Structural Engineering Department is acknowledged for the preparation of the final report.

## EXECUTIVE SUMMARY

This report provides guidance in the use of the NASGRO<sup>®</sup> fracture mechanics and fatigue crack growth analysis software to perform fitness-for-service (FFS) assessments of crack-like flaws in typical pressure system components in accordance with procedures outlined in Part 9 of the 2021 edition of API 579-1/ASME FFS-1. While multiple sections of this report provide necessary background on the use of the various analytical modules of NASGRO, this report is not intended as a substitute for the NASGRO reference manual, nor is it intended as a substitute for API 579. Familiarity with both is required to understand and effectively apply the guidance provided in this document.

NASGRO has been enhanced to perform fitness-for-service analyses of safety-critical ground-based steel pressure vessels and other non-flight structures using approaches contained in the API and ASME standards. The guidelines for performing FFS assessment procedures for crack-like flaws outlined in this report are based on the well-known Failure Assessment Diagram (FAD). The objective of this report was to provide guidance in the use of NASGRO and the FAD to perform FFS assessments and fatigue crack growth analyses. Key features and recent enhancements to NASGRO that enable analyses to be performed aligned with API 579 approaches are reviewed. In some cases, there may be slight differences in formulations between NASGRO and API 579 and these are documented.

Four representative example analyses were presented in Section 13.0 and were intended to illustrate the use of NASGRO for different FFS analyses of “real-world” pressure vessel applications. While these examples considered typical pressure vessel geometries and materials, they should only be treated as “notional” demonstrations of the NASGRO software capabilities and features.

A key aspect of the examples presented herein is the use of different choices for material properties such as the fatigue crack growth relationship and the fracture toughness. In general, it was shown that the API 579 material property choices produce results that are conservative relative to the NASGRO database materials. It is recommended that analysts be aware of these differences when setting up an analysis.

Comparisons between results obtained with NASGRO and the INSPECT software were made for two of the examples. These benchmark comparisons produced reasonably good agreement between the SIFs and final crack sizes; however key differences were noted between the value of  $L_r$  used in the FAD. These differences are most likely due to the difference between a local and global failure computation used by the two programs. It is recommended that future NASGRO enhancements include the output of the reference stress and  $L_r$  values for both the local and global failure conditions, with an option for the analyst to choose which one to use for the FAD.

Lastly, additional benchmark analyses are recommended between NASGRO and other FFS software programs to identify and understand differences such as those noted above.

## ACRONYMS AND SYMBOLS

### Organizations

API	American Petroleum Institute
ASME	American Society of Mechanical Engineers
NASA	National Aeronautics and Space Administration
OSMA	NASA Office of Safety and Mission Assurance
SwRI	Southwest Research Institute

### Technical Abbreviations

FAD	Failure Assessment Diagram
FAL	Failure Assessment Line
FCG	Fatigue Crack Growth
FEA/FEM	Finite Element Analysis/Finite Element Model
FFS	Fitness For Service
GUI	Graphical User Interface
LPV	Layered Pressure Vessel
SIF	Stress Intensity Factor
WF	Weight Function
WRS	Weld Residual Stress

### Mathematical Symbols

a	crack depth
c	crack length
x	distance
t	thickness
W	width
da/dN	fatigue crack growth rate
C, n, p, q	NASGRO equation parameters
R	stress ratio
S	stress
$\Delta S$	stress range
K	stress intensity factor
$\Delta K$	stress intensity factor range
$K_{Ic}, K_c, K_{Ic}$	fracture toughness
$\sigma_{ys}$	yield stress
$K_r$	FAD toughness ratio
$L_r$	FAD load ratio

# TABLE OF CONTENTS

	Page
<b>ACKNOWLEDGEMENTS .....</b>	<b><i>ii</i></b>
<b>EXECUTIVE SUMMARY .....</b>	<b><i>iii</i></b>
<b>ACRONYMS AND SYMBOLS.....</b>	<b><i>iv</i></b>
<b>LIST OF FIGURES .....</b>	<b><i>viii</i></b>
<b>LIST OF TABLES .....</b>	<b><i>xi</i></b>
<b>1 INTRODUCTION AND OBJECTIVES .....</b>	<b>1</b>
1.1 ORGANIZATION OF REPORT .....	2
1.2 USE OF THIS REPORT .....	2
<b>2 OVERVIEW OF FITNESS-FOR-SERVICE ANALYSES .....</b>	<b>3</b>
2.1 DEFINITION OF CRACK-LIKE FLAWS .....	3
2.1.1 Flaw Characterization .....	3
2.2 API 579 ASSESSMENT PROCEDURES .....	3
2.2.1 API 579 Assessment Levels.....	3
2.3 STRESS INTENSITY FACTORS .....	8
2.4 LIMIT LOADS.....	8
2.5 FAILURE ASSESSMENT DIAGRAM .....	8
2.6 FRACTURE ASSESSMENT .....	9
2.7 FATIGUE CRACK GROWTH ANALYSIS .....	9
<b>3 OVERVIEW OF NASGRO ANALYSIS MODULES.....</b>	<b>11</b>
3.1 NASSIF .....	12
3.2 NASCCS .....	12
3.3 NASFAD.....	13
3.4 NASFLA .....	13
3.5 NASMAT .....	13
<b>4 NASGRO STRESS INTENSITY FACTOR (SIF) SOLUTIONS .....</b>	<b>14</b>
4.1 GENERAL.....	14
4.2 OVERVIEW OF FREQUENTLY USED NASGRO SIF SOLUTIONS FOR FFS ASSESSMENTS	14
4.3 NASGRO LIMIT LOAD SOLUTIONS.....	15
4.4 CROSS-REFERENCE TO API 579 SIF SOLUTIONS .....	16
4.5 CRACK SHAPE TRANSITIONS .....	23
4.5.1 NASGRO Defaults.....	23
4.5.2 API 579 Criteria for Surface and Embedded Crack Transitions.....	23
<b>5 MATERIAL PROPERTIES FOR FFS ANALYSES .....</b>	<b>25</b>
5.1 STRENGTH.....	25
5.2 FRACTURE TOUGHNESS.....	25
5.3 FATIGUE CRACK GROWTH RATE.....	25
<b>6 NASGRO MATERIAL PROPERTIES.....</b>	<b>27</b>

6.1	THE NASGRO FATIGUE CRACK GROWTH (FCG) DATABASE .....	27
6.1.1	Material Selection .....	27
6.1.2	Data Source .....	27
6.1.3	Data Format .....	27
6.1.4	NASGRO Equation.....	28
6.1.5	Walker Equation .....	29
6.1.6	Tabular FCG Data.....	29
6.1.7	1-D Tabular FCG Data Example .....	30
6.1.8	2-D Tabular FCG Data Example .....	30
6.1.9	API 579 and ASME Tabular Data (Paris Equations).....	31
<b>7</b>	<b>FRACTURE TOUGHNESS OPTIONS IN NASGRO.....</b>	<b>35</b>
7.1	NASGRO TOUGHNESS PROPERTIES AND DEPENDANCE ON THICKNESS .....	35
7.2	DEFAULT TOUGHNESS VALUES AND OPTION TO CHOOSE TOUGHNESS BY CRACK TIP..	35
7.3	OPTION TO USE API 579 AND ASME TOUGHNESS VALUES.....	36
<b>8</b>	<b>RESIDUAL STRESS INPUT FOR NASGRO.....</b>	<b>38</b>
8.1	GENERAL CAPABILITIES .....	38
8.2	INPUT OF POLYNOMIAL RESIDUAL STRESS DISTRIBUTIONS.....	40
8.3	CHOOSING API 579 WELD RESIDUAL STRESS (WRS) POLYNOMIAL INPUTS .....	40
<b>9</b>	<b>BACKGROUND ON THE FAILURE ASSESSMENT DIAGRAM (FAD) CAPABILITY IN NASGRO .....</b>	<b>44</b>
9.1	COMPARISON OF BASIC FAD APPROACHES USED BY NASGRO AND API 579.....	44
9.1.1	Definition of $K_r$ .....	46
9.1.2	Definition of $L_r$ .....	46
9.1.3	Computation of Failure Assessment Lines (FALs) Used in NASGRO.....	46
<b>10</b>	<b>NASCCS INPUT SETUP .....</b>	<b>47</b>
<b>11</b>	<b>NASFAD INPUT SETUP .....</b>	<b>48</b>
11.1	OBJECTIVE.....	48
11.2	ACTIVATION .....	48
11.3	CRACK CASE SELECTION.....	49
11.4	MATERIAL SELECTION .....	49
11.5	NASFAD OPTIONS .....	50
11.5.1	FAD Assessment Option.....	52
11.5.2	Critical Crack Size Option .....	53
11.5.3	Failure Stress Option.....	55
<b>12</b>	<b>NASFLA INPUT SETUP .....</b>	<b>57</b>
12.1	NASFLA OUTPUT.....	60
<b>13</b>	<b>REPRESENTATIVE EXAMPLES.....</b>	<b>61</b>
13.1	LPV OUTER LAYER SURFACE CRACK.....	62
13.2	NOZZLE CORNER CRACK.....	68
13.3	INTERNAL CIRCUMFERENTIAL SURFACE CRACK IN A PIPE WITH WELD RESIDUAL STRESS .....	75

13.4 FAD ANALYSIS OF EMBEDDED CRACKS IN A SPHERE.....	84
<b>14 SUMMARY AND RECOMMENDATIONS.....</b>	<b>91</b>
<b>15 REFERENCES.....</b>	<b>93</b>

## LIST OF FIGURES

Figure		Page
FIGURE 2.2.1-1.	API 579 LEVEL 2 ASSESSMENT PROCEDURE FOR A NON-GROWING CRACK-LIKE FLAW .....	5
FIGURE 2.2.1-2.	API 579 ASSESSMENT PROCEDURES TO EVALUATE GROWING CRACK-LIKE FLAWS .....	6
FIGURE 2.2.1-3.	API 579 METHODOLOGY FOR CRACK GROWTH ANALYSIS.....	7
FIGURE 2.5-1.	SCHEMATIC REPRESENTATION OF FAILURE ASSESSMENT DIAGRAM .....	9
FIGURE 3.0-1.	NASGRO OPENING SCREEN .....	11
FIGURE 3.0-2.	NASGRO CRACK CASE GEOMETRY SELECTION SCREEN .....	12
FIGURE 4.5.2-1.	NASGRO GUI SCREEN FOR SC30 SHOWING CHECK BOX TO ACTIVATE API 579 TRANSITION CRITERIA .....	24
FIGURE 6.1.2-1.	NASFLA GUI MENU FOR MATERIAL DATA SOURCE SELECTION.....	27
FIGURE 6.1.3-1.	NASFLA GUI MENU FOR MATERIAL DATA FORMAT SELECTION .....	28
FIGURE 6.1.4-1.	EXAMPLE NASFLA MATERIAL SCREEN SHOWING NASGRO EQUATION DATA FOR A285 GR C STEEL .....	29
FIGURE 6.1.7-1.	EXAMPLE NASFLA MATERIAL SCREEN SHOWING 1-D TABULAR FCG DATA FOR A106 GR B STEEL .....	30
FIGURE 6.1.8-1.	EXAMPLE NASFLA MATERIAL SCREEN SHOWING 2-D TABULAR FCG DATA FOR AOS 1146A LPV WRAPPER STEEL.....	31
FIGURE 6.1.9-1.	EXAMPLE NASFLA MATERIAL SCREEN SHOWING 1-D TABULAR FCG DATA FOR THE API 579 BARSOM PARIS EQUATION FOR FERRITIC-PEARLITE STEEL.....	33
FIGURE 6.1.9-2.	EXAMPLE NASFLA MATERIAL SCREEN SHOWING 2-D TABULAR FCG DATA FOR THE ASME SECTION VIII, DIV3 PARIS EQUATION FOR A CARBON AND LOW ALLOY STEEL .....	34
FIGURE 7.2-1.	NASFLA MATERIAL SCREEN GUI TOOL FOR USER-DEFINED $K_C$ BY TIP CLASS .....	36
FIGURE 7.3-1.	API 579 FRACTURE TOUGHNESS CHECKBOX IN MATERIAL GUI (DEFAULT) ..	37
FIGURE 8.1-1.	RESIDUAL STRESS INPUT OPTIONS FOR UNIVARIANT WEIGHT FUNCTION SIF MODELS.....	39
FIGURE 8.3-1.	GUI LAYOUT FOR USER TO SPECIFY POLYNOMIAL COEFFICIENTS WITH BUTTON TO OPTIONALLY SELECT API 579 WRS POLYNOMIAL EQUATION ....	41
FIGURE 8.3-2.	GUI DISPLAY OF API 579 WRS POLYNOMIAL EQUATION MENU.....	42
FIGURE 8.3-3.	RESIDUAL STRESS POLYNOMIAL INPUT SCREEN SHOWING SELECTION OF AN API 579 WRS EQUATION AND THE POLYNOMIAL COEFFICIENTS .....	43
FIGURE 10.0-1.	NASCCS INPUT OPTIONS SCREEN .....	47
FIGURE 11.2-1.	INITIAL NASFAD GUI ANALYSIS TABS .....	48
FIGURE 11.4-1.	NASFAD MATERIAL SCREEN .....	49
FIGURE 11.5-1.	NASFAD OPTIONS SCREEN (FAD ASSESSMENT OPTION) .....	50
FIGURE 11.5-2.	NASFAD OPTIONS SCREEN (CRITICAL CRACK SIZE OPTION).....	51
FIGURE 11.5-3.	NASFAD OPTIONS SCREEN (FAILURE STRESS OPTION).....	51
FIGURE 11.5.1-1.	NASFAD RESULTS IN THE OUTPUT SCREEN FOR “FAD ASSESSMENT” OPTION .....	52
FIGURE 11.5.1-2.	NASFAD PLOTTING OPTIONS SCREEN.....	52

FIGURE 11.5.1-3.	NASFAD RESULTS PLOTTED FROM THE GUI FOR THE “FAD ASSESSMENT” OPTION .....	53
FIGURE 11.5.2-1.	NASFAD CRITICAL CRACK SIZE RESULTS DISPLAYED IN THE COMPUTATIONS SCREEN.....	54
FIGURE 11.5.2-2.	NASFAD RESULTS PLOTTED FROM THE GUI FOR THE “CRITICAL CRACK SIZE” OPTION.....	55
FIGURE 11.5.3-1.	NASFAD FAILURE STRESS RESULTS DISPLAYED IN THE COMPUTATIONS SCREEN .....	56
FIGURE 12.0-1.	MANUAL INPUT OF MEMBRANE TENSION STRESS, $S_0$ , ON THE NASFLA LOAD BLOCKS SCREEN WITH $S_0(\text{MIN}) = 0.0$ AND $S_0(\text{MAX}) = 20.0$ KSI.....	58
FIGURE 12.0-2.	MANUAL INPUT OF MEMBRANE TENSION STRESS, $S_0$ , ON THE NASFLA LOAD BLOCKS SCREEN WITH $S_0(\text{MIN}) = 0.0$ AND $S_0(\text{MAX}) = 20.0$ KSI.....	58
FIGURE 12.0-3.	NASFLA OUTPUT OPTIONS SCREEN SHOWING DEFAULT CHOICES .....	59
FIGURE 12.0-4.	NASFLA COMPUTATIONS SCREEN SHOWING RUN BUTTON .....	59
FIGURE 13.1-1.	NASFLA GEOMETRY INPUT SCREEN FOR SURFACE CRACK IN PLATE (SC30).....	63
FIGURE 13.1-2.	NASFLA MATERIAL INPUT SCREEN FOR AOS 1146A WRAPPER PLATE.....	64
FIGURE 13.1-3.	NASFLA MATERIAL INPUT SCREEN FOR AOS 1146A WRAPPER PLATE SHOWING SELECTION OF API 579 LOWER BOUND FRACTURE TOUGHNESS.....	65
FIGURE 13.1-4.	CRACK GROWTH CURVES SHOWING TRANSITION FROM.....	66
FIGURE 13.1-5.	FAILURE ASSESSMENT DIAGRAM SHOWING TRANSITION FROM .....	66
FIGURE 13.1-6.	FAILURE ASSESSMENT DIAGRAM USING API 579 LOWER BOUND TOUGHNESS ( $K_C = 40.1$ KSI $\sqrt{\text{IN}}$ ) WITHOUT TRANSITION .....	67
FIGURE 13.2-1.	NASFLA MATERIAL INPUT SCREEN FOR API 579 FERRITIC-PEARLITE STEEL.....	70
FIGURE 13.2-2.	NASFLA GEOMETRY INPUT SCREEN FOR NOZZLE CORNER CRACK USING API 579 SOLUTION KNCC1 .....	71
FIGURE 13.2-3.	NASFLA GEOMETRY INPUT SCREEN FOR NOZZLE CORNER CRACK USING NASGRO WEIGHT FUNCTION MODEL CC28.....	71
FIGURE 13.2-4.	NORMALIZED STRESS DISTRIBUTION AT NOZZLE CORNER FROM FEA FOR INPUT TO CC28 WEIGHT FUNCTION SIF MODEL .....	72
FIGURE 13.2-5.	NOZZLE CORNER CRACK GROWTH CURVE FOR CC27 ( $a/c = 1$ ).....	73
FIGURE 13.2-6.	NOZZLE CORNER CRACK FAD FOR CC27 .....	73
FIGURE 13.2-7.	NOZZLE CORNER CRACK GROWTH CURVES FOR CC28.....	74
FIGURE 13.2-8.	NOZZLE CORNER CRACK FAD FOR CC28 .....	74
FIGURE 13.3-1.	NASFLA GEOMETRY INPUT SCREEN FOR INTERNAL CIRCUMFERENTIAL SURFACE CRACK IN A CYLINDER (SC34).....	76
FIGURE 13.3-2.	NASFLA PLOT OF WELD RESIDUAL STRESS POLYNOMIAL EQUATION 9D.9 FROM SECTION 9D.5.1 OF API 579 FOR A FULL PENETRATION CIRCUMFERENTIAL WELD IN A CYLINDER.....	78
FIGURE 13.3-3.	NASFLA MATERIAL INPUT SCREEN FOR UPPER BOUND WELDED JOINT PARIS EQUATION FROM API 579 TABLE 9F.5 .....	79
FIGURE 13.3-4.	NASFLA MATERIAL INPUT SCREEN FOR UPPER BOUND WELDED JOINT PARIS EQUATION FROM API 579 TABLE 9F.5 .....	80
FIGURE 13.3-5.	NASFLA LOAD BLOCKS SCREEN.....	81
FIGURE 13.3-6.	CRACK GROWTH CURVES FOR SC34 FOR A106 GR B STEEL MATERIAL.....	82

FIGURE 13.3-7.	FAD FOR SC34 FOR A106 GR B STEEL MATERIAL .....	82
FIGURE 13.3-8.	CRACK GROWTH CURVES FOR SC34 FOR UPPER BOUND WELD MATERIAL ....	83
FIGURE 13.3-9.	FAD FOR SC34 FOR UPPER BOUND WELD MATERIAL .....	83
FIGURE 13.4-1.	NASFAD GEOMETRY SCREEN FOR EC05 SHOWING CHOICE OF API 579 WRS EQUATION .....	86
FIGURE 13.4-2.	NASFAD PLOT OF WELD RESIDUAL STRESS POLYNOMIAL EQUATION 9D.9 FROM SECTION 9D7.1 OF API 579 FOR FULL PENETRATION CIRCUMFERENTIAL WELD IN A SPHERE .....	87
FIGURE 13.4-3.	NASFAD MATERIAL PROPERTY SCREEN FOR A REPRESENTATIVE A200 SERIES STEEL .....	88
FIGURE 13.4-4.	NASFAD OPTIONS SCREEN SHOWING CRACK SIZES AND WRS SCALE FACTOR.....	89
FIGURE 13.4-5.	NASFAD PLOT OF FAD FOR TWO CRACKS .....	90

## LIST OF TABLES

Table		Page
TABLE 4.4-1.	CROSS-REFERENCE MATRIX FOR CRACKS IN FLAT PLATE.....	17
TABLE 4.4-2.	CROSS-REFERENCE MATRIX FOR CRACKS IN FLAT PLATE WITH A HOLE.....	18
TABLE 4.4-3.	CROSS-REFERENCE MATRIX FOR CRACKS IN CYLINDERS.....	19
TABLE 4.4-4.	CROSS-REFERENCE MATRIX FOR CRACKS IN SPHERES .....	21
TABLE 4.4-5.	CROSS-REFERENCE MATRIX FOR CRACKS IN OTHER COMPONENTS .....	22
TABLE 6.1.9-1.	MATERIALS WITH 1-D & 2-D TABULAR PARIS EQUATION DATA FROM API 579 (2021) AND ASME SECTION VIII, DIV. 3 (2023) CONTAINED IN THE NASGRO DATABASE.....	32
TABLE 9.1-1.	DIFFERENCES BETWEEN FITNET-BASED NASGRO FFS AND API 579 ASME FFS .....	45
TABLE 13.2-1.	COMPARISON OF RESULTS FOR CC27 AND CC28 .....	69
TABLE 13.3-1.	COMPARISON OF ANALYSIS RESULTS FOR CIRCUMFERENTIAL SURFACE CRACK IN A PIPE .....	77
TABLE 13.4-1.	COMPARISON OF ANALYSIS RESULTS FOR TWO EMBEDDED CRACKS IN A SPHERE .....	85

# 1 INTRODUCTION AND OBJECTIVES

The objective of this document is to provide guidance in the use of the NASGRO<sup>®</sup> fracture mechanics and fatigue crack growth analysis software [1]<sup>1</sup> to perform fitness-for-service (FFS) assessments of crack-like flaws in typical pressure system components in accordance with procedures outlined in Part 9 of the 2021 edition of API 579-1/ASME FFS-1, hereinafter simply referred to as API 579 [2]. While multiple sections of this report provide necessary background on the use of the various analytical modules of NASGRO, this report is not intended as a substitute for the NASGRO reference manual, nor is it intended as a substitute for API 579. Familiarity with both is required to understand and effectively apply the guidance provided in this document.

The NASGRO fracture mechanics and fatigue crack growth analysis software is a general-purpose suite of analysis modules that are used to perform structural integrity analyses and lifetime predictions for a wide range of structures and mechanical components in many industries around the world. Initial development of the NASGRO software began at NASA Johnson Space Center in the 1980s for fracture control of the Space Shuttle and subsequently grew into a specialized engineering software package that was being used for the analysis of aging aircraft structural integrity in the 1990s. Beginning in 2000, Southwest Research Institute<sup>®</sup> (SwRI<sup>®</sup>) took over industrial distribution and support of NASGRO and established the NASGRO Consortium comprised of primarily aerospace industry companies. Since 2000, SwRI has had the responsibility as manager of the NASGRO Consortium under the terms of a Space Act Agreement first signed between the NASA Johnson Space Center and SwRI in 2000 and renewed in subsequent years.

While the underlying fracture mechanics and fatigue crack growth analysis technology contained in NASGRO is generally applicable for the analysis of cracks in any metallic structure, the historical focus of the feature developments in the NASGRO software had been on aerospace structural applications. More recently, NASGRO has been enhanced to perform fitness-for-service analyses of safety-critical ground-based steel pressure vessels and other non-flight structures using approaches contained in the API and ASME standards. These efforts facilitate the broader use of NASGRO for the analysis and sustainment of ground-based pressure systems. They were funded incrementally over the last ten years by the NASA Office of Safety and Mission Assurance (OSMA) Pressure Systems program and expand the application of NASGRO to industries beyond its initial aerospace focus.

The guidelines for performing fitness-for-service assessment procedures for crack-like flaws outlined in this report are based on the well-known Failure Assessment Diagram (FAD) as covered in Part 9 of API 579 [2] and Appendix X of the NASGRO Reference Manual [1]. In NASGRO, the FAD is considered an alternative (advanced) failure criterion that combines the failure criteria for crack instability (unstable fracture) with the plastic limit load, including their interaction. The FAD approach is capable of assessing the acceptability of a component containing a crack-like flaw as well as being used as a failure criterion for a propagating crack under cyclic loading in a remaining life analysis.

---

<sup>1</sup> Numbers in square brackets [ ] refer to references listed in Section 15.0.

Therefore, the objective of this report is to provide guidance in the use of NASGRO and the FAD to perform FFS assessments and fatigue crack growth analyses. Key features and recent enhancements to NASGRO that enable analyses to be performed more consistent with API 579 approaches are reviewed. In some cases, there may be slight differences in formulations between NASGRO and API 579 and these are documented. Lastly, examples for a number of key geometries are provided.

## **1.1 Organization of Report**

An overview of the fitness-for-service approach is first presented in Section 2 of this report, briefly summarizing the analysis approach outlined in API 579 and providing background on key concepts and the use of the Failure Assessment Diagram for fracture assessment and as a failure criterion for fatigue crack growth analysis and remaining life assessment. Section 3 of the report provides an overview of the NASGRO software and its modules that are relevant to FFS analysis applications. Specific NASGRO stress intensity factor solutions that are frequently used in FFS assessments are presented in Section 4 along with discussions and comments about their defaults and use relative to similar solutions listed in API 579. Section 5 summarizes the key material properties that are needed to perform a FFS analysis while Section 6 describes the NASGRO material database and how to access the different material models and data that are available.

While Sections 2 through 6 can be considered essential background information, the following three sections (7 through 9) provide specific details of NASGRO capabilities for FAD assessments. Section 7 outlines the approach NASGRO uses to model fracture toughness as well as an option to use API 579 fracture toughness values. Section 8 provides guidance on how NASGRO modules can include the effect of residual stress distributions in tabular or polynomial form and, in particular, describes how to access the library of API 579 Annex D weld residual stress polynomial equations. The implementation of the FAD capability in NASGRO is presented in Section 9.

The next three sections of the report (10, 11 and 12) provide guidance on using the three key modules of NASFLA for integrity assessments: NASCCS to compute critical crack size; NASFAD to perform a FAD assessment and compute critical crack size using the FAD; and NASFLA to compute remaining life. Each of these sections include details of providing the required input data and a discussion of how NASGRO presents the calculated results. Lastly, Section 13, presents a number of example problems that illustrate the application of NASGRO for FFS analyses, followed by a final section providing a summary and recommendations.

## **1.2 Use of this Report**

This report has been prepared for the use and benefit of NASA; however, the information contained herein is applicable to many industries and clients outside of NASA. Neither SwRI nor anyone acting on its behalf makes any warranty or representation, express or implied, of merchantability or fitness for a particular purpose nor assumes any liability (direct, indirect, foreseeable or consequential) with respect to NASA's or anyone else's use of the report or use of the NASGRO software. SwRI disclaims all liability for any loss or damage that may arise as a result of NASA's or anyone else's use of the report, the information provided herein, or the use of the NASGRO software.

## **2 OVERVIEW OF FITNESS-FOR-SERVICE ANALYSES**

### **2.1 Definition of Crack-Like Flaws**

A “flaw” is defined as a discontinuity, defect or irregularity that is detected by inspection (or assumed to exist) in a metallic component. A “crack-like” flaw considers such flaws to be represented by a planar crack for the purpose of analysis. A crack-like flaw is therefore characterized by a crack length and depth and a sharp root radius (*i.e.*, a crack tip). These crack-like flaws may be through-wall cracks, surface cracks, corner cracks or embedded cracks. In the remainder of this report the term “crack” will be used for simplicity.

#### **2.1.1 Flaw Characterization**

API 579 provides guidelines for the characterization of existing or postulated cracks for the purposes of performing fracture mechanics analyses. These idealizations are discussed in Section 9.3.6 of API 579 and guidelines are provided in API 579 Figures 9.1 to 9.8 for idealization of single cracks as well as co-planar and non-planar flaws. These guidelines provide “rules” to combine individual flaws that are in close proximity to each other into a larger virtual flaw for the purpose of performing a fracture assessment and/or a fatigue crack growth analysis. This is because multiple flaws in close proximity to each other may interact and be more severe than single flaws considered to act alone.

The NASGRO software does not contain the capability to assess multiple cracks and their proximity to one another and combine them into a single crack based on any interaction criteria. When confronted with cracks in close proximity to each other, the analyst needs to make a determination as to whether they should be combined using the API 579 interaction criteria prior to performing a fracture assessment with NASGRO. The combined virtual crack size and shape would then be input to a NASGRO stress intensity factor model.

### **2.2 API 579 Assessment Procedures**

It is not the intent of this document to replicate the contents of API 579, however, some discussion is provided as background to aid the reader in connecting API 579 methods to the capabilities of the NASGRO software. Part 9 of API 579 (including the Annexes) provides extensive detail of the API 579 assessment procedures. References to relevant sections of API 579 are made herein as appropriate.

#### **2.2.1 API 579 Assessment Levels**

Three levels of assessment procedures are specified by API 579 for evaluation of components containing cracks. Levels 1 and 2 are intended for components that are not anticipated to experience service load conditions resulting in crack growth. A Level 3 assessment is required when Levels 1 and 2 cannot be applied, yield overly conservative results, or when advanced stress analyses are needed. The focus of using NASGRO for FFS analyses is to perform Level 2 and 3 assessments using the Failure Assessment Diagram (FAD).

An overview of the Level 2 assessment procedure for *non-growing* cracks using the FAD is provided in API 579 Figure 9.11, reproduced here as Figure 2.2.1-1. An overview of the Level 3 assessment procedure for *growing* cracks using the FAD is provided in API 579 Figure 9.21, reproduced here as Figure 2.2.1-2. The analytical aspects of these two procedures can be accomplished using the NASGRO software with the NASGRO crack growth analysis following the methodology shown in API 579 Figure 9.22, reproduced here as Figure 2.2.1-3.

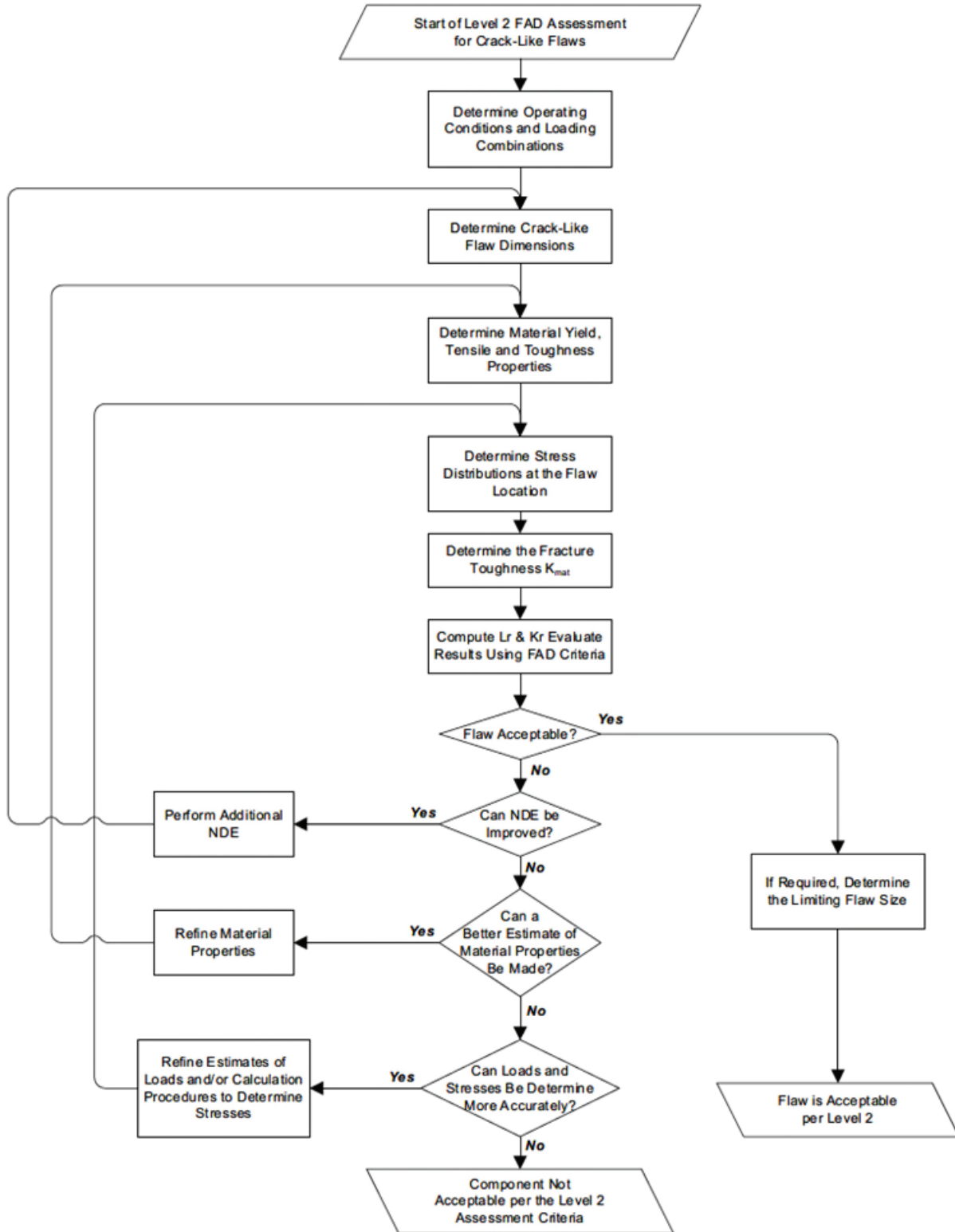


Figure 2.2.1-1. API 579 Level 2 Assessment Procedure for a Non-Growing Crack-Like Flaw  
[Ref. API 579 Figure 9.11, used with permission]

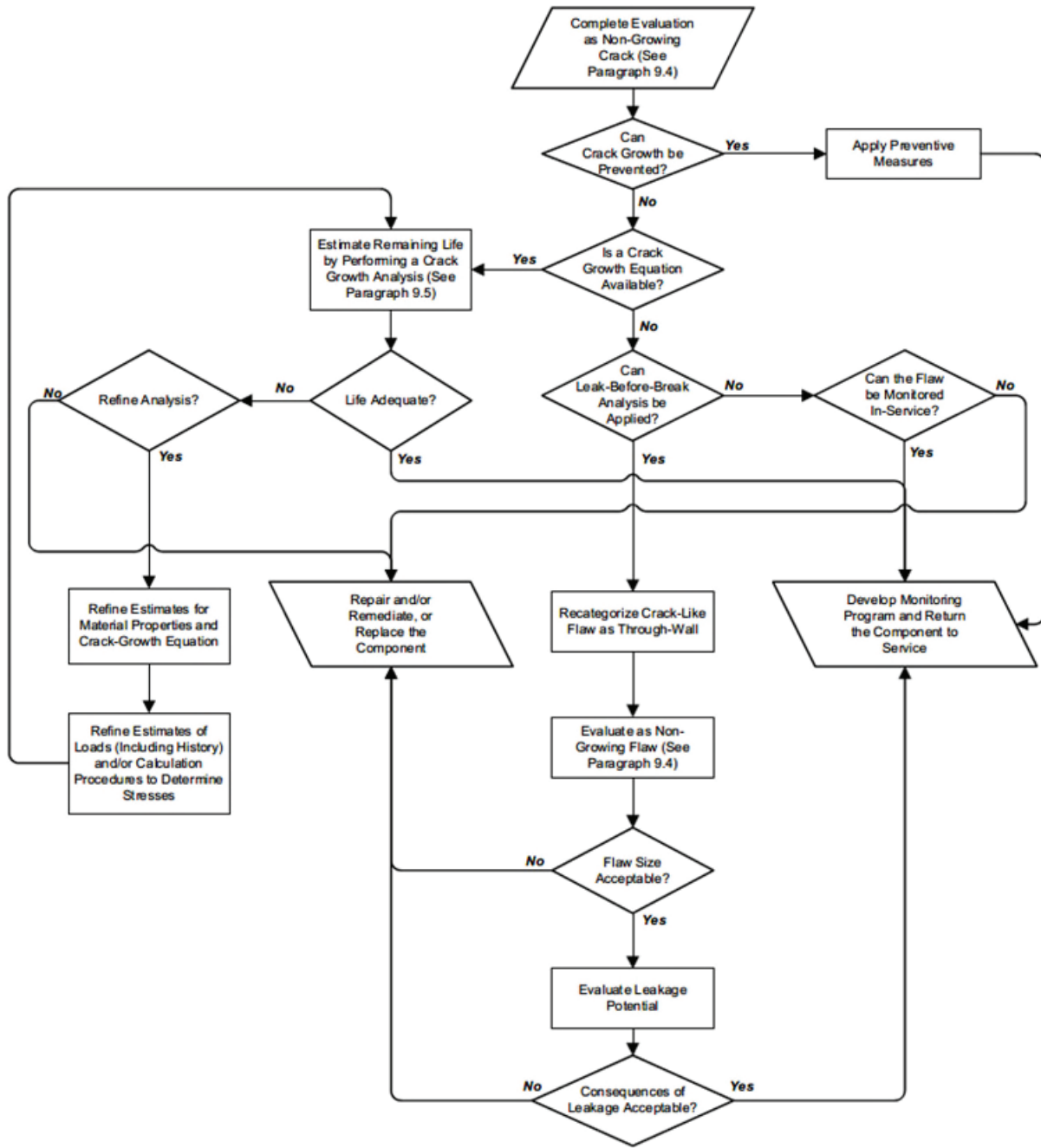


Figure 2.2.1-2. API 579 Assessment Procedures to Evaluate Growing Crack-Like Flaws [Ref. API 579 Figure 9.21, used with permission]

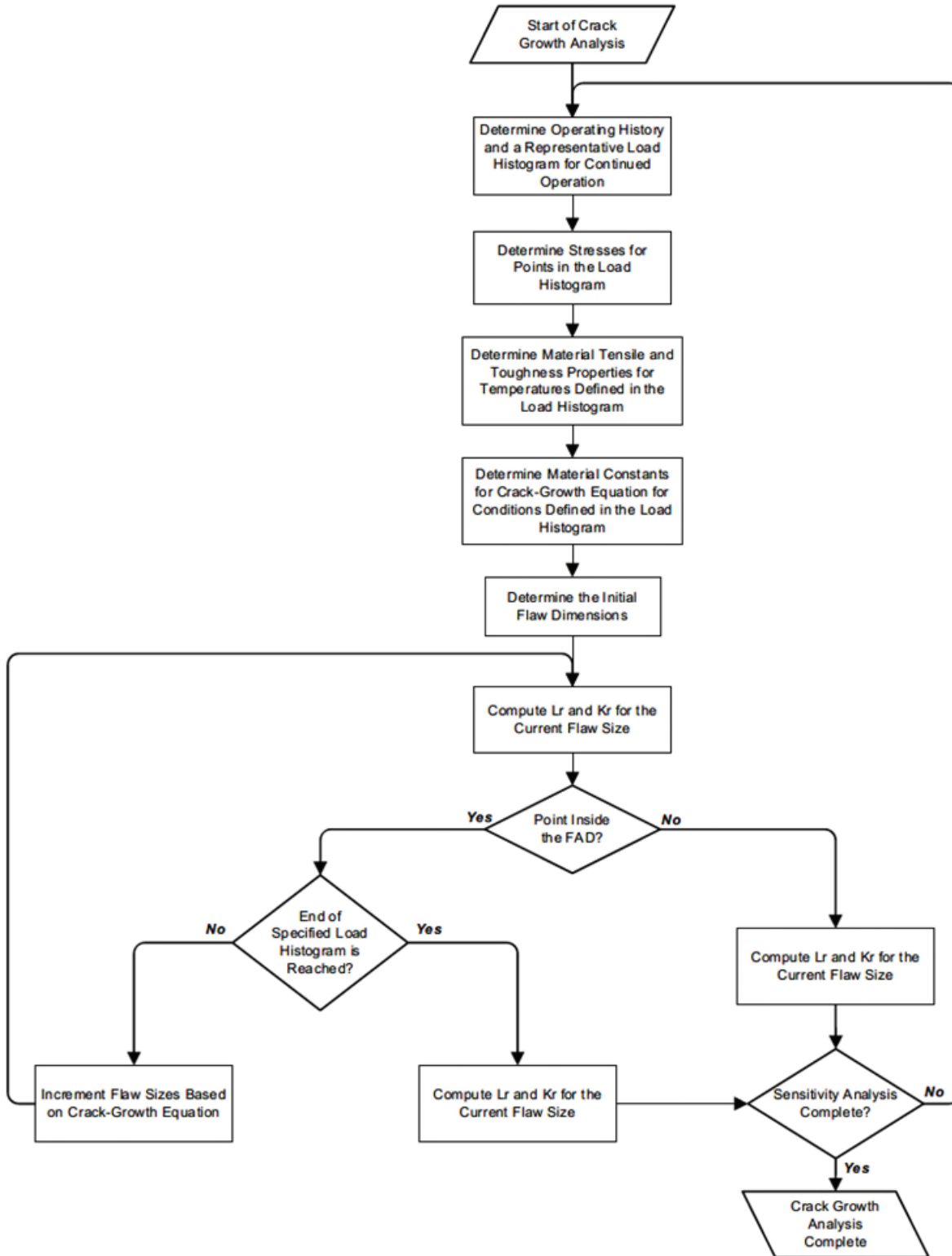


Figure 2.2.1-3. API 579 Methodology for Crack Growth Analysis  
 [Ref. API 579 Figure 9.22, used with permission]

### 2.3 Stress Intensity Factors

The stress intensity factor (SIF) is a measure of the severity of a crack in an elastic solid and is closely related to the stress field in the vicinity of the crack tip. There is a direct relationship between the SIF and the energy release rate that governs the criticality of a crack. Since the range of SIF ( $\Delta K$ ) during a fatigue loading cycle governs the crack growth rate, knowledge of the SIF for a given crack geometry is essential in any fatigue crack growth computation.

### 2.4 Limit Loads

The plastic limit load of the cracked structure must be calculated and compared to the total applied load as part of the FAD assessment procedure. Solutions for plastic limit loads for common geometries are available in the literature and documented in the NASGRO, FITNET and API 579 references [1-3].

### 2.5 Failure Assessment Diagram

An in-depth discussion on the theory and background of the FAD approach is outside the scope of this report; however, a brief review is presented herein for reference. Detailed documentation of the FAD approach can be found in References [1 through 5].

The Failure Assessment Diagram (FAD) is a graph of the failure envelope of a cracked structure, expressed in terms of the two parameters  $K_r$  (the toughness ratio) and  $L_r$  (the load ratio) defined as follows:

$K_r = K_{app}/K_{mat}$  = ratio of the applied stress intensity factor to the appropriate material fracture toughness value (such as  $K_c$  or  $K_{Ic}$ )

$L_r = P/P_L$  = ratio of the total applied load contributing to the primary stresses to the plastic limit load of the cracked structure

The failure envelope is called the Failure Assessment Line (FAL). For the approaches currently included in NASGRO, the FAL is dependent only on the tensile properties of the material through the relationship  $K_r = f(L_r)$ . The FAL incorporates a cut-off at  $L_r = L_{r\ max}$ , which defines the plastic collapse limit of the structure.

To use the FAD approach, assessment points with coordinates  $(K_r, L_r)$  calculated based on the applicable loads, crack type and crack size(s), and material properties are compared with the FAL. A schematic example is shown in Figure 2.5-1. Assessment points that lie inside the envelope defined by the FAL indicate non-failure, while assessment points that lie outside the FAL indicate failure. For many fatigue crack growth analyses, the assessment points will initially be far inside the FAL envelope and will gradually grow towards the FAL envelope as the crack grows sub-critically (e.g., from point A to point B in Figure 2.5-1). Since point B is on the FAL, the analysis would terminate when first reaching this unacceptable condition.

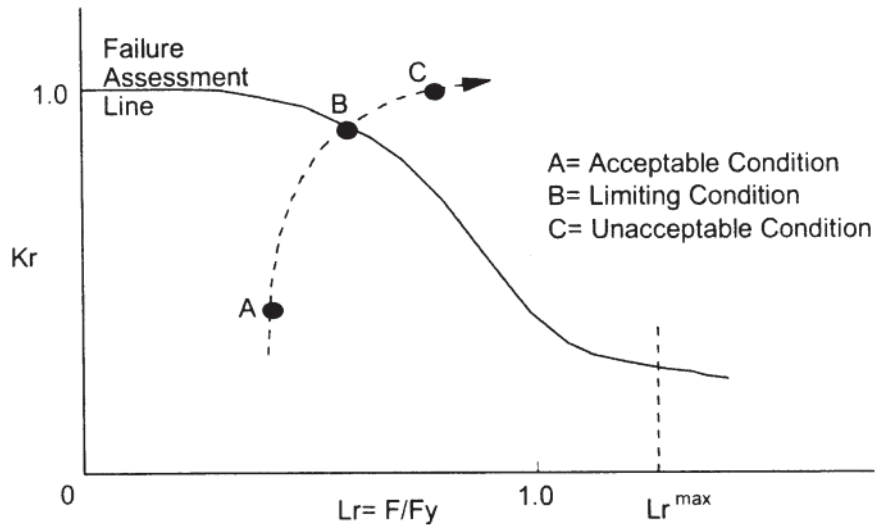


**Figure 2.5-1. Schematic Representation of Failure Assessment Diagram**

## 2.6 Fracture Assessment

A fracture assessment can be performed according to the API 579 Level 1 and Level 2 procedures to assess fracture stability of a crack under loading conditions that are not anticipated to cause the crack to grow in service, *i.e.*, static load conditions. These analyses can be performed in NASGRO in a number of ways using NASSIF, NASCCS, or NASFAD. NASSIF can compute the SIF directly and the user can manually compare the calculated SIF to a known fracture toughness value. NASCCS can be used to compute a critical crack size for a specific loading and material properties and that result can be compared to an existing crack size. However, NASFAD is the module used to perform a fracture assessment using the FAD criterion. NASFAD computes the assessment point with coordinates  $(K_r, L_r)$  based on the applicable loads, crack type, crack size, and material properties and compares (plots) the result relative to the FAL as shown in Figure 2.5-1. If the assessment point resides inside the FAL, the crack is stable. NASFAD can also be used to compute the critical crack size using the FAD criterion.

## 2.7 Fatigue Crack Growth Analysis

If a cracked component with a known crack size is determined to be acceptable using the FAD criteria, and it will experience cyclic loadings in subsequent continued use, it is necessary to perform a fatigue crack growth analysis to compute the remaining life of the cracked component.

The remaining life can then be used to establish inspection intervals and plan for monitoring and/or eventual replacement of the component. Alternatively, a fatigue crack growth analysis can be performed in a damage tolerant design process to estimate the life of a component assuming an initial crack size that may exist in the material, for example as a weld defect or some other material discontinuity or damage. The NASFLA module in NASGRO is used to perform fatigue crack growth analyses. NASFLA will propagate an initial crack subject to a specified cyclic loading (stress spectrum) until the critical crack size is reached and failure occurs. Failure in NASFLA can occur by a number of criteria: failure by fracture, failure by net section yielding, or failure by the FAD criterion.

### 3 OVERVIEW OF NASGRO ANALYSIS MODULES

NASGRO is a suite of computer programs comprised of eight analysis modules designed to perform fracture mechanics and fatigue crack growth analyses. Five of these modules are relevant for performing fitness-for-service analyses and their function is briefly summarized below. Extensive detail on the operation of each NASGRO module is provided in the NASGRO Reference Manual [1].

The NASGRO software module includes a large library of component geometries, crack shapes, and applied stress fields, as well as a large library of material properties for fatigue crack growth and fracture. Each of the NASGRO modules access these libraries in different ways depending on their function via a graphical user interface (GUI) specifically designed for each module. The individual modules are accessed from the opening screen via buttons as shown in Figure 3.0-1.

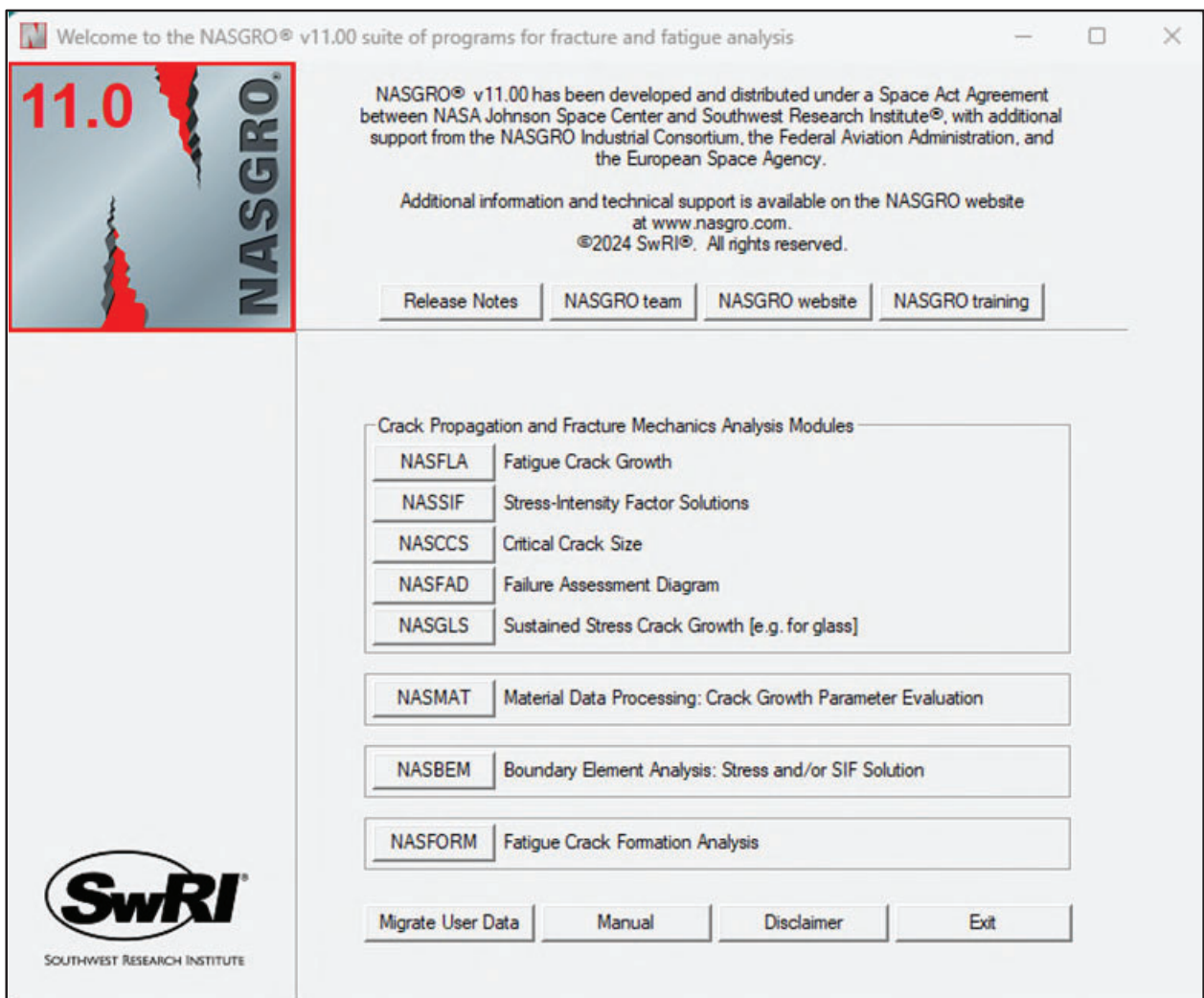
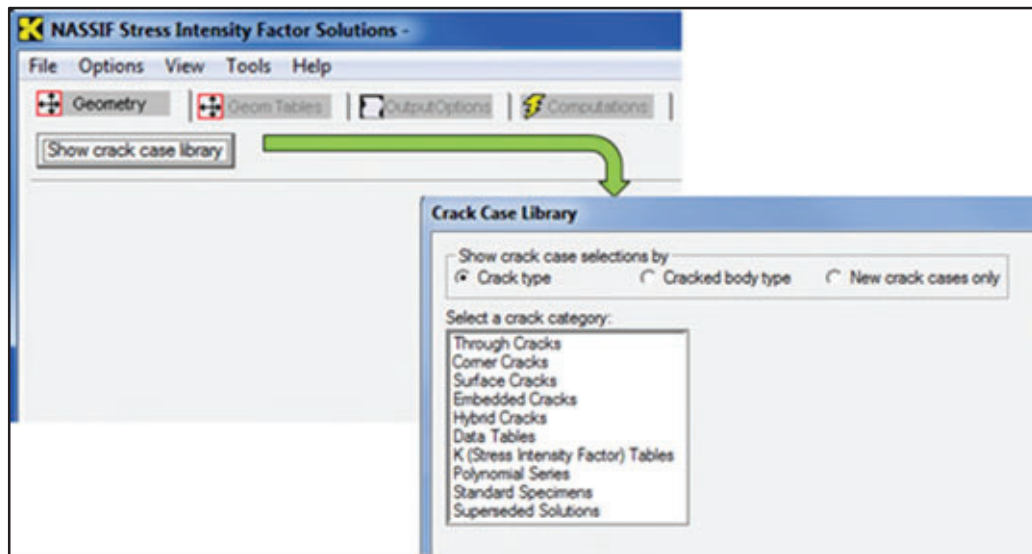


Figure 3.0-1. NASGRO Opening Screen

To perform an analysis, the user selects the desired NASGRO module. From the opening (home) screen in NASGRO the desired module is selected by clicking on its button as shown in Figure 3.0-1. This activates the NASFLA Geometry GUI as shown in Figure 3.0-2 for most of the analysis modules (except NASMAT, NASFORM and NASBEM). Clicking on the Show crack case library button activates a menu of crack categories (or cracked body types) as shown in Figure 3.0-2. Note that the menu of crack cases can be scrolled through to visually display the list of different SIF model geometries available in NASGRO. Then, clicking on the Select button loads the model into the GUI enabling the analyst to enter the geometry parameters for the selected crack case. Depending on the complexity of the fracture mechanics model selected, the GUI screen offers different options and choices to enter geometry, loadings, etc.



**Figure 3.0-2. NASGRO Crack Case Geometry Selection Screen**

### 3.1 NASSIF

NASSIF is used to compute and tabulate values of the stress intensity factor (SIF) in standard ( $K$ ) or normalized non-dimensional forms (commonly referred to as geometry or correction factors). Values are computed and tabulated (or plotted) for each crack tip of the crack case being analyzed. This module can also be used to compute the net section stresses, which is a measure commonly used with failure criteria in NASFLA and NASCCS.

### 3.2 NASCCS

NASCCS determines the critical crack size associated with specified “failure” criteria for a given geometry, loading and material properties. These criteria include failure by fracture, failure by net section yield, or exceedance of the threshold SIF range for fatigue crack growth (below which no growth will occur). The dual criteria of failure by fracture and by net section yielding is the default. This module does not consider the failure assessment diagram as a failure criterion.

### 3.3 NASFAD

NASFAD provides the capability to use the Failure Assessment Diagram (FAD) to assess the criticality of crack-like flaws. The NASFAD module in NASGRO is used to perform a Level 2 fracture assessment using the FAD failure criterion given a crack size, material properties and applied stresses. The principal result of the analysis is a determination of whether or not the crack is in the “safe” area of the FAD (Point A) or in the “unsafe” area (Point B) as shown in Figure 2.5-1. The NASFAD analysis provides a plot of the FAD showing the assessment point ( $K_r, L_r$ ). There is no crack growth performed by the NASFAD module. However, NASFAD contains options to compute a critical crack size and a failure stress using the FAD criterion.

### 3.4 NASFLA

The NASFLA module in NASGRO is used to compute fatigue crack growth as a function of cyclically applied stresses. The principal result of the analysis is a crack growth curve plotting crack size (depth and length) as a function of applied stress cycles until reaching a critical crack size (failure). When choosing to invoke a FAD failure criterion, the NASFLA analysis also provides a plot of the FAD showing the locus of the assessment points ( $K_r, L_r$ ) calculated as the crack grows to the limiting condition (point B) on the FAD, reaching a critical crack size determined by the FAD criterion. NASFLA can be used to perform a Level 3 assessment.

### 3.5 NASMAT

NASMAT is a material data processing program containing a large library of fatigue crack growth rate ( $da/dN$  vs  $\Delta K$ ) and fracture toughness ( $K_c$ ) data. Users can select, view, edit, and curve fit the library data or enter and save their own data into the NASMAT user database. Options exist to curve fit data to the NASGRO equation and the Walker Equation. NASMAT also provides the capability to determine the parameters ( $A_k$  and  $B_k$ ) of the relationship between fracture toughness and thickness that is used in NASGRO. The resulting material properties and fit parameters are suitable for direct entry into NASCCS, NASFAD and the NASGRO modules.

## 4 NASGRO STRESS INTENSITY FACTOR (SIF) SOLUTIONS

### 4.1 General

The general form of the stress intensity factor solutions in NASGRO is given by the following equation

$$K = (S_0F_0 + S_1F_1 + S_2F_2 + S_3F_3) \sqrt{\pi a}$$

where the  $S_i$  represent stress quantities such as tension ( $S_0$ ), bending ( $S_1, S_2$ ), or bearing ( $S_3$ ) stresses. The  $F_i$  are the geometry (correction) factors associated with each stress component and  $a$  is the crack depth or crack length  $c$ , depending on the solution being used. Additionally, for the NASGRO weight function models, the  $S_0, S_1, S_2$  and  $S_3$  stresses can be used to individually represent any type of nonlinear stress gradient specified in tabular form as a function of normalized distance over the cross-section of the model. Important elements of the SIF solutions such as the finite width correction factor and the factors accounting for the crack shape (aspect ratio,  $a/c$ ) are automatically included in the NASGRO SIF solutions and do not need to be calculated separately. The NASSIF module in NASGRO is used to compute stress intensity factors. The process requires the analyst to choose the desired model and specify the geometry parameters, crack size, and stress components using the NASSIF graphical user interface (GUI). The NASFLA, NASCCS and NASFAD modules all use the SIF solutions contained in the NASSIF module with a similar input GUI.

### 4.2 Overview of Frequently Used NASGRO SIF Solutions for FFS Assessments

The NASGRO software contains over 110 different SIF solutions. The theoretical background for each of these solutions is provided in Appendix C of the NASGRO Reference Manual [1]. While any of these solutions could be employed for general purpose fracture and fatigue crack growth analyses, only a subset of them is enabled to perform an analysis using the FAD failure criteria. This “FAD-enabled” set of solutions represents common geometries that arise in the FFS analysis of pressure systems (as well as other applications).

The following is a list of NASGRO SIF solutions that are available for use with the FAD failure criteria:

**TC06:** Through crack in hollow sphere

**TC07:** Through crack (axial) in hollow cylinder

**TC08:** Through crack (circumferential) in thin cylinder

**TC11:** Through crack (offset) in plate – univariant WF

**TC12:** Through crack at edge of plate – univariant WF

**TC15:** Through crack at edge of variable thickness plate – univariant WF

**CC09:** Quarter-elliptical corner crack in plate – bivariant WF

**CC11:** Quarter-elliptical corner crack in plate – univariant WF

- CC27:** Quarter-elliptical corner crack at pressure vessel nozzle – from API 579
- CC28:** Quarter-elliptical corner crack at pressure vessel nozzle – bivariant WF
- SC04:** Semi-elliptical surface crack (axial) in hollow cylinder – univariant WF
- SC05:** Semi-elliptical surface crack (circumferential) in hollow cylinder
- SC06:** Constant depth surface crack (circumferential) in hollow cylinder – univariant WF
- SC30:** Semi-elliptical surface crack (offset) in plate – univariant WF
- SC31:** Semi-elliptical surface crack (offset) in plate – bivariant WF
- SC34:** Semi-elliptical surface crack in a hollow cylinder – univariant WF
- SC36:** Semi-elliptical surface crack in a sphere – univariant WF
- EC04:** Elliptical embedded crack (offset) in plate – bivariant WF
- EC05:** Elliptical embedded crack (offset) in plate – univariant WF

Note that the majority of these crack cases (except TC06, TC07, TC08, CC27 and SC05) are weight function solutions for univariant or bivariant stress gradients on the crack plane.

### **4.3 NASGRO Limit Load Solutions**

Determination of the load ratio,  $L_r$ , for use in the FAD, requires computing the ratio of the total applied load contributing to the primary stresses to the plastic limit load of the cracked structure. The conditions at which failure of a cracked body is imminent due to plastic collapse of the net section are traditionally denoted as the plastic limit load. Plastic limit load solutions from various sources have been collected into compendia similar to published volumes of stress intensity factor solutions [2, 3, 4]. Plastic limit loads are generally expressed in terms of applied uniform tension and linear bending stresses. Therefore, if the applied loading takes the form of an arbitrary stress gradient, it is first necessary to determine the equivalent tension and bending stresses that produce the same net force and net moment. The specific equations for plastic limit load employed in NASGRO are documented in detail in Appendix X of the NASGRO Reference Manual. The equations used to calculate the global and local plastic limit loads in NASGRO are taken from the FITNET compendium [3], independently derived [1], or from API 579 [2] depending on the crack geometry.

Established structural integrity procedures generally specify that the plastic limit load should be calculated based on minimum (not mean) material strength properties (e.g., yield strength). If these are not available, mean values can be employed, but the result will be less conservative.

Only primary (mechanical) stresses can contribute to plastic collapse. Secondary stresses such as residual or thermal stresses do not contribute to plastic collapse and hence should not be included in the plastic limit load check. NASGRO correctly treats residual stresses as secondary stresses for the purposes of plastic limit load checks. This includes both residual stresses that are explicitly input as residual stresses via the NASGRO GUIs as well as calculated residual stresses arising from shakedown analysis.

#### 4.4 Cross-Reference to API 579 SIF Solutions

NASGRO and API 579 each have their own nomenclature for SIF solutions and it can be somewhat problematic to make an apples-to-apples parallel list for the different models. Therefore, a comparison matrix (table) was developed to cross-reference existing API 579 stress intensity factor solutions with corresponding NASGRO SIF solutions. This matrix (included here as Tables 4.4-1 through 4.4-5) was derived from API 579 Table 9B.1 and modified to include a column of notes and a column containing NASGRO SIF solution names corresponding to API 579 solution names. In a few cases, additional rows were added for relevant NASGRO SIF solutions that do not have a corresponding counterpart in the API 579 SIF list. An “X” in the tables indicates that there is not a direct counterpart between API 579 and NASGRO or vice versa.

The objective of these tables is to provide guidance to users of NASGRO in choosing NASGRO SIF solutions that correspond to API 579 solutions they may have been accustomed to using. For example, the table indicates that for a circumferentially oriented surface crack in a cylinder (API 579 solutions KCSCCE1, 2 & 3) the NASGRO SC34 model can be used.

**Table 4.4-1. Cross-Reference Matrix for Cracks in Flat Plate**

Component Geometry	Crack Geometry	Notes	Crack Loading	API 579 Stress Intensity Factor Solution	API 579 Reference Stress Solution	NASGRO Stress Intensity Factor Solution
<b>Plate</b>	Through-Wall Crack	Center Crack	Through-Wall Membrane and Bending Stress	KPTC (9B.3.1)	RPTC (9C.3.1)	TC01, TC11
	Surface Crack, Infinite Length		Through-Wall Fourth Order Polynomial Stress Distribution	KPSCL1 (9B.3.2)	RPSCL (9C.3.2)	X
	Surface Crack, Infinite Length		Through-Wall Arbitrary Stress Distribution	KPSCL2 (9B.3.3)	RPSCL (9C.3.3)	X
	Surface Crack, Semi-Elliptical Shape	Center Crack	Through-Wall Membrane and Bending Stress	KPSCE1 (9B.3.4)	RPSCE1 (9C.3.4)	SC01, SC02
	Surface Crack, Semi-Elliptical Shape	Center Crack	Through-Wall Fourth Order Polynomial Stress Distribution	KPSCE2 (9B.3.5)	RPSCE2 (9C.3.5)	SC02, SC30
	Surface Crack, Semi-Elliptical Shape	Center Crack	Through-Wall Arbitrary Stress Distribution	KPSCE3 (9B.3.6)	RPSCE3 (9C.3.6)	SC30
	Surface Crack, Semi-Elliptical Shape	Off-Center Crack	Bivariant Through-Wall Arbitrary Stress Distribution	X	X	SC30
	Surface Crack, Semi-Elliptical Shape	Off-Center Crack	Bivariant Through-Wall Arbitrary Stress Distribution	X	X	SC31
	Embedded Crack, Infinite Length		Through-Wall Fourth Order Polynomial Stress Distribution	KPECL (9B.3.7)	RPECL (9C.3.7)	X
	Embedded Crack, Elliptical Shape	Center Crack (on width)	Through-Wall Membrane and Bending Stress	KPECE1 (9B.3.8)	RPECE1 (9C.3.8)	EC05
	Embedded Crack, Elliptical Shape	Center Crack (on width)	Through-Wall Fourth Order Polynomial Stress Distribution	KPECE2 (9B.3.9)	RPECE2 (9C.3.9)	EC05
	Embedded Crack, Elliptical Shape	Off-Center Crack (on width)	Through-Wall Fourth Order Polynomial Stress Distribution	X	X	EC05
	Embedded Crack, Elliptical Shape	Off-Center Crack (on width)	Bivariant Through-Wall Arbitrary Stress Distribution	X	X	EC04

**Table 4.4-2. Cross-Reference Matrix for Cracks in Flat Plate with a Hole**

Component Geometry	Crack Geometry	Notes	Crack Loading	API 579 Stress Intensity Factor Solution	API 579 Reference Stress Solution	NASGRO Stress Intensity Factor Solution
<b>Plate with a Hole</b>	Single Hole, Through-Wall Single Edge Crack	Infinite Plate, Biaxial Stress	Through-Wall Membrane and Bending Stress	KPHTC1 (9B.4.1)	RPHTC1 (9C.4.1)	TC09
	Single Hole, Through-Wall Double Edge Crack	Infinite Plate, Biaxial Stress	Through-Wall Membrane and Bending Stress	KPHTC2 (9B.4.2)	RPHTC2 (9C.4.2)	X
	Single Hole, Surface Crack, Semi-Elliptical Shape	Center Hole (on width) Center Crack (on thickness)	Membrane Stress	KPHSC1 (9B.4.3)	RPHSC1 (9C.4.3)	SC11
	Single Hole, Corner Crack, Semi-Elliptical Shape	Center Hole (on width)	Through-Wall Membrane and Bending Stress	KPHSC2 (9B.4.4)	RPHSC2 (9C.4.4)	CC16
	Single Hole, Corner Crack, Semi-Elliptical Shape	Off-Center Hole (on width)	Through-Wall Membrane and Bending Stress	X	X	CC16

**Table 4.4-3. Cross-Reference Matrix for Cracks in Cylinders**

Component Geometry	Crack Geometry	Notes	Crack Loading	API 579 Stress Intensity Factor Solution	API 579 Reference Stress Solution	NASGRO Stress Intensity Factor Solution
Cylinder	Through-Wall Crack, Longitudinal Direction		Through-Wall Membrane and Bending Stress	KCTCL (9B.5.1)	RCTCL (9C.5.1)	TC07
	Through-Wall Crack, Circumferential Direction		Through-Wall Membrane and Bending Stress	KCTCC1 (9B.5.2)	RCTCC1 (9C.5.2)	X
	Through-Wall Crack, Circumferential Direction		Pressure with a Net Section Axial Force and Bending Moment	KCTCC2 (9B.5.3)	RCTCC2 (9C.5.3)	X
	Surface Crack, Longitudinal Direction, Infinite Length		Internal Pressure (Lame Stress Distribution)	KCSCLL1 (9B.5.4)	RCSCLL1 (9C.5.4)	X
	Surface Crack, Longitudinal Direction, Infinite Length		Through-Wall Fourth Order Polynomial Stress Distribution	KCSCLL2 (9B.5.5)	RCSCLL2 (9C.5.5)	X
	Surface Crack, Longitudinal Direction, Infinite Length		Through-Wall Arbitrary Stress Distribution	KCSCLL3 (9B.5.6)	RCSCLL3 (9C.5.6)	X
	Surface Crack, Circumferential Direction, 360°		Pressure with Net Section Axial Force and Bending Moment	KCSCCL1 (9B.5.7)	RCSCCL1 (9C.5.7)	X
	Surface Crack, Circumferential Direction, 360°		Through-Wall Fourth Order Polynomial Stress Distribution & Net Section Bending Moments	KCSCCL2 (9B.5.8)	RCSCCL2 (9C.5.8)	SC06
	Surface Crack, Circumferential Direction, 360°		Through-Wall Arbitrary Stress Distribution	KCSCCL3 (9B.5.9)	RCSCCL3 (9C.5.9)	SC06
	Surface Crack, Longitudinal Direction, Semi-Elliptical Shape		Internal Pressure (Lame Stress Distribution)	KCSCLE1 (9B.5.10)	RCSCLE1 (9C.5.10)	SC04
	Surface Crack, Longitudinal Direction, Semi-Elliptical Shape		Through-Wall Fourth Order Polynomial Stress Distribution	KCSCLE2 (9B.5.11)	RCSCLE2 (9C.5.11)	SC04
	Surface Crack, Longitudinal Direction, Semi-Elliptical Shape		Through-Wall Arbitrary Stress Distribution	KCSCLE3 (9B.5.12)	RCSCLE3 (9C.5.12)	SC04
	Surface Crack, Circumferential Direction, Semi-Elliptical Shape		Internal Pressure (Lame Stress Distribution) with Net Section Axial Force	KCSCCE1 (9B.5.13)	RCSCCE1 (9C.5.13)	SC34
	Surface Crack, Circumferential Direction, Semi-Elliptical Shape		Through-Wall Fourth Order Polynomial Stress Distribution with Net Section Bending Moment	KCSCCE2 (9B.5.14)	RCSCCE2 (9C.5.14)	SC34

**Table 4.4-3. Cross-Reference Matrix for Cracks in Cylinders (continued)**

	Crack Geometry	Notes	Crack Loading	API 579 Stress Intensity Factor Solution	API 579 Reference Stress Solution	NASGRO Stress Intensity Factor Solution
<b>Cylinder</b>	Surface Crack, Circumferential Direction, Semi-Elliptical Shape		Through-Wall Arbitrary Stress Distribution	KCSCE3 (9B.5.15)	RCSCE3 (9C.5.15)	SC34
	Embedded Crack, Longitudinal Direction, Infinite Length		Through-Wall Fourth Order Polynomial Stress Distribution	KCECLL (9B.5.16)	RCECLL (9C.5.16)	X (EC05)
	Embedded Crack, Circumferential Direction, 360°		Through-Wall Fourth Order Polynomial Stress Distribution	KCECCL (9B.5.17)	RCECCL (9C.5.17)	X
	Embedded Crack, Longitudinal Direction, Elliptical Shape		Through-Wall Fourth Order Polynomial Stress Distribution	KCECLE (9B.5.18)	RCECLE (9C.5.18)	X (EC05)
	Embedded Crack, Circumferential Direction, Elliptical Shape		Through-Wall Fourth Order Polynomial Stress Distribution	KCECCE (9B.5.19)	RCECCE (9C.5.19)	X

**Table 4.4-4. Cross-Reference Matrix for Cracks in Spheres**

Component Geometry	Crack Geometry	Notes	Crack Loading	API 579 Stress Intensity Factor Solution	API 579 Reference Stress Solution	NASGRO Stress Intensity Factor Solution
Sphere	Through-Wall Crack		Through-Wall Membrane and Bending Stress	KSTC (9B.6.1)	RSTC (9C.6.1)	TC06
	Surface Crack, Circumferential Direction, 360°		Internal Pressure (Lame Stress Distribution)	KSSCCL1 (9B.6.2)	RSSCCL1 (9C.6.2)	X
	Surface Crack, Circumferential Direction, 360°		Through-Wall Fourth Order Polynomial Stress Distribution	KSSCCL2 (9B.6.3)	RSSCCL2 (9C.6.3)	X
	Surface Crack, Circumferential Direction, 360°		Through-Wall Arbitrary Stress Distribution	KSSCCL3 (9B.6.4)	RSSCCL3 (9C.6.4)	X
	Surface Crack, Circumferential Direction, Semi-Elliptical Shape		Internal Pressure (Lame Stress Distribution)	KSSCCE1 (9B.6.5)	RSSCCE1 (9C.6.5)	SC36
	Surface Crack, Circumferential Direction, Semi-Elliptical Shape		Through-Wall Fourth Order Polynomial Stress Distribution	KSSCCE2 (9B.6.6)	RSSCCE2 (9C.6.6)	SC36
	Surface Crack, Circumferential Direction, Semi-Elliptical Shape		Through-Wall Arbitrary Stress Distribution	KSSCCE3 (9B.6.7)	RSSCCE3 (9C.6.7)	SC36
	Embedded Crack, Circumferential Direction, 360°		Through-Wall Fourth Order Polynomial Stress Distribution	KSECCL (9B.6.8)	RSECCL (9C.6.8)	X
	Embedded Crack, Circumferential Direction, Elliptical Shape	Plate Solutions	Through-Wall Fourth Order Polynomial Stress Distribution	KSECCE (9B.6.9)	RSECCE (9C.6.9)	EC05

**Table 4.4-5. Cross-Reference Matrix for Cracks in Other Components**

Component Geometry	Crack Geometry	Notes	Crack Loading	API 579 Stress Intensity Factor Solution	API 579 Reference Stress Solution	NASGRO Stress Intensity Factor Solution
Elbow and Pipe Bend	General Solution		See Discussion in Paragraph 9B.7.	(9B.7)	(9C.7)	X
	Corner Cracks, Radial Direction, Quarter-Circular Shape		Membrane Stress	KNCC1 (9B.8.1)	RNCC1 (9C.8.1)	CC27
Nozzle or Piping Tee	Corner Cracks, Radial Direction, Quarter-Circular Shape		Cubic Polynomial Stress Distribution	KNCC2 (9B.8.2)	RNCC2 (9C.8.2)	CC28
	Surface Cracks at Nozzles - General Solution		See Discussion in Paragraph 9B.8.	(9B.8.3)	(9C.8.3)	X
Ring- Stiffened Cylinder	Surface Crack at the Toe of One Fillet Weld, Circumferential Direction -		Pressure (Membrane and Bending Stress)	KRCSCL1 (9B.9.1)	RRCSCCL1 (9C.9.1)	X
	Surface Crack at the Toe of Both Fillet Welds, Circumferential Direction -		Pressure (Membrane and Bending Stress)	KRCSCL2 (9B.9.2)	RRCSCCL2 (9C.9.2)	X
Sleeve Reinforced Cylinder	General Solution		See Discussion in Paragraph 9B.10.	(9B.10)	(9C.10)	X
Round Bar or Bolt	Round Bar, Surface Crack, 360°		Membrane and Bending Stress	KBSC1 (9B.11.1)	RBSC1 (9C.11.1)	X
	Round Bar, Surface Crack, Straight Front Shape		Membrane and Bending Stress	KBSC2 (9B.11.2)	RBSC2 (9C.11.2)	X
	Round Bar, Surface Crack, Semi-Circular Shape		Membrane and Bending Stress	KBSC3 (9B.11.3)	RBSC3 (9C.11.3)	SC07, SC35
	Bolt, Surface Crack, Semi-Elliptical or Straight Front Shape		Membrane and Bending Stress	KBSC4 (9B.11.4)	RBSC4 (9C.11.4)	SC08
Cracks at Fillet Welds	Surface Crack, Infinite Length		Membrane and Bending Stress	KFWSCE1 (9B.12.1)	RFWSCE1 (9C.12.1)	SC30
	Cracks at Fillet Welds in Tee Juncions in Pressurized Components - General Solution		See Discussion in Paragraph 9B.12.2	(9B.12.2)	(9C.12.1.3)	SC30
Cracks in Clad or Weld Overlayed Plate	General Solution		See Discussion in Paragraph 9B.13.	(9B.13)	(9C.13)	X

## 4.5 Crack Shape Transitions

During a fatigue crack growth analysis, corner and surface cracks may grow to the point where the crack depth reaches the thickness prior to fracture instability. Embedded cracks may break through to the surface prior to fracture instability. A frequent example of this type of behavior is a leak-before-break situation where a surface crack in a pressure vessel grows subcritically and becomes a through-wall crack without failure, resulting in a leak. NASGRO automatically accounts for these transitions in crack shape and SIF solution in the NASFLA module. In some cases, more than one transition is possible, for example, an embedded crack transitioning to a surface crack and then to a through-wall crack.

### 4.5.1 NASGRO Defaults

NASGRO provides crack transition capabilities for many crack cases for NASFLA analysis, *i.e.* crack propagation from one geometrical configuration to another. During crack transition, the simulation will switch from the original crack case to a degraded crack case (or a succession of them). In such cases, appropriate data need to be furnished for the degraded crack case, including geometrical dimensions, crack sizes and loading. This transfer of data between models occurs automatically within NASFLA and the output reflects when these transitions occur in terms of crack size and cycles and plots of the crack growth curves illustrating that a transition has occurred. Appendix D of the NASGRO reference manual provides details about the crack transitions for each SIF solution that has transitions available. It is important to note that different NASGRO SIF models transition at different crack sizes, *e.g.*,  $a/t$ .

### 4.5.2 API 579 Criteria for Surface and Embedded Crack Transitions

The crack transition criteria in NASGRO differ from those contained in the API 579 “recategorization” guidelines. For example, the API 579 guidelines require transition to a through crack at an  $a/t$  of 0.80 whereas the NASGRO weight function surface crack models transition to a through crack at an  $a/t$  of 0.95 (*e.g.*, SC30 & SC31). The API 579 crack transition criteria are more conservative than the default transition criteria used in NASFLA.

An option within NASGRO to allow the user to choose crack transition criteria based on the API flaw recategorization guidelines for surface and embedded cracks in Section 9.3.6.6 of API 579 (2021) has been implemented in NASFLA beginning with v11.0. This new transition criteria option is implemented in NASFLA via a check box on the geometry page for applicable crack cases. The transition criteria that already exist in NASGRO remain the defaults.

Figure 4.5.2-1 shows a NASFLA crack case geometry screen containing the check box for selecting the use of the API 579 transition criteria. The default is to use the existing NASGRO transitions. The API 579 transition criteria are only available for the following surface crack and embedded crack cases: SC01, SC02, SC03, SC04, SC05, SC30, SC31, EC04 and EC05.

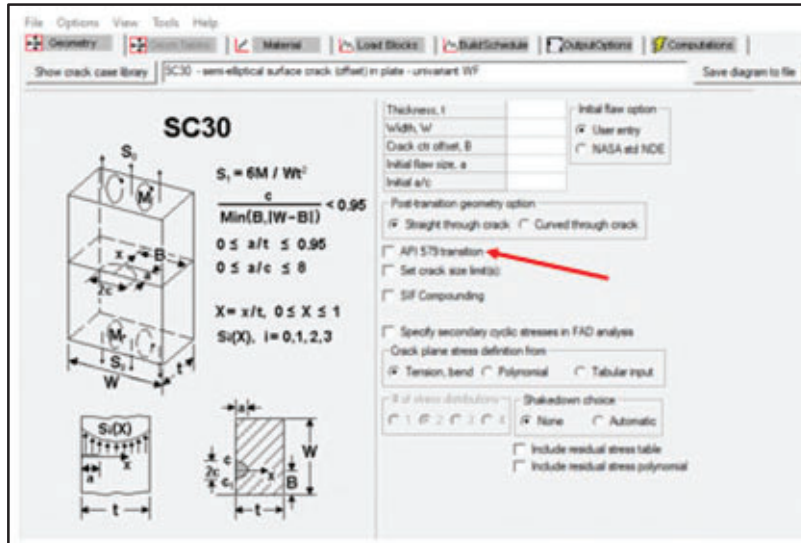


Figure 4.5.2-1. NASGRO GUI Screen for SC30 Showing Check Box to Activate API 579 Transition Criteria

Note that the user must specify the use of the API 579 transition criteria for each individual crack case on the Geometry page. Also note that these new criteria apply only to the list of surface and embedded crack cases provided above. The API 579 transition criteria do not apply to any other NASGRO crack cases, *e.g.*, corner cracks. When the API 579 transition criteria option is selected, a statement in the output file is printed to that effect.

The crack shape transitions for embedded cracks and surface cracks using the API 579 criteria are documented with additional detail in Section 9 of Appendix D of the NASGRO reference manual. This includes a listing of the API 579 transition equations, flaw dimensions before and after transition, and a table comparing the API 579 transition criteria to the default NASGRO transition criteria.

## 5 MATERIAL PROPERTIES FOR FFS ANALYSES

Required material properties for fitness-for-service analyses are specified in Section 9.3.5 of API 579 and include the yield and tensile (ultimate) strength, the fracture toughness and the fatigue crack growth rate model. Values of these properties and parameters of the fatigue crack growth rate model, *i.e.*, the NASGRO equation, are contained in the NASGRO material property database. In addition, the elastic modulus (Young's modulus) and Poisson's ratio may also be needed, however, the NASGRO database does not contain values for these quantities.

In this report, the US (English) system of units is used. That is the default units system in NASGRO. However, NASGRO does have the ability to accommodate a number of different variants on metric systems of units.

### 5.1 Strength

Yield and ultimate tensile strengths are required to account for a number of aspects of a FFS analysis ranging from a simple net-section yield failure criterion to the computation the plastic limit load and including the effects of plasticity on the crack driving force. In addition, the yield stress can be used to estimate residual stress distributions and to account for the effect of thickness on fracture toughness. In NASGRO, if the FAD criterion is not used, failure is considered to occur if the net section stress exceeds the flow stress of the specified material, defined as the average of the yield and ultimate strengths. If the FAD criterion is used, then the yield stress is used to compute the load ratio,  $L_r$ .

### 5.2 Fracture Toughness

The fracture toughness of a material is a measure of its resistance to failure by rapid crack extension (instability) resulting in fracture. It is a material property that is dependent on temperature, environment and component thickness. Generally, the fracture toughness is defined as the plane strain fracture toughness,  $K_{Ic}$ , which is considered a lower bound value for high constraint conditions. For lower constraint conditions, *i.e.*, thinner geometries, the fracture toughness increases as the thickness decreases and is labeled  $K_c$ . In NASGRO, crack instability is usually assumed to occur if  $K_{max}$  exceeds the fracture toughness ( $K_{Ic}$  or  $K_c$ ) of a material. If the FAD failure criterion is used, then  $K_{Ic}$  or  $K_c$  are used in computing the toughness ratio,  $K_r$ .

### 5.3 Fatigue Crack Growth Rate

Remaining life calculations require the use of a relationship that relates crack growth rate ( $da/dN$ ) to applied cyclic stress or load spectrum cycles where a stress cycle ( $\Delta S$ ) results in a SIF cycle ( $\Delta K$ ) that causes subcritical crack growth. These relationships (equations) use the applied  $\Delta K$  to compute the fatigue crack growth rate and usually account for dependence on the stress ratio,  $R$ , defined as  $S_{min}/S_{max}$  for a given cycle. Crack growth rate calculations in NASGRO use a relationship called the NASGRO equation. Other equations are available in the literature, such as the Walker equation that is also available in NASGRO. The parameters of the NASGRO equation for many materials have been obtained from curve fits to experimental fatigue crack growth rate test results and are included in the NASGRO material property database.

In addition to the NASGRO equation and Walker equation, the NASGRO software also offers tabular  $da/dN$  approaches to perform crack growth calculations. The NASGRO material database contains a smaller number of tabular data sets and NASFLA provides the capability to enter user-defined sets of tabular fatigue crack growth rate data. The tabular  $da/dN$  approach utilizes a series of discrete  $da/dN$  vs  $\Delta K$  data points for one or more stress ratios. These tables are not made directly from test data points, but rather from tabular fits of test data. During crack propagation analysis, the crack growth rate under the applied stress intensity factor and/or stress ratio is calculated by interpolating within the user-provided  $da/dN$  vs  $\Delta K$  tables rather than using an equation.

## 6 NASGRO MATERIAL PROPERTIES

The NASGRO material database is contained within the NASGRO program and has numerous sources including government reports and handbooks, contractor reports, and journal articles. Citations for the reference (source) of all materials in the database can be displayed from within the program.

### 6.1 The NASGRO Fatigue Crack Growth (FCG) Database

#### 6.1.1 Material Selection

From the opening NASGRO screen (Figure 3.0-1), clicking on the NASFLA button will provide access to the Materials tab in the main NASFLA menu. Then, selecting the Materials tab provides access to the NASGRO materials files, where properties are accessed from the NASFLA database files automatically. Detailed information on interaction models in NASFLA is provided in Section 2.1.7 of the NASGRO Reference Manual.

The Materials tab provides a list of five crack growth interaction models that are available in NASFLA, however, the default is non-interaction. A non-interaction model is deemed appropriate for API 579 FFS analyses.

#### 6.1.2 Data Source

The default “Data source” is the NASGRO material file. The other options are to obtain the material properties either from a user-defined file or to enter new data from scratch. Options are also available to choose from files for multiple temperatures (NASFLA database or user files) as shown in Figure 6.1.2-1.

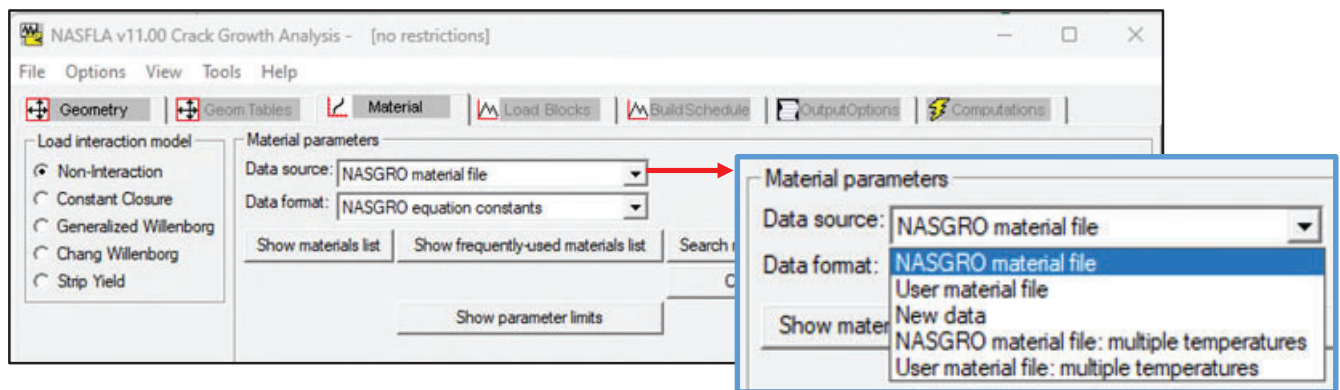
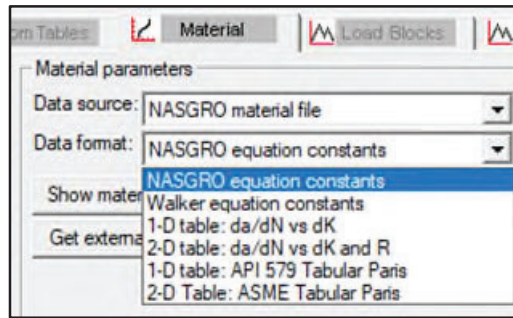


Figure 6.1.2-1. NASFLA GUI Menu for Material Data Source Selection

#### 6.1.3 Data Format

Next, the “Data format” is selected from one of the following: NASGRO equation, Walker equation, 1-D table, or a 2-D table. Two additional 1-D and 2-D table options are available to choose tabular Paris equation representations for materials specified by API 579 and the ASME Boiler and Pressure Vessel Code. See Figure 6.1.3-1.



**Figure 6.1.3-1. NASFLA GUI Menu for Material Data Format Selection**

Once the Data source and Data format are chosen, the “Show materials list” button can be used to display the materials in the database via a series of down-select menu choices.

### 6.1.4 NASGRO Equation

Crack growth rate calculations in NASGRO use a relationship called the NASGRO equation given by:

$$\frac{da}{dN} = C \left[ \left( \frac{1-f}{1-R} \right) \Delta K \right]^n \frac{\left( 1 - \frac{\Delta K_{th}}{\Delta K} \right)^p}{\left( 1 - \frac{K_{max}}{K_c} \right)^q}$$

where  $N$  is the number of applied fatigue cycles,  $a$  is the crack length,  $R$  is the stress ratio,  $\Delta K$  is the stress intensity factor range, and  $C$ ,  $n$ ,  $p$ , and  $q$  are empirically derived constants. The NASGRO equation is a “full-range” crack growth model in that it can represent all three crack growth regions (near threshold, linear, and instability) as well as account for the dependence of FCG rate on the stress ratio,  $R$ . Closure is modeled using the Newman crack opening function,  $f$ . For background and theory supporting the NASGRO equation, the reader is referred to the NASGRO reference manual (Sections 2.1.1 to 2.1.3) [1].

When choosing a material from the NASGRO material database for use in a NASFLA fatigue crack growth analysis the material GUI screen is displayed showing all the material constants and parameters for that material choice. Figure 6.1.4-1 is an example of the NASGRO equation data display for A285 Gr C steel. A plot of the NASGRO equation fit to the test data can be displayed by clicking on the “View Basic Fit” button.

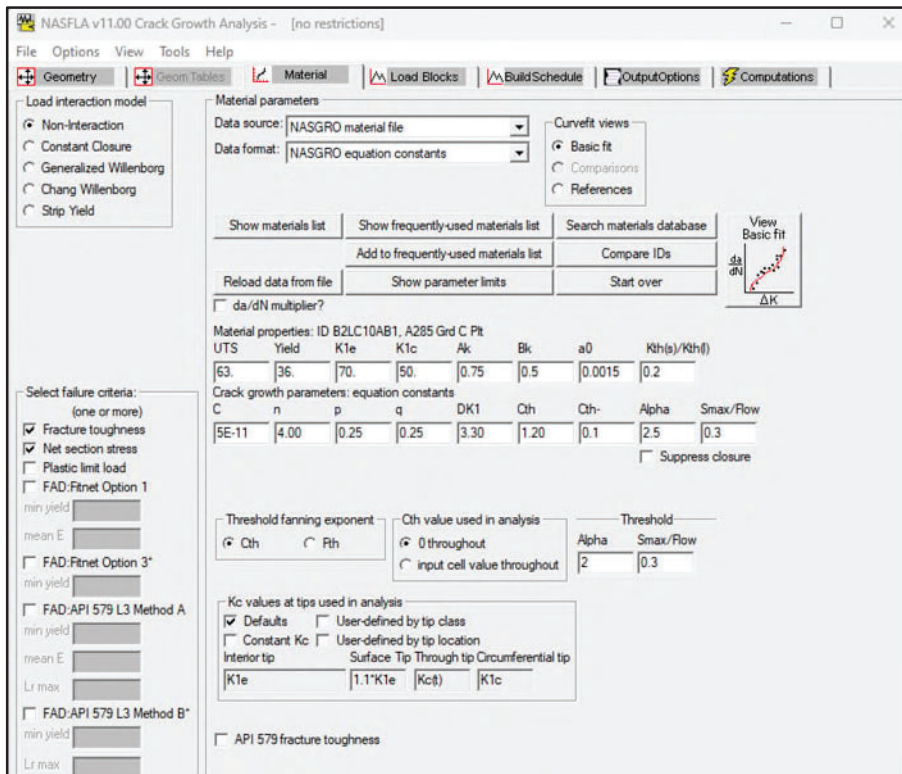


Figure 6.1.4-1. Example NASFLA Material Screen Showing NASGRO Equation Data for A285 Gr C Steel

### 6.1.5 Walker Equation

As shown in Figure 6.1.3-1, the Walker equation is also available in NASFLA and is given by:

$$\frac{da}{dN} = C \left[ \frac{\Delta K}{(1-R)^{1-m}} \right]^n$$

where  $C$ ,  $n$ , and  $m$  are empirically derived constants. The Walker equation is a crack growth model that is best used to represent the linear or Paris region of FCG rate data and it includes the influence of the stress ratio,  $R$ . However, in the NASGRO material database, much fewer materials are fit to the Walker equation than the NAGRO equation.

### 6.1.6 Tabular FCG Data

As shown in Figure 6.1.3-1, NASGRO also provides four kinds of tabular  $da/dN$  approaches:

- 1) 1-D table of  $da/dN$  vs.  $\Delta K$ ;
- 2) 1-D table of  $da/dN$  vs.  $\Delta K_{eff}$ ;
- 3) 2-D table of  $da/dN$  vs.  $\Delta K$  &  $R$ .
- 4) 1-D and 2-D tabular Paris data from API 579 & ASME Section VIII, Div3

The choice of which type of tabular data to use will depend on the availability of the material data in the database (in tabular form) and the anticipated cyclic loading (single R or multiple R values in the stress history). Appendix G of the NASGRO Reference Manual lists all the materials in the NASGRO database that are available in tabular form. Relevant examples of choices for select pressure vessel materials are presented below.

### 6.1.7 1-D Tabular FCG Data Example

An example of a 1-D tabular data set is shown in Figure 6.1.7-1 obtained by selecting the data source as the NASGRO material file and then the data format to be 1-D table da/dN vs.  $\Delta K$ . The material chosen is A106 Gr B steel. A plot of the FCG data in the table can be made by clicking on the plot button in the GUI.

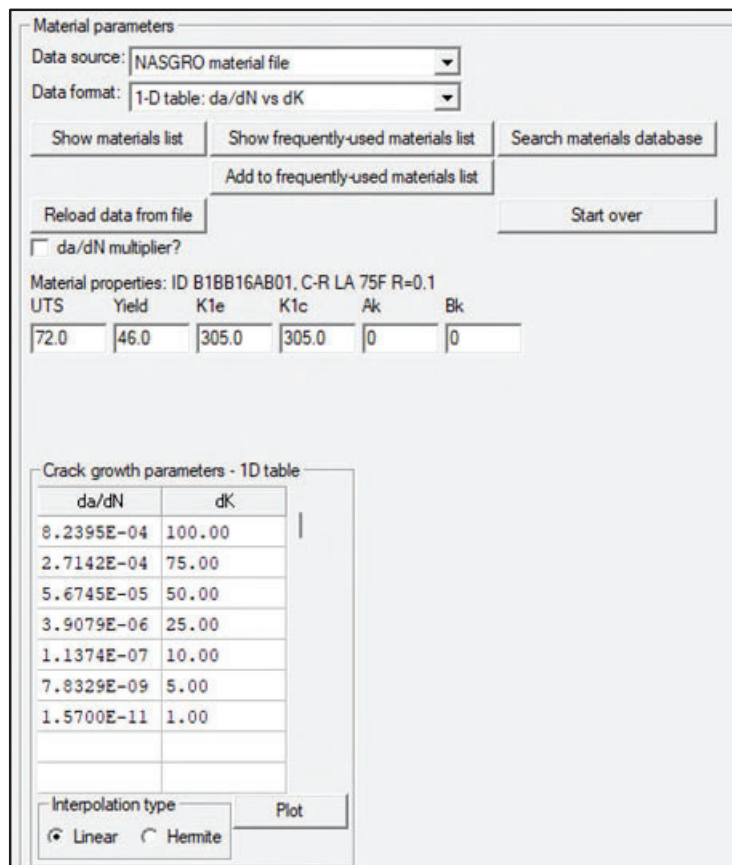


**Figure 6.1.7-1. Example NASFLA Material Screen Showing 1-D Tabular FCG Data for A106 Gr B Steel**

### 6.1.8 2-D Tabular FCG Data Example

An example of a 2-D tabular data set is shown in Figure 6.1.8-1 obtained by selecting the data source as the NASGRO material file and then the data format to be 2-D table da/dN vs.  $\Delta K$  and R. The material chosen is AOS 1146a, a wrapper plate steel from the NASA layered

pressure vessel (LPV) program [6]. A plot of the FCG data in the table can be made by clicking on the plot button in the GUI using the default linear-linear interpolation option.

Material parameters

Data source: NASGRO material file

Data format: 2-D table: da/dN vs dK and R

Show materials list   Show frequently-used materials list   Search materials database

Add to frequently-used materials list

Reload data from file   Start over

da/dN multiplier?

Material properties: ID E2FD12AB01, AOS 1146a Wrapper Plate: T-L

UTS	Yield	K1e	K1c	Ak	Bk
134	101	66.85	66.85	0	0

Crack growth parameters - 2D table

da/dN data type

Diff da/dN set for each R    Same da/dN set for all R

R ->	.1	R ->	.7	R ->	
da/dN	dK	da/dN	dK	da/dN	dK
0.000977712	60.5222	0.000979938	25.2115		
0.000411867	59.0577	0.000172881	24.4653		
0.000183827	56.9271	0.000044430	22.7422		
0.000100484	50.9855	0.000015248	21.0093		

Interpolation type for R:  Linear    Cubic spline    Walker logic

Interpolation type for dK:  Linear    Hermite

Set options and plot

**Figure 6.1.8-1. Example NASFLA Material Screen Showing 2-D Tabular FCG Data for AOS 1146a LPV Wrapper Steel**

### 6.1.9 API 579 and ASME Tabular Data (Paris Equations)

The Paris fatigue crack growth rate equations described in API 579 and ASME Section VIII, Div. 3 [7] are included in the NASGRO material files and stored in a format consistent with current NASGRO 1-D and 2-D table formats through conversion. The inclusion of these material categories facilitates the application of the NASGRO program to be in line with the selection of materials and their fatigue crack growth properties in boiler and pressure vessel industry. A total of ten (10) material IDs were added to the NASGRO tabular material property database. They can be chosen by selecting the NASGRO material file as the “Data source”

and using the “Data format” pull-down menu to select either the 1-D API 579 tabular Paris option or the 2-D ASME tabular option as shown in Figure 6.1.3-1.

Complete details of these materials and how the Paris equations have been converted to tabular form, including threshold behavior where applicable, are provided in Section 5 of Appendix A in the NASGRO Reference Manual. Table 6.1.9-1 provides a list of the materials that are contained in the NASGRO database using a tabular representation of the Paris equation.

**Table 6.1.9-1. Materials with 1-D & 2-D Tabular Paris Equation Data from API 579 (2021) and ASME Section VIII, Div. 3 (2023) Contained in the NASGRO Database**

<b>Table format</b>	<b>Materials; Conditions; Environment</b>	<b>Code</b>
1-D	<b>[B] API 579 Barsom; steel</b>	
	Ferritic-pearlite; Table 9F.4, C = 3.60E-10, n = 3.00	B1FPAPI2
	Martensitic; Table 9F.4, C = 6.60E-09, n = 2.25	B1MAAPI1
	Austenitic; Table 9F.4; C = 3.00E-10, n = 3.25	B1SSAPI3
	<b>[W] API 579 Welded Joint; steel</b>	
	Mean weld; Table 9F.5, C = 7.40E-10, n = 2.75	W1MNAPI5
Upper bound weld; Table 9F.5, C = 1.33E-09, n = 2.75	W1UPAPI4	
2-D	<b>[A] ASME Section VIII, Div 3</b>	
	High strength low alloy steel; Table KD-430, C = 1.95E-10, n = 3.26	A1HSASME2
	Carbon and low alloy steel; Table KD-430, C = 2.00E-10, n = 3.07	A1LAASME1
	Martensitic precipitation hardened steel; Table KD-430; C = 2.38E-10, n = 3.15	A1PHASME3
	Austenitic stainless steel; Table KD-430, C = 1.10E-10, n = 3.30	A1SSASME4
	Aluminum alloys; Table KD-430, C = 7.01E-10, n = 3.26	A2ALASME5

Figures 6.1.9-1 and 6.1.9-2 show examples of the material selection screens for the 1-D Barsom Paris equation materials and the 2-D ASME Section VIII Paris equation materials, respectively. It is important to note that the GUI cells for strength and toughness are empty and need to be filled in by the user. Neither API 579 or ASME Section VIII, Div 3 list strengths or toughness values corresponding to these Paris FCG rate equations. See Section 7 of this report for discussion of toughness properties in NASGRO.

Materials List ( Data source: NASGRO material file, Data format: 1-D table: API 579 Tabular Paris, material file: ParisTBC.XML)

Sort order for all material selections  
 by code     by description

Select material category [1D table]: [B] API 579 Barsom [W] API 579 Welded Joint	Select alloy group: [J] Steel	Select alloy and heat treatment: [FP] Ferritic-Pearlite [MA] Martensitic [SS] Austenitic Stainless Steel	Select product form/orientation/environment: [API2] Table 9F.4, C = 3.60E-10, n = 3.00
--	----------------------------------	---	---

Material parameters

Data source: NASGRO material file

Data format: 1-D table: API 579 Tabular Paris

Show materials list    Show frequently-used materials list    Search materials database

Add to frequently-used materials list

Reload data from file    Start over

da/dN multiplier?

Material properties: ID B1FPAPI2, API2 Table 9F.4, C = 3.60E-10, n = 3.00

UTS	Yield	K1e	K1c	Ak	Bk
				0.00	0.00

Crack growth parameters - 1D table

da/dN	dK
0.10000E-02	0.14060E+03
0.28710E-03	0.92740E+02
0.82450E-04	0.61180E+02
0.23670E-04	0.40360E+02
0.67970E-05	0.26630E+02
0.19520E-05	0.17570E+02
0.56040E-06	0.11590E+02
0.16090E-06	0.76460E+01
0.46200E-07	0.50440E+01

Interpolation type    Plot

Linear     Hermite

**Figure 6.1.9-1. Example NASFLA Material Screen Showing 1-D Tabular FCG Data for the API 579 Barsom Paris Equation for Ferritic-Pearlite Steel**

Materials List ( Data source: NASGRO material file, Data format: 2-D table: ASME Tabular Paris, material file: ParisTBC.XML)

Sort order for all material selections  
 by code     by description

Select material category [2D table]: [A] ASME Section VIII, Div 3	Select alloy group: [1] Steel [2] Aluminum	Select alloy and heat treatment: [HS] High Strength Low Alloy [LA] Carbon and Low Alloy [PH] Martensitic Precipitation Hardened [SS] Austenitic Stainless Steel	Select product form/orientation/environment: [ASME1] Table KD-430, C = 2.00E-10, n = 3.07
--	--	---	--

Material parameters

Data source: NASGRO material file

Data format: 2-D table: ASME Tabular Paris

Show materials list    Show frequently-used materials list    Search materials database

Add to frequently-used materials list

Reload data from file    Start over

da/dN multiplier?

Material properties: ID A1LAASME1, ASME1 Table KD-430, C = 2.00E-10, n = 3.07

UTS	Yield	K1e	K1c	Ak	Bk
				0.00	0.00

Crack growth parameters - 2D table

da/dN data type  
 Diff da/dN set for each R     Same da/dN set for all R

R ->	-0.10000E+0	R ->	-0.20000E+0	R ->	-0.10000E+0
da/dN	dK	da/dN	dK	da/dN	dK
0.10000E-02	0.16729E+04	0.10000E-02	0.45624E+03	0.10000E-02	0.30416E+03
0.22602E-03	0.10306E+04	0.31514E-03	0.31322E+03	0.34959E-03	0.21599E+03
0.51086E-04	0.63492E+03	0.99316E-04	0.21503E+03	0.12221E-03	0.15337E+03
0.11546E-04	0.39115E+03	0.31299E-04	0.14762E+03	0.42724E-04	0.10891E+03

Interpolation type for R  
 Linear     Cubic spline     Walker logic

Interpolation type for dK  
 Linear     Hermite

Set options and plot

Figure 6.1.9-2. Example NASFLA Material Screen Showing 2-D Tabular FCG Data for the ASME Section VIII, Div3 Paris Equation for a Carbon and Low Alloy Steel

## 7 FRACTURE TOUGHNESS OPTIONS IN NASGRO

### 7.1 NASGRO Toughness Properties and Dependence on Thickness

Fracture toughness properties of a material are essential for reliable fitness-for-service assessments and fatigue crack growth analyses. These include plane strain fracture toughness ( $K_{Ic}$ ) values, part-through fracture toughness ( $K_{Ie}$ ) values, and any other available fracture toughness ( $K_c$ ) values as a function of thickness.  $K_{Ie}$  values are especially important because flaws in real structures are often part-through (surface or corner) cracks. The main reason that fracture toughness depends on thickness is that differences in constraint produce changes in the stress state in the material. Thin structures, where the constraint is small, experience a plane stress condition with a higher toughness, whereas thicker structures that are in plane strain have more constraint and a lower toughness.

The following relationship has been adopted in NASGRO, for through crack problems, to describe the  $K_c$  vs. thickness behavior for various materials:

$$K_c/K_{Ic} = 1 + B_k e^{- (A_k t/t_0)^2}$$

where: 
$$t_0 = 2.5 (K_{Ic}/\sigma_{ys})^2$$

and  $t$  is the thickness of the component being analyzed. These equations are used by NASGRO to calculate a  $K_c$  value to substitute into the NASGRO equation for through cracks. Values of the material properties  $K_{Ic}$  and  $\sigma_{ys}$  and the parameters  $A_k$  and  $B_k$  are contained in the material property database. For part-through crack geometries,  $K_c$  in the NASGRO equation is set equal to a constant value of  $K_{Ie}$ , again contained in the NASGRO material properties files. Section 2.1.4 of the NASGRO reference manual provides additional details on how fracture toughness is modeled in NASGRO.

The toughness and strength material properties and the fit parameters  $A_k$  and  $B_k$  displayed in the NASFLA material GUI are used in analyses by default, however these values may be edited and changed by the user if desired. For many applications, it is desired (or required) to use the lower bound plane strain fracture toughness,  $K_{Ic}$ , to be conservative, or because of uncertainty in the thickness dependence relationship. In this case, the user can set  $B_k$  equal to zero which results in  $K_c = K_{Ic}$ . Also,  $K_{Ie}$  can be manually set to  $K_{Ic}$ .

### 7.2 Default Toughness Values and Option to Choose Toughness by Crack Tip

In NASFLA, NASCCS and NASFAD, the default  $K_c$  values are set tip-by-tip according to the following NASGRO rules:

- Through cracks:  $K_c(t)$ .
- Corner cracks:  $1.1 \times K_{Ie}$  for all crack tips.
- Surface cracks:  $1.1 \times K_{Ie}$  for surface crack tips, and  $K_{Ie}$  for interior crack tips.
- Embedded cracks:  $K_{Ie}$  for all crack tips.
- Circumferential cracks:  $K_{Ic}$ .

The default  $K_c$  values for each of the crack cases based on the above NASGRO rules are listed in Appendix U of the NASGRO reference manual. However, NASGRO also provides the capability to allow a user to define their own  $K_c$  values, which overwrite the default  $K_c$  values set by the NASGRO rules listed above in fatigue life analysis.

NASGRO offers three options for a user to define their own  $K_c$  values. There are four kinds of crack tip classes in NASGRO crack models: interior crack tip, surface crack tip, through crack tip, and circumferential crack tip. Figure 7.2-1 shows the GUI tool that appears on the material screen in NASFLA. The default is to use the toughness rules listed above and the other three check boxes allow the user to define a constant  $K_c$  for all crack tips or define toughness by tip class or location. Section 3 of Appendix U of the NASGRO reference manual provides details on each of these three options.

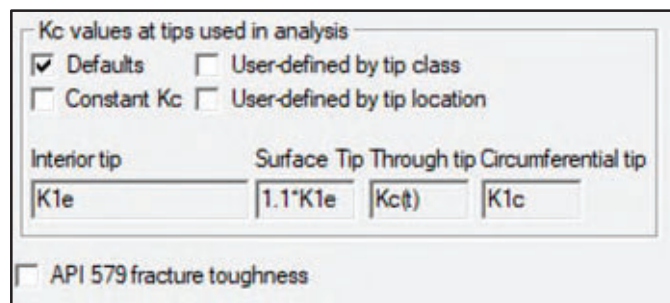


**Figure 7.2-1. NASFLA Material Screen GUI Tool for User-Defined  $K_c$  by Tip Class**

### 7.3 Option to Use API 579 and ASME Toughness Values

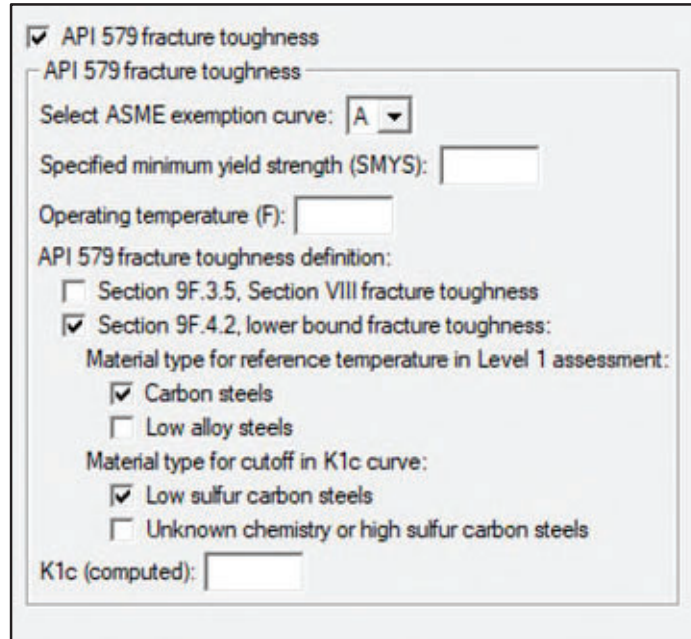
NASGRO v11.0 provides the capability for a user to calculate fracture toughness ( $K_{Ic}$ ) values using the methodology listed in the 2021 edition of API 579 [2] and the ASME B&PV Code [6, 8]. This new feature was implemented as an option on the NASGRO material screens for NASFLA and NASFAD. To activate this capability, a check box is provided on the material screen of the GUI, just below the user-defined toughness box, as shown in Figure 7.3-1.

Use of this feature presumes that the analyst is familiar with the relevant sections of API 579 and the ASME code in order to make appropriate choices in the GUI as described in the following. Checking the box to activate this feature displays a number of options for computing a fracture toughness as shown in Figure 7.3-1.

The user first needs to specify the ASME Exemption Curve designation (A, B, C, or D) according to Table 3.2 and Figure 3.5 of API 579 using the pull-down menu. Next, the Minimum Specified Yield Strength (MYS), and the operating temperature need to be specified.

Once this choice and these values are specified, there are two options available for computing a lower bound fracture toughness. The first option is to use the ASME B&PV Code, Section VIII, Div 1 & 2 fracture toughness approach listed as Equation 9F.43 in API 579. The second (default) option is the approach from Section XI of the ASME B&PV Code [8] that applies to ferritic materials and uses the reference temperature, Equation 9F.45 in API 579. The reference

temperature is determined using API 579 Table 9.2, the exemption curve designation, and the MYS. Note that use of this latter approach is restricted to two generic types of steels and a material cut-off of the toughness curve can be chosen.



The image shows a software interface for configuring API 579 fracture toughness. It includes a checked checkbox for 'API 579 fracture toughness', a dropdown menu for 'ASME exemption curve' set to 'A', and input fields for 'Specified minimum yield strength (SMYS)', 'Operating temperature (F)', and 'K1c (computed)'. Under 'API 579 fracture toughness definition', there are two checked options: 'Section 9F.4.2, lower bound fracture toughness' and 'Carbon steels' for the reference temperature. For the 'K1c curve' cutoff, 'Low sulfur carbon steels' is checked, while 'Unknown chemistry or high sulfur carbon steels' is unchecked.

**Figure 7.3-1. API 579 Fracture Toughness Checkbox in Material GUI (Default)**

Once the above choices are completed, the fracture toughness is computed and displayed in the GUI. This toughness value will then be used as the critical fracture toughness to determine the critical crack size in NASFLA as well as in determining the toughness ratio when using the FAD failure criteria in NASFLA and NASFAD.

## 8 RESIDUAL STRESS INPUT FOR NASGRO

### 8.1 General Capabilities

An option to superimpose a user-supplied static residual stress is available for many of the univariant and all the bivariant weight function SIF solutions in NASGRO. A detailed discussion of NASGRO residual stress capability is provided in Section 11.6 of Appendix C of the NASGRO reference manual.

Residual stresses can only be included in SIF solutions that utilize weight functions. In FFS assessments of pressure vessels, residual stresses are usually considered to exist in welds; however, residual stresses may also result from other manufacturing processes such as shot peening, laser shock peening, cold expansion of holes, forging, or machining processes. The static residual stress distribution must be defined by the user and is applied at each step in the stress history and is not affected by the spectrum scale factors. The user must obtain (by measurement or calculation) the residual stress fields outside of NASGRO and then input the results into NASGRO as an additional stress gradient.

Residual stress input follows the same general protocols as regular stress gradient input, although fewer options are available. Residual stress input can be provided in tabular or polynomial series form. For univariant stress intensity factor solutions, residual stresses can be entered directly from the keyboard into the GUI, entered from a file, or entered by specifying the coefficients of a sixth order polynomial as shown in Figure 8.1-1. For direct keyboard entry, the residual stress table has a blue-grey background to remind the user that this is the entry point for the static residual stress gradient, not the regular stress gradient, Figure 8.1-1(a). For file entry, the standard NASGRO file format for univariant stress gradients is applicable, Figure 8.1-1(b).

Crack plane stress definition from  
 Tension/bend  Polynomial  Tabular input

# of stress distributions:  1  2  3  4

Shakedown choice:  None  Automatic

Optimize point spacing  Include residual stress table  
 Include residual stress polynomial

Input stresses from file  Input full stress tensor

Display stress quantity:  
 S0  S1  S2  S3  RS

Tens./Comp stress gradients  
 t1/t2 stress gradients

X	Resid stress

(a) Keyboard Entry of Univariant Residual Stress Table

Crack plane stress definition from  
 Tension/bend  Polynomial  Tabular input

# of stress distributions:  1  2  3  4

Shakedown choice:  None  Automatic

Optimize point spacing  Include residual stress table  
 Include residual stress polynomial

Input stresses from file  Input full stress tensor

Display stress quantity:  
 S0  S1  S2  S3  RS

Tens./Comp stress gradients  
 t1/t2 stress gradients

RS file:

(b) File Entry of Univariant Residual Stress Table

Crack plane stress definition from  
 Tension/bend  Polynomial  Tabular input

# of stress distributions:  1  2  3  4

Shakedown choice:  None  Automatic

Optimize point spacing  Include residual stress table  
 Include residual stress polynomial

Input stresses from file  Input full stress tensor

Display stress quantity:  
 S0  S1  S2  S3  RS

Tens./Comp stress gradients  
 t1/t2 stress gradients

	Coef 0	Coef 1	Coef 2	Coef 3	Coef 4	Coef 5	Coef 6
RS							

(c) Keyboard Entry of Coefficients for Sixth Order Polynomial Univariant Residual Stress Equation

Figure 8.1-1. Residual Stress Input Options for Univariant Weight Function SIF Models

## 8.2 Input of Polynomial Residual Stress Distributions

Residual stress gradients are commonly characterized in the form of a polynomial function of normalized thickness ( $X = x/t$ , ranging from 0.0 to 1.0). Both API 579 and BS 7910 contain polynomial functions for through-thickness residual stress gradients for common weld geometries. In NASGRO, input of a univariant residual stress gradient (Figure 8.1-1(c)) in the form of a polynomial series requires specification of the coefficients of the following sixth order polynomial:

$$\sigma(X) = C_0 + C_1 X + C_2 X^2 + C_3 X^3 + C_4 X^4 + C_5 X^5 + C_6 X^6$$

Any of the coefficients  $C_i$  may be set equal to zero. For the univariant polynomial series residual stress input format, the ability to apply a scale factor to the entire polynomial is provided on the load blocks page, with the default scale factor equal to 1.0. A similar procedure is available for bivariate residual stress distributions and is described in Section 11.6 of Appendix C of the NASGRO reference manual.

## 8.3 Choosing API 579 Weld Residual Stress (WRS) Polynomial Inputs

To enable easier use of the commonly used API 579 equations for weld residual stresses, NASGRO has a new capability to simplify this process by providing the user the capability to choose from a menu of API 579 WRS equations (from Annex 9D) and not have to manually enter polynomial coefficients into the GUI.

The API 579 WRS polynomial equations are univariate and this option can only be used for NASGRO univariate WF solutions. An example of the GUI screen was given above in Figure 8.1-1(c) for a univariate WF case showing the checked box for including RS input in the form of a sixth order polynomial. Beginning with NASGRO v11.0, a new feature provides a button below the input grid for the polynomial coefficients for activating the option to select the API 579 WRS polynomial equations as shown in Figure 8.3-1.

This new option provides a button below the input grid for the polynomial coefficients for activating the option to select the API 579 WRS polynomial equations. This option is applicable to the cases when the crack plane stress is defined from remote (tension/bend) stresses or from tabular input. It is available in both the NASFLA and NASFAD modules of NASGRO.

Crack plane stress definition from

Tension, bend  Polynomial  Tabular input

# of stress distributions:  1  2  3  4

Shakedown choice:  None  Automatic

Optimize point spacing  Include residual stress table

Include residual stress polynomial

Input stresses from file

Plot stresses

	Coef 0	Coef 1	Coef 2	Coef 3	Coef 4	Coef 5	Coef 6
RS							

< >

Select WRS API 579 polynomial equation (not selected)

**Figure 8.3-1. GUI Layout for User to Specify Polynomial Coefficients with Button to Optionally Select API 579 WRS Polynomial Equation**

Clicking on the button to select the API 579 WRS polynomial equations activates a menu for the user to choose the desired equation. Figure 8.3-2 lists the section numbers, equation numbers and figure numbers from API 579 Annex 9D (2021 edition) along with specific details about the weld, crack location, heat input and material. The user must be familiar with Annex 9D to be able to choose the appropriate WRS equation for their application. Note that these WRS equations pertain only to ferritic steel and austenitic stainless steel welds. The equation selection is made by clicking on the row in the table and the row is then turned blue as shown. Only one equation is allowed to be selected.

Once the desired equation has been selected, the user needs to click on the “Use selected WRS equation” button at the bottom of the table. The GUI then returns to the NASFLA geometry screen as shown in Figure 11.6.4, displaying the polynomial coefficients and a description of the equation that has been selected as shown in Figure 8.3-3. A plot of the chosen WRS distribution can then be made using the Plot Stresses button. A scale factor can then be applied to the RS polynomial curve on the Load Blocks page. This scaling factor is frequently the yield stress.

API 579 WRS Equations Menu							
Post weld heat treatment:							
API 579 section	API 579 eqn num	API 579 fig num	Weld info	Crack location	Weld heat input	Materials	
9D.4.1	9D.3	none	PWHT	Perpendicular to weld			
9D.4.1	9D.4	none	PWHT	Parallel to weld			
Cylindrical shells:							
API 579 section	API 579 eqn num	API 579 fig num	Weld info	Crack location	Weld heat input	Materials	
9D.5.1	9D.7	9D.1	Full pen circumferential	Circumferential flaw, WRS perpendicular to weld	High	Ferritic and austenitic stainless steel welds	
9D.5.1	9D.8	9D.1	Full pen circumferential	Circumferential flaw, WRS perpendicular to weld	Medium	Ferritic steel welds	
9D.5.1	9D.9	9D.1	Full pen circumferential	Circumferential flaw, WRS perpendicular to weld	Low	Ferritic and medium/low heat austenitic stainless steel welds	
9D.5.2	9D.16-18	9D.1	Full pen circumferential	Longitudinal flaw, WRS parallel to weld		Thickness dependent	
9D.6.1	9D.22	9D.1	Full pen longitudinal	Longitudinal flaw, WRS perpendicular to weld			
9D.6.2	9D.25	9D.1	Full pen longitudinal	Longitudinal flaw, WRS parallel to weld			
Spheres and heads:							
API 579 section	API 579 eqn num	API 579 fig num	Weld info	Crack location	Weld heat input	Materials	
9D.7.1	9D.7	9D.6	Full pen circumferential	Circumferential flaw, WRS perpendicular to weld	High	Ferritic and austenitic stainless steel welds	
9D.7.1	9D.8	9D.6	Full pen circumferential	Circumferential flaw, WRS perpendicular to weld	Medium	Ferritic steel welds	
9D.7.1	9D.9	9D.6	Full pen circumferential	Circumferential flaw, WRS parallel to weld	Low	Ferritic and medium/low heat austenitic stainless steel welds	
9D.7.2	9D.16-18	9D.6	Full pen circumferential	Meridional flaw, WRS perpendicular to weld		Thickness dependent	
9D.8.1	9D.22	9D.6	Full pen meridional	Meridional flaw, WRS perpendicular to weld			
9D.8.2	9D.25	9D.6	Full pen meridional	Circumferential flaw, WRS parallel to weld			
Corner joints (nozzles):							
API 579 section	API 579 eqn num	API 579 fig num	Weld info	Crack location	Weld heat input	Materials	
9D.10.1	9D.28	9D.7.8	Full pen	WRS perpendicular to weld			
9D.10.2	9D.36	9D.7.8	Full pen	WRS parallel to weld			
Piping branch connections:							
API 579 section	API 579 eqn num	API 579 fig num	Weld info	Crack location	Weld heat input	Materials	
9D.10.4.1	9D.45	none	Full pen	WRS perpendicular to weld		Ferritic steel welds	
9D.10.4.1	9D.46	none	Full pen	WRS perpendicular to weld		Austenitic stainless steel welds	
9D.10.4.2	9D.47	none	Full pen	WRS parallel to weld		Ferritic steel welds	
9D.10.4.2	9D.48	none	Full pen	WRS parallel to weld		Austenitic stainless steel welds	
(Note: Green highlighting indicates thickness-dependent polynomial equations.)							
Clear equation selection					Use selected WRS equation		Cancel

Figure 8.3-2. GUI Display of API 579 WRS Polynomial Equation Menu

Crack plane stress definition from

Tension, bend  Polynomial  Tabular input

# of stress distributions:  1  2  3  4

Shakedown choice

None  Automatic

Optimize point spacing  Include residual stress table

Include residual stress polynomial

Input stresses from file

Plot stresses

	Coef 0	Coef 1	Coef 2	Coef 3	Coef 4	Coef 5	Coef 6
RS	1.00	-0.22	-3.06	1.88	0.00		

Select WRS API 579 polynomial equation (selected)

Section (9D.5.1) Full penetration circumferential welds in cylindrical shells

Equation (9D.7) Circumferential flaw; WRS perpendicular to weld  
High weld heat input; Ferritic and austenitic stainless steel welds

Clear selected WRS API 579 polynomial equation

Polynomial gradient direction:  (click to change)

**Figure 8.3-3. Residual Stress Polynomial Input Screen Showing Selection of an API 579 WRS Equation and the Polynomial Coefficients**

When selecting an API 579 WRS equation, the default is to have the gradient oriented in the direction (forward) such that the crack is at  $x/t$  equal to zero in the model. The “forward/reverse gradient” button is provided for the user to flip the gradient in case the defect is on the back side of the plate, or to align the defect initiation site with the gradient direction. The original “forward” coefficients are recalculated when changing to “reverse” and displayed in the cells and the reversed gradient can also be plotted.

## 9 BACKGROUND ON THE FAILURE ASSESSMENT DIAGRAM (FAD) CAPABILITY IN NASGRO

The NASFAD module in NASGRO is used to perform a fracture assessment using the FAD failure criteria given a crack size, material properties and applied stresses. The principal result of the analysis is a determination of whether or not the crack is in the “safe” area of the FAD (Point A) or in the “unsafe” area (Point B) as shown in Figure 2.5-1. The NASFAD analysis provides a plot of the FAD showing the assessment point ( $K_r, L_r$ ).

The NASFLA module in NASGRO is used to compute fatigue crack growth as a function of cyclically applied stresses using a FAD failure criterion. The NASFLA analysis provides a plot of the FAD showing the locus of the assessment points ( $K_r, L_r$ ) calculated as the crack grows to the limiting condition (point B) on the FAD, reaching a critical crack size determined by the FAD criterion.

### 9.1 Comparison of Basic FAD Approaches Used by NASGRO and API 579

The FAD approach has been developed and used by numerous organizations over the last few decades. In 2008, the European FITNET project [4] developed and published a specific implementation of the FAD approach which largely harmonizes various methods previously in use. The NASGRO implementation of FAD originally followed the FITNET approach, although not all FITNET FAD options were implemented in NASGRO. Beginning with NASGRO v8.2, the ASME FFS/API-579 failure assessment diagram methods were incorporated into NASGRO. The failure assessment diagram methods in NASGRO have been updated for the 2021 version of ASME FFS/API-579 [2]. Each of these approaches is described in the sections that follow, including a brief summary of their differences in the context of describing the ASME/API approach.

Table 9.1-1 provides a comparison of the differences between the FITNET-based and API 579 based FFS approaches that are contained in NASGRO. Extensive detail on both approaches is provided in Appendix X of the NASGRO reference manual and a number of key aspects of each are discussed here.

**Table 9.1-1. Differences Between FITNET-Based NASGRO FFS and API 579 ASME FFS**

	<b>FITNET-based NASGRO FFS</b>	<b>API/ASME FFS</b>
<b>Equation for <math>K_r</math> ratios</b>	$K_r = \frac{K_I^P}{K_c} + \frac{K_I^S}{K_c} + \rho$ <p>where <math>\rho</math> is the plasticity correction given by <math>\rho = \psi - \phi \cdot (K_I^S/K_{I,p}^S - 1)</math>. The stress intensity factors in the equations are defined as</p> <p><math>K_I^P</math>: SIF with primary load  <math>K_I^S</math>: SIF with secondary load  <math>K_{I,p}^S</math>: plastically-corrected SIF with secondary load</p> <p>and <math>\psi</math> and <math>\phi</math> are interpolated values from tables.</p>	$K_r = \frac{K_I^P}{K_c} + \frac{\Phi K_I^{SR}}{K_c}$ <p>where <math>\Phi</math> is the plasticity interaction factor determined through interpolation and depends on the API-579 edition. The SIFs in the equations are given by</p> <p><math>K_I^P</math>: SIF with primary load  <math>K_I^{SR}</math>: SIF with secondary load and residual stress  <math>K_{I,p}^{SR}</math>: plastically-corrected SIF with secondary load and residual stress</p>
<b>FALs used by FITNET Option 1 and ASME Level 3 Method A</b>	$f(L_r) = \begin{cases} \frac{0.3 + 0.7e^{-\mu L_r^6}}{\sqrt{1 + 0.5L_r^2}} & L_r \leq 1 \\ f(1) \cdot L_r^{\frac{N-1}{2N}} & 1 \leq L_r \leq L_r^{max} \\ 0 & L_r \geq L_r^{max} \end{cases}$ <p>where <math>\mu = \min(0.001 E/\sigma_y, 0.6)</math>, <math>N = 0.3 \cdot (1 - \sigma_y/\sigma_u)</math>, and <math>L_r^{max} = 0.5 \cdot (1 + \sigma_u/\sigma_y)</math> with <math>\sigma_u</math> is the ultimate strength.</p>	$f(L_r) = (1 - 0.14L_r^2) \cdot (0.3 + 0.7e^{-0.65L_r^6})$ <p>for <math>L_r \leq L_r^{max}</math>. The extent of <math>L_r^{max}</math> axis depends on the material. It's governed by the following.</p> <ol style="list-style-type: none"> <li><math>L_r^{max} = 1</math> for materials with yield point plateau (strain hardening exponent &gt; 15)</li> <li><math>L_r^{max} = 1.25</math> for ASTM A508</li> <li><math>L_r^{max} = 1.25</math> for C-Mn steels</li> <li><math>L_r^{max} = 1.80</math> for austenitic stainless steels</li> <li><math>L_r^{max} = \sigma_f/\sigma_y = 0.5 \cdot (1 + \sigma_u/\sigma_y)</math> for other materials where <math>\sigma_f</math> is the flow stress.</li> <li><math>L_r^{max} = 1</math> for unknown materials</li> </ol>
<b>FALs used by FITNET Option 3 and ASME Level 3 Method B</b>	$f(L_r) = \begin{cases} \left( \frac{E\varepsilon_r}{\sigma_r} + 0.5 \frac{L_r^2}{\frac{E\varepsilon_r}{\sigma_r}} \right)^{-0.5} & L_r \leq L_r^{max} \\ 0 & L_r > L_r^{max} \end{cases}$ <p>where <math>\sigma_r</math> and <math>\varepsilon_r</math> are true stress and strain and <math>L_r^{max} = 0.5 \cdot (1 + \sigma_u/\sigma_y)</math>. The relationship between <math>\sigma_r</math> and <math>\varepsilon_r</math> are governed by a Ramberg-Osgood type of equation with constants <math>\sigma_0</math>, <math>\varepsilon_0 = \sigma_0/E</math>, <math>\alpha</math>, and <math>\beta</math> being defined.</p> $\frac{\varepsilon_r}{\varepsilon_0} = \frac{\sigma_r}{\sigma_0} + \alpha \left( \frac{\sigma_r}{\sigma_0} \right)^\beta$	$f(L_r) = \begin{cases} \left( \frac{E\varepsilon_r}{L_r\sigma_y} + \frac{L_r^3\sigma_y}{2E\varepsilon_r} \right)^{-0.5} & L_r \leq L_r^{max} \\ 0 & L_r > L_r^{max} \\ 1 & L_r = 0 \end{cases}$ <p>where <math>L_r^{max}</math> is material-specific (see FAL for ASME Level 3 Method A). The true stress and strain curve is derived from discrete engineering stress and strain data pairs accurately defined at very fine ratios of applied stress to yield stress. In the ASME FFS specifications, the ratios are in terms of 0.1 intervals with more refinement near <math>\sigma_r/\sigma_y = 1</math>.</p>

### 9.1.1 Definition of $K_r$

Examination of the specifications of both FFS approaches shows that although both approaches are quite similar, there exist some subtle differences on the way failure assessment lines (FALs) are constructed and also on how the interaction between primary and secondary loads is defined. The latter is used to provide the plasticity correction in the definition of  $K_r$  ratios. The first row of Table 9.1-1 lists the definitions used in computing  $K_r$  for illustrating the differences of each approach. As evident in the side-by-side comparison the major difference comes from the definition of  $K_r$  ratios. Both FITNET and API 579 require the determination of a plasticity interaction or correction factor. Additional details (not included in the table) are the various definitions of quantities relating to plasticity interaction provided in Appendix X of the NASGRO reference manual.

### 9.1.2 Definition of $L_r$

In NASGRO, the computation of the load ratio,  $L_r$ , is essentially the same between the FITNET approach and the API 579 approach. It is the ratio of the total applied load that contributes to the primary stresses to the plastic limit load of the cracked structure. Or, alternatively, computed as the ratio of the reference stress to the yield stress. Only primary stresses are considered in computing the load ratio. Plastic limit load equations for each FAD-enabled SIF model in NASGRO are provided in Section 5 of Appendix of the NASGRO reference manual.

### 9.1.3 Computation of Failure Assessment Lines (FALs) Used in NASGRO

The FITNET and API 579 approaches in NASGRO each include two analysis methods that are used to define the FAL that incorporate progressively more detailed representations of material behavior. As shown in Table 9.1-1, the current NASGRO implementation incorporates FITNET Option 1 and Option 3 while the API 579 approach incorporates ASME Level 3 (Method A) and ASME Level 3 (Method B). These two options differ primarily in the definition of the FAL. For the approaches currently included in NASGRO, the FAL is dependent only on the tensile properties of the material through the relationship  $K_r = f(L_r)$ . In each approach, the FAL incorporates a cut-off at  $L_r = L_r^{\max}$ , which defines the plastic collapse limit of the structure. However, the definition of  $L_r^{\max}$  varies between approaches as shown in Table 9.1-1.

The simpler approaches shown in the second row of the table FITNET Option 1 and ASME Level 3 (Method A) only require the yield strength (and the modulus of elasticity for FITNET). Note that the API 579 ASME approach provide cut-offs for  $L_r^{\max}$  as a function of different material types. The default value for  $L_r^{\max}$  in NASGRO is 1.0.

The third row of Table 9.1-1 outlines the approaches in each case that use a more detailed representation of material behavior, specifically the true stress, true strain curve that models the elastic-plastic constitutive behavior of the material. In NASGRO, the Ramberg-Osgood equation is used to represent the true stress true strain curve. However, the NASGRO materials database does not contain parameters of the Ramberg-Osgood equation and the user needs to manually be entered the parameters on the NASFLA material page. An analysis tool to curve-fit tabular true stress-strain data to the Ramberg-Osgood equation is available in NASGRO and its operation is described in Section 6 of Appendix X of the NASGRO reference manual.

## 10 NASCCS INPUT SETUP

NASCCS is a relatively easy-to-use module for determining critical crack size. After NASCCS is launched, the geometric parameters are input in the geometry menu. For weight function cases, the load distributions are also input in the geometry menu. The mechanical properties such as the critical stress intensity and the critical stress, as well as stress scale factors, are specified in the CCS Options menu as shown in Figure 10.0-1. Also, the criterion for calculating critical crack size is specified in this menu.

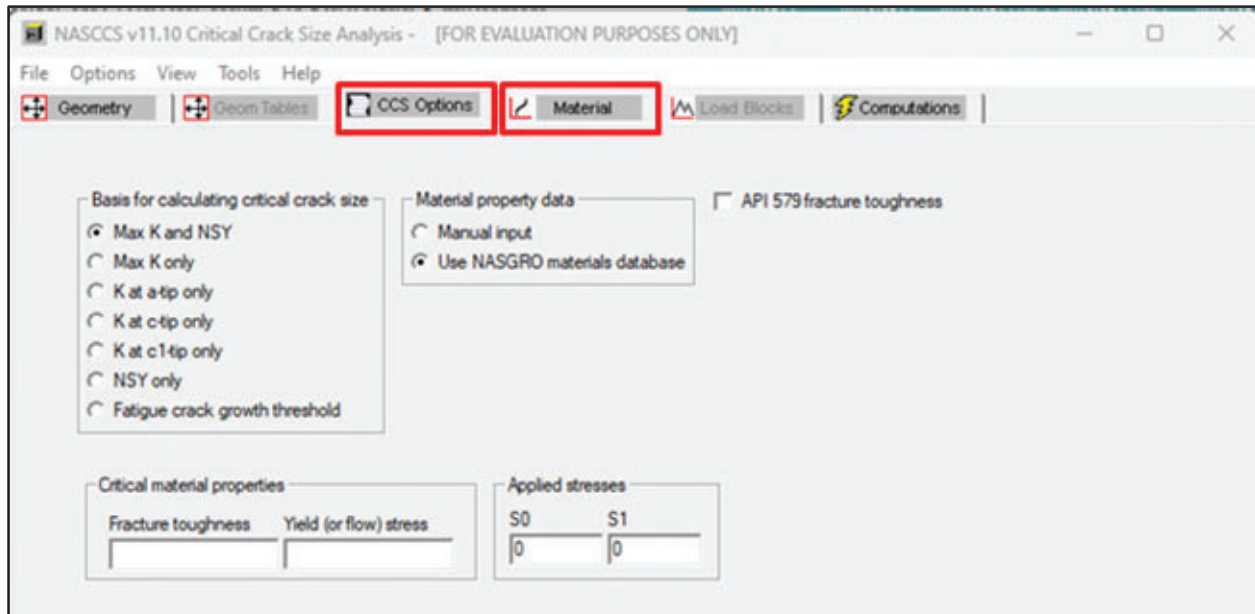


**Figure 10.0-1. NASCCS Input Options Screen**

In prior versions of NASGRO, the material property information in NASCCS required manual input and there was not any link to the NASGRO material database. Beginning with NASGRO v11.1, NASCCS now includes the capability to access the NASGRO (NASFLA) material database as an option. The manual input of material properties (from v11.0 and earlier) is the default and remains unchanged. In NASCCS for v11.1, the previously existing tab named “Output Options” has been removed and renamed “CCS Options” as shown in Figure 10-1. Clicking on the “Use NASGRO Material Database” provides access to a new Material tab and the material ID chooser similar to what exists in NASFLA. A checkbox is also provided to allow the use of API 579 fracture toughness values as was described in Section 7.3 for NASFLA and NASFAD.

Depending on the crack case, and the number of crack tips, a number of different options for calculating the critical crack size can be selected as the basis for determination from the list of radio buttons shown in the GUI. Additional detail describing these options is provided in Section 3.4 of the main NASGRO reference manual. Note that NASCCS *does not* use the failure assessment diagram as a criterion to determine critical crack size; that capability is provided in the NASFAD module discussed below.

## 11 NASFAD INPUT SETUP

The NASFAD module enables the NASGRO user to employ the Failure Assessment Diagram (FAD) approach for assessment of crack-like flaws. This module is somewhat analogous to the existing NASSIF and NASCCS modules in NASGRO, but in “FAD space.” No fatigue crack growth analysis is performed in the NASFAD module. (NASFLA has the capability to perform fatigue crack growth analyses and utilize the FAD as a failure criterion.)

The features of the NASFAD module share many of the capabilities contained in other NASGRO modules. These include geometry selection and definition, material selection, stress intensity factor and limit load calculation, and FAD plotting and output.

### 11.1 Objective

The primary objective of the NASFAD module is to provide the capability to compute and plot assessment points ( $L_r$ ,  $K_r$ ) for known (detected or assumed) crack sizes and graphically compare them to the FAD failure assessment line (FAL). Here  $K_r = K_{app}/K_{mat}$  = ratio of the applied stress intensity factor to the appropriate material fracture toughness value (such as  $K_{Ic}$  or  $K_{IIc}$ ), and  $L_r = P/P_L$  = ratio of the total applied load contributing to the primary stresses to the plastic limit load of the cracked structure.

The NASFAD module provides the following capabilities as options:

- Plot ( $L_r$ ,  $K_r$ ) assessment point(s) vs FAD failure assessment line
- Compute critical crack size (for a given load and material)
- Compute failure stress (for a given crack size and material)
- Use API 579 Level 3/Method A or B
- Use FITNET Option 1 or 3

### 11.2 Activation

The NASFAD module is activated from the main NASGRO opening screen (Figure 3-1) by clicking on the NASFAD button. This, in turn, displays a set of tabs in the GUI similar to other NASGRO modules for choosing the crack geometry and material (Figure 11.2-1). The key difference from the other NASGRO modules is the “FAD Options” tab, which initially appears grayed-out.



Figure 11.2-1. Initial NASFAD GUI Analysis Tabs

### 11.3 Crack Case Selection

The crack case selection process for NASFAD is identical to that used in all the other NASGRO modules. However, the only crack cases that are available are those crack cases that are FAD-enabled, as listed in Section 4.2. As is true for NASSIF, the crack size (depth, aspect ratio) is not specified on the geometry screen for NASFAD. Additionally, a number of the FAD-enabled crack cases (TC11, SC30, SC31, EC04 and EC05) require specification of the crack center offsets (B, or  $B_t$  and  $B_w$ ). For NASFAD, the specification of the offset parameter(s) for these crack cases is not shown on the geometry screen but occurs on the FAD Analysis Options screen as discussed in Section 11.5.1.

### 11.4 Material Selection

NASFAD allows the user to choose a material from the NASGRO material database in a similar manner as is done in NASFLA. However, since NASFAD does not perform crack growth calculations, only the material data necessary to perform a FAD assessment are displayed, as shown in Figure 11.4-1. Similar to the material screen in NASFLA, the FAD failure criteria options are displayed on the left-hand side of the screen. The options for toughness values at different crack tips used in the analysis are also available. Also, if desired, the analyst can check the box to use an API 579 toughness; this option is shown in Figure 11.4-1.

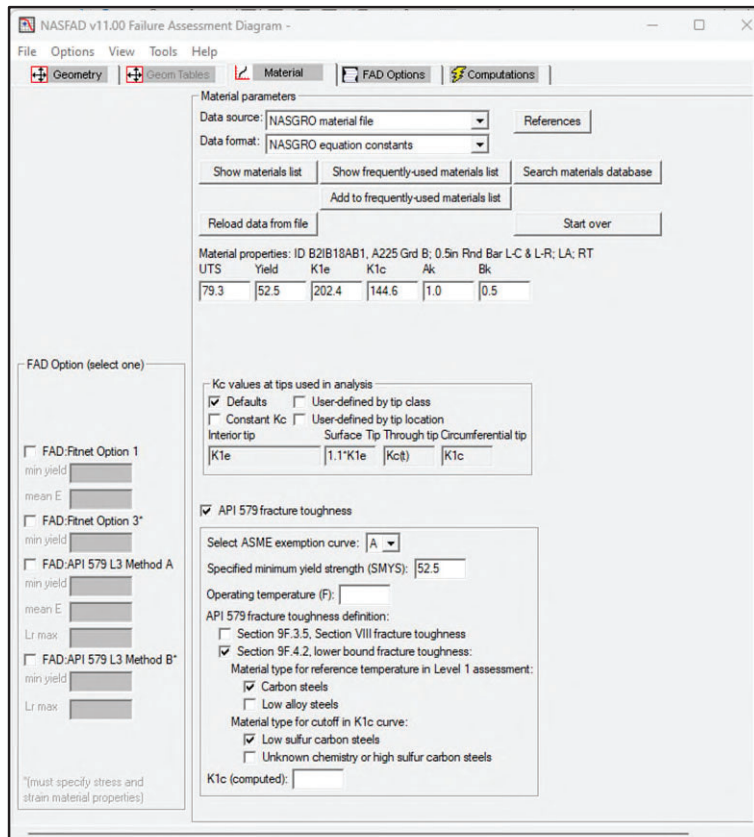


Figure 11.4-1. NASFAD Material Screen

## 11.5 NASFAD Options

Once the geometry and material are chosen and defined, the “FAD Options” tab becomes active and the user can supply crack size information and applied stresses for use in the FAD assessment. The FAD analysis options box is displayed in the upper right corner of the “FAD Analysis Options” screen with radio buttons provided to choose between three options; see Figures 11.5-1, 11.5-2 and 11.5-3. The first option allows the user to plot  $(L_r, K_r)$  assessment point(s) versus the FAL; this option is referred to as the “standard” FAD assessment. It allows the user to assess whether a crack (or a set of cracks) is within the “safe” or “unsafe” side of the FAL. The second option allows the user to compute a critical crack size using the FAD failure criteria. The third option computes a failure stress using the FAD criterion for a given crack size and material choice.

The lower portion of the NASFAD options screen provides input tools for the user to enter (multiple) crack sizes, shapes and offsets for the crack case that has been selected on the Geometry page. Consequently, what is displayed here is a function of the individual crack case chosen. This display and its functionality are intended to be nearly identical to the process for specification of crack sizes used in NASSIF. The notable additions are boxes that require the user to input the crack center offset locations (B, or Bt and Bw) for crack cases that require this input parameter(s).

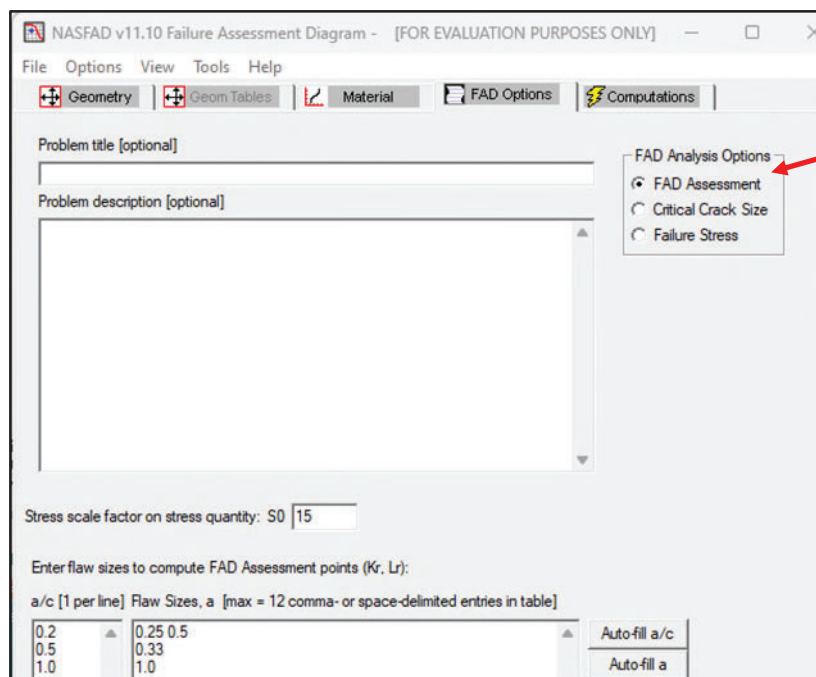


Figure 11.5-1. NASFAD Options Screen (FAD Assessment Option)

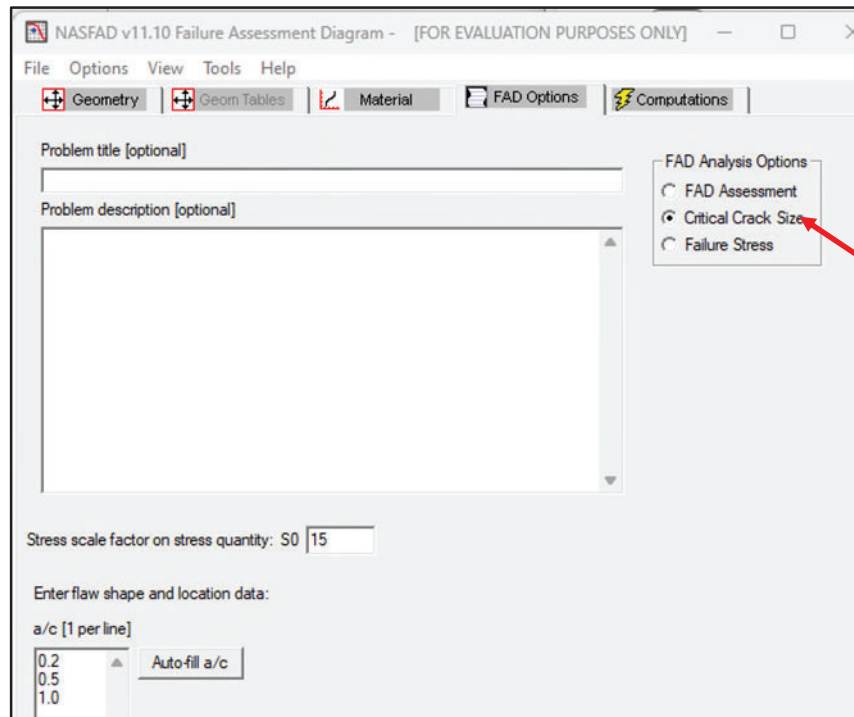


Figure 11.5-2. NASFAD Options Screen (Critical Crack Size Option)

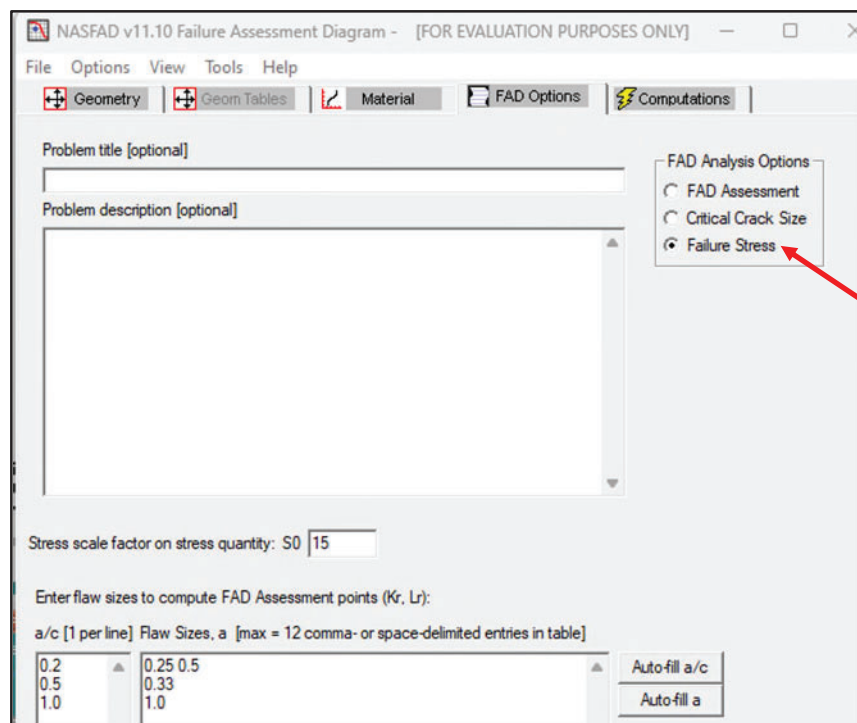


Figure 11.5-3. NASFAD Options Screen (Failure Stress Option)

### 11.5.1 FAD Assessment Option

Once the flaw sizes and stresses are specified as shown in Figures 11.5-1 to 3, the “Computations” tab can be clicked to run the FAD analysis. For the standard FAD assessment option, NASFAD generates an *out2* file that contains geometry information for each input crack for the crack case being considered. Each crack analyzed has a separate line in the *out2* file and the number of columns depends on the crack case being analyzed (*i.e.*, the number of crack tips from one to four). Each crack analyzed is automatically given a crack number or label by NASFAD for reference when plotting on the FAD.

Figure 11.5.1-1 provides an example of the NASFAD output screen for the “FAD Assessment” option. This example shows the printed NASFAD results for two different axial surface cracks on the inside of a pressurized cylinder (SC04) listing the calculated FAD assessment point values ( $L_r$ ,  $K_r$ ) for each crack tip ( $a$  and  $c$ ).

Crack Number	Crack Sizes		STATUS	ASME3MA: $L_r$ vs $K_r$ @ Applied		
	$a$	$c$		A: $L_r$	A: $K_r(a)$	A: $K_r(c)$
1	0.2500	1.2500	DONE	0.7655	0.2388	0.1233
2	0.5000	2.5000	DONE	0.9296	0.3542	0.1851

Figure 11.5.1-1. NASFAD Results in the Output Screen for “FAD Assessment” Option

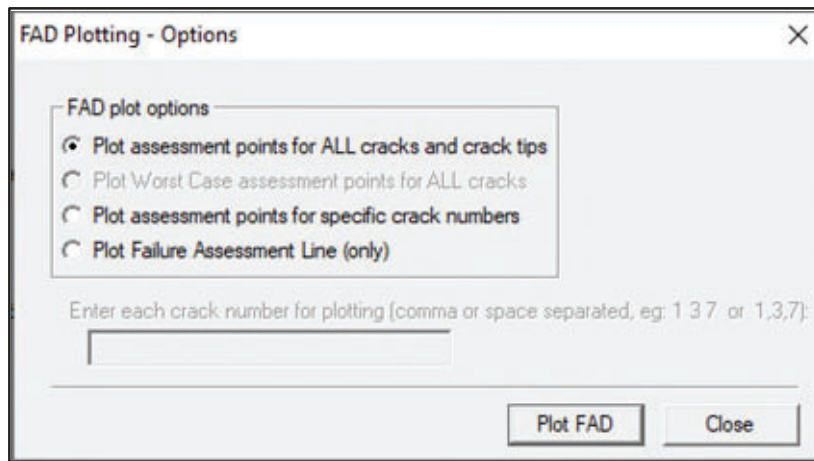
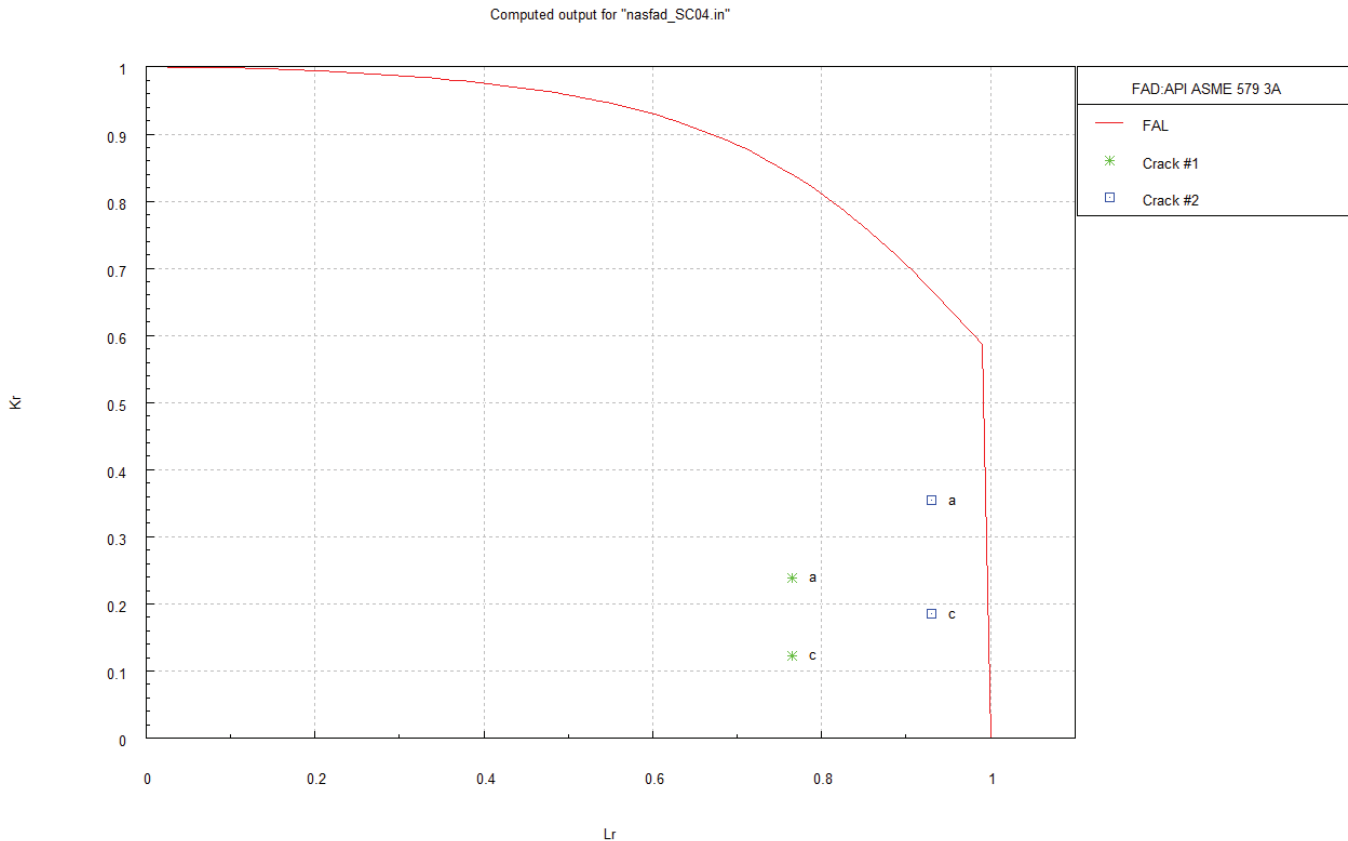


Figure 11.5.1-2. NASFAD Plotting Options Screen

A plot of the FAD is available from the Computations screen by clicking on the “Plot FAD” button. (The data to be plotted is obtained from the *out2* file.) This button provides the user a number of plotting options, as listed in Figure 11.5.1-2. In the list of plotting choices shown in Figure 11.5-2, an “assessment point” is the pair of calculated values ( $L_r$ ,  $K_r$ ) computed for each crack tip of each crack. Depending on the crack case being analyzed, there could be from one to four assessment points available. The first option allows the user to plot the assessment point for all tips and all cracks. (The second option is planned, but not yet available and is grayed-out.) The

third option allows the user to select a specific number of cracks for which to plot the assessment points. The cracks are automatically numbered in the *out2* file as described above. For the first three options, the FAL is also plotted. The last option allows the user to plot only the FAL for this geometry and material.

Using the NASFAD plotting options screen, these results can be plotted using the first plotting option above as shown in Figure 11.5.1-3. Alternatively, the third option can be used to request results for only these two cracks from a larger group. In this notional example, the second crack is closer to the FAL and would be considered more severe.



**Figure 11.5.1-3. NASFAD Results Plotted from the GUI for the “FAD Assessment” Option**

### 11.5.2 Critical Crack Size Option

For the critical crack size calculation option, the main difference on the NASFAD Options screen is that there is an input for crack shape but not crack size. Compare Figures 11.5-1 and 11.5-2. Once the flaw shapes and stresses are specified, the “Computations” tab can be clicked to run the FAD analysis (see Figure 11.5-2). The output can be displayed by the NASFAD GUI output screen in similar fashion to the FAD Assessment option, and the *out1* file contains the NASGRO header information, problem title, an echo of the crack case and loading information, the FAD method used and material ID and properties information. For the critical crack size FAD assessment option, the *out1* file also contains the results of the iteration and convergence to the critical crack sizes.

NASFAD generates an *out2* file that contains geometry information for each input crack for the crack case being considered. Each crack analyzed has a separate line in the *out2* file and the number of columns depends on the crack case being analyzed (*i.e.*, the number of crack tips from one to four). Each crack analyzed is automatically given a crack number or label by NASFAD for reference when plotting on the FAD.

A plot of the FAD is available from the Computations screen by clicking on the “Plot FAD” button. (The data to be plotted is obtained from the *out2* file.) This button provides the user a number of plotting options, as was shown in Figure 11.5.1-2. The functionality is identical to that described above for the FAD Assessment option.

As an example, Figure 11.5.2-1 shows the NASFAD critical crack size results for three different axial surface cracks (three different aspect ratios, *a/c*) on the inside of a pressurized cylinder (SC04) listing the calculated FAD assessment point values ( $L_r$ ,  $K_r$ ) for each critical crack tip (*a* and *c*). Using the NASFAD plotting options screen, these results can be plotted with the first plotting option above as shown in Figure 11.5.2-2. Since the calculated FAD assessment point values ( $L_r$ ,  $K_r$ ) were determined for critical crack sizes, they fall precisely on the FAL.

###Crack case being analyzed: SC04							
Number	a	c	a/c	A:Lr	A:Kr(a)	A:Kr(c)	
1	0.5791524E+00	0.2895762E+01	0.2000000E+00	1.000	0.3894		x
2	0.8230245E+00	0.1646049E+01	0.5000000E+00	1.000	0.3682		x
3	0.1148350E+01	0.1148350E+01	0.1000000E+01	1.000	0.3101		x

**Figure 11.5.2-1. NASFAD Critical Crack Size Results Displayed in the Computations Screen**

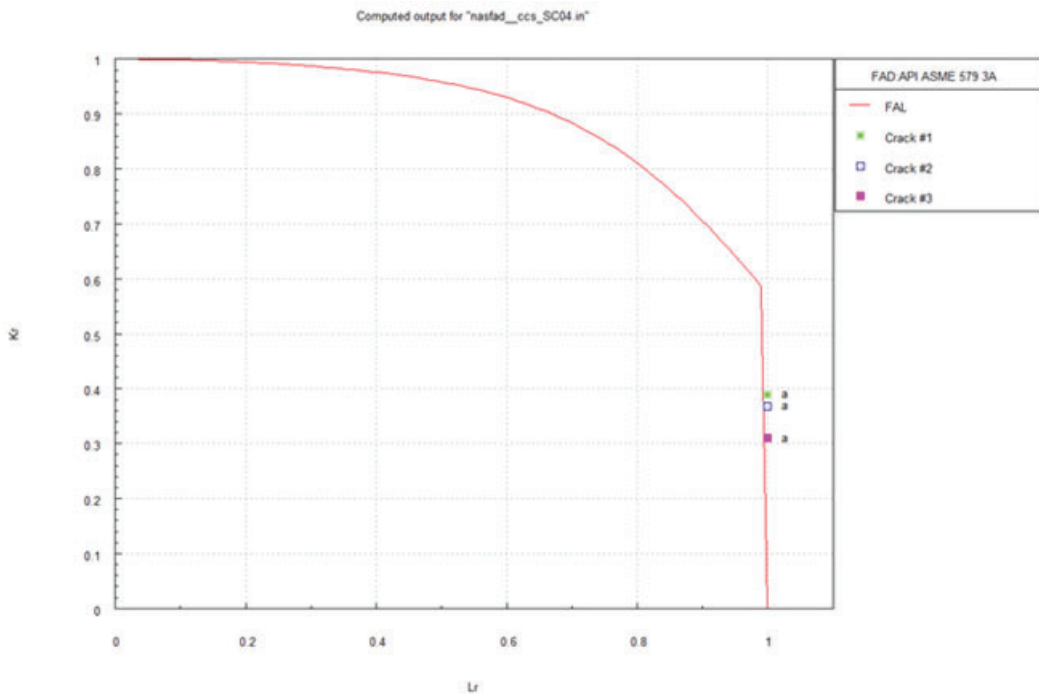


**Figure 11.5.2-2. NASFAD Results Plotted from the GUI for the “Critical Crack Size” Option**

### 11.5.3 Failure Stress Option

For the failure stress calculation option, similar to the FAD assessment option, there is an input for crack shape and crack size as shown in Figure 11.5-3. Note, however, that specific values of stresses are not specified. Stresses should be input in normalized (tabular) form on the geometry screen or with unit scale factors on the FAD Options screen.

The option to compute the failure stress for a given crack size/shape and material in NASFAD computes the assessment point for a given crack size that lies on the FAL and then back-solves for the stress that would produce this critical point,  $(L_r, K_r)_{\text{critical}}$ . The  $(L_r, K_r)_{\text{critical}}$  point is found by computing the intersection of the FAL curve with a curve defined by a number of  $(L_r, K_r)$  points in FAD space. These points are computed for a number of different applied stress levels and the curve must go through  $(0, 0)$ . The numerical method to compute the intersection of these two curves was developed and implemented for NASFAD in NASGRO v10.0. Once the  $(L_r, K_r)_{\text{critical}}$  point is determined, the applied stress corresponding to the critical point can be back-calculated.

Once the flaw shapes and sizes are specified, the “Computations” tab can be clicked to run the FAD analysis. The output is displayed by the NASFAD GUI output screen and the *out1* file contains the NASGRO header information, problem title, an echo of the crack case and loading information, the FAD method used and material ID and properties information. For the FAD failure stress option, the *out1* file also contains the results of the iteration and convergence to the failure stress. NASFAD generates an *out2* file that contains geometry information for each input crack for the crack case being considered. Each crack analyzed has a separate line in the *out2* file and the number of columns depends on the crack case being analyzed (*i.e.*, the number of crack

tips from one to four). There is no plotting output for the NASFAD failure stress option; the output is simply the failure stress value (or stress scale factor, SSF) for the specified crack size and shape.

As an example, Figure 11.5.3-1 shows the NASFAD failure stress results for two different axial surface cracks (two different aspect ratios,  $a/c$ ) on the inside of a pressurized cylinder (SC04) listing the calculated FAD assessment point values ( $L_r$ ,  $K_r$ ) and the corresponding failure load.

```
[FINAL RESULT]: minimal SSF gathered from all tips = 0.14809E+02 with tip location = a-tip
a = 0.25000E+00, c = 0.50000E+00, a/c = 0.50000E+00
Failure loads: S0 = 0.14809E+02
(Lr,Kr) from ASME L3MA = ( 0.100E+01, 0.245E+00)
```

```
[FINAL RESULT]: minimal SSF gathered from all tips = 0.15852E+02 with tip location = a-tip
a = 0.25000E+00, c = 0.25000E+00, a/c = 0.10000E+01
Failure loads: S0 = 0.15852E+02
(Lr,Kr) from ASME L3MA = ( 0.100E+01, 0.193E+00)
```

**Figure 11.5.3-1. NASFAD Failure Stress Results Displayed in the Computations Screen**

## 12 NASFLA INPUT SETUP

NASFLA is the primary module in NASGRO and is used to perform fatigue crack growth calculations (remaining life). It is activated by clicking on the NASFLA button on the opening screen (Figure 3.0-1). Previous sections of this report have described the choices available for specifying the geometry of the crack case and the material properties. The same process is used for NASFLA as for NASCCS and NASFAD. NASFLA will propagate an initial crack subject to a specified cyclic loading (stress spectrum) until the critical crack size is reached and failure occurs. Therefore, a key input for a NASFLA analysis is the initial flaw size that is specified on the geometry screen for the crack case being analyzed (crack depth and aspect ratio). Failure in NASFLA can occur by a number of criteria: failure by fracture, failure by net section yielding, or failure by the FAD criterion, depending on choices made on the material screen.

In NASFLA, once the geometry and materials screens have been completed, clicking on the Load Blocks tab lets the analyst specify the cyclic loadings (stresses) for the crack growth analysis as shown in Figure 12.0-1. For this example, the simple (manual) cycles and stress input is used in Figure 12.0-1 where the step containing 100 tension cycles from zero to 20.0 ksi will be repeated over and over until final failure occurs. Note that the scale factors for each stress component default to zero and must be manually entered by the user (in this case a scale factor of one was entered for S0). For complicated stress spectra, the use of the NASGRO “long block” format is recommended. It facilitates stress history inputs via a data file. A complete description of the many NASFLA options for specifying stress spectra for crack growth analysis is provided in Section 2.2.7 of the NASGRO Reference Manual [1].

The Build Schedule tab is then used to specify how many times to repeat the steps (block) shown in Figure 12.0-2. In this simple example, the block of 100 steps is shown to be repeated 1000 times. Next, the Output Options tab can be used to customize the output (frequency of printing results). Figure 12.0-3 shows the Output Options screen illustrating the default choices used by NASFLA. The default is to print the output at the end of every schedule and at the end of every block. Alternatively, the analyst can request output by a specified crack growth interval. In some cases, specifying a small crack growth interval for results output can help in understanding the results of the analyses, particularly when crack shape transitions occur. None of these output interval settings have any effect on the calculated crack growth rates and lifetimes. However, recognize that specifying a very small crack growth output interval will produce a larger output file, but this level of detail may be desired.

Finally, the Computations tab must be clicked and the “Run” button selected to perform the crack growth calculations as shown in Figure 12.0-4. The default input filename saved for a NASFLA analysis is *nasfla.in* and this can be changed by the user since the Run button originally appears as “Save+Run”. A summary of the analysis results is then displayed in the center of the screen.

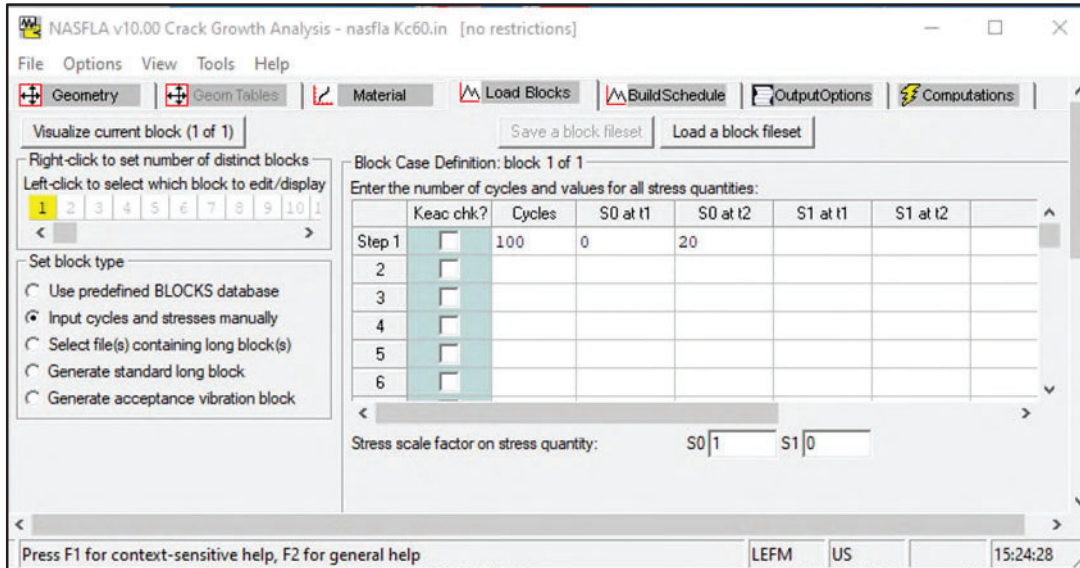


**Figure 12.0-1. Manual Input of Membrane Tension Stress, S0, on the NASFLA Load Blocks Screen with S0(min) = 0.0 and S0(max) = 20.0 ksi**

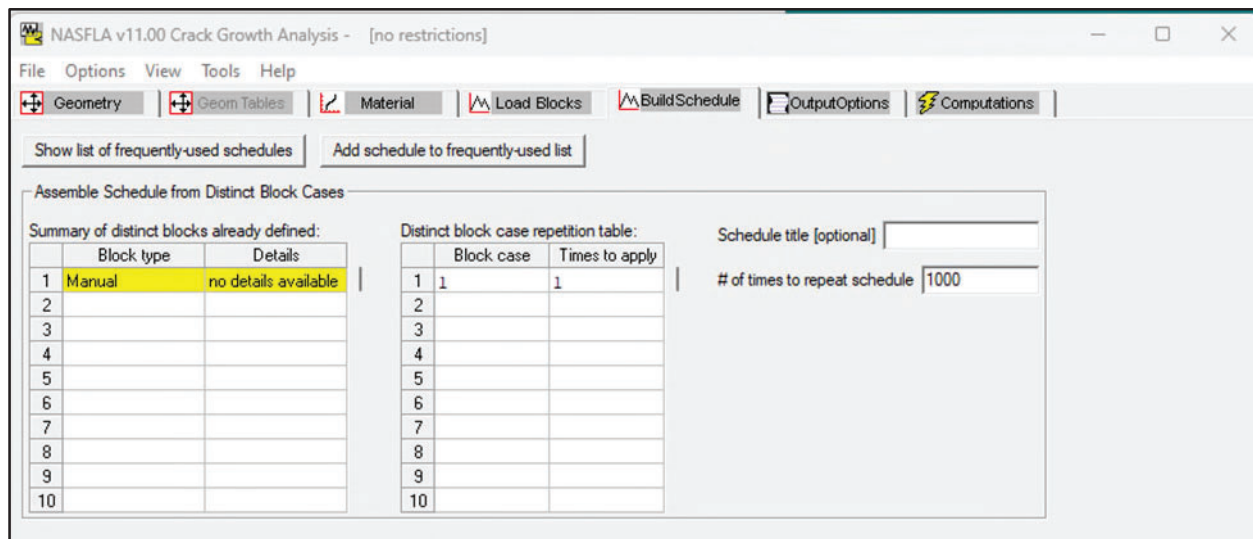


**Figure 12.0-2. Manual Input of Membrane Tension Stress, S0, on the NASFLA Load Blocks Screen with S0(min) = 0.0 and S0(max) = 20.0 ksi**

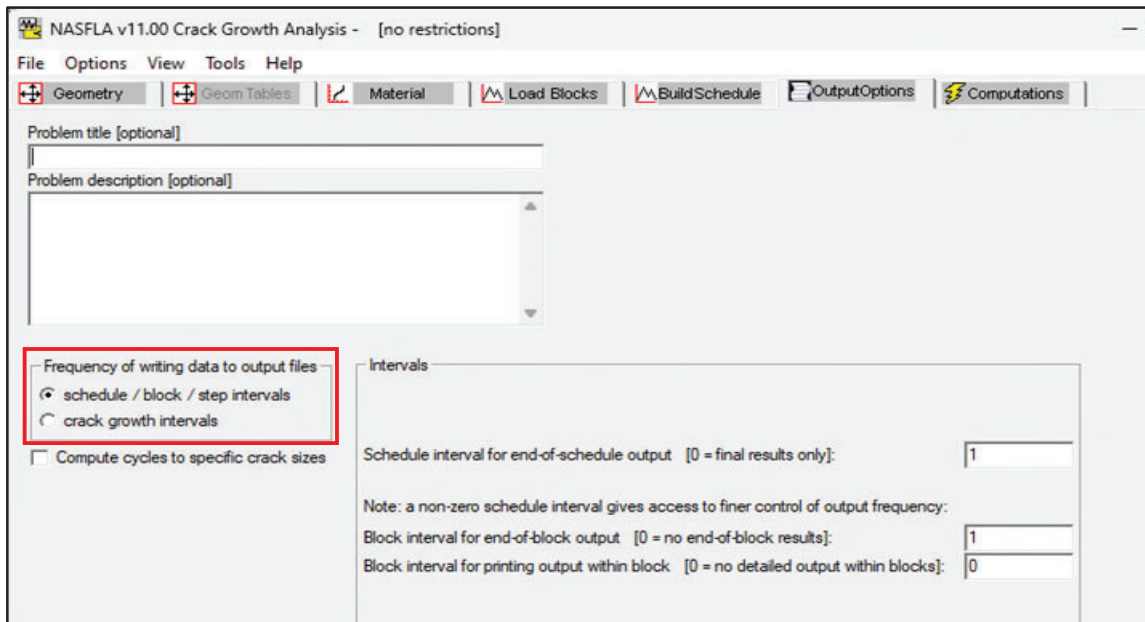


Figure 12.0-3. NASFLA Output Options Screen Showing Default Choices

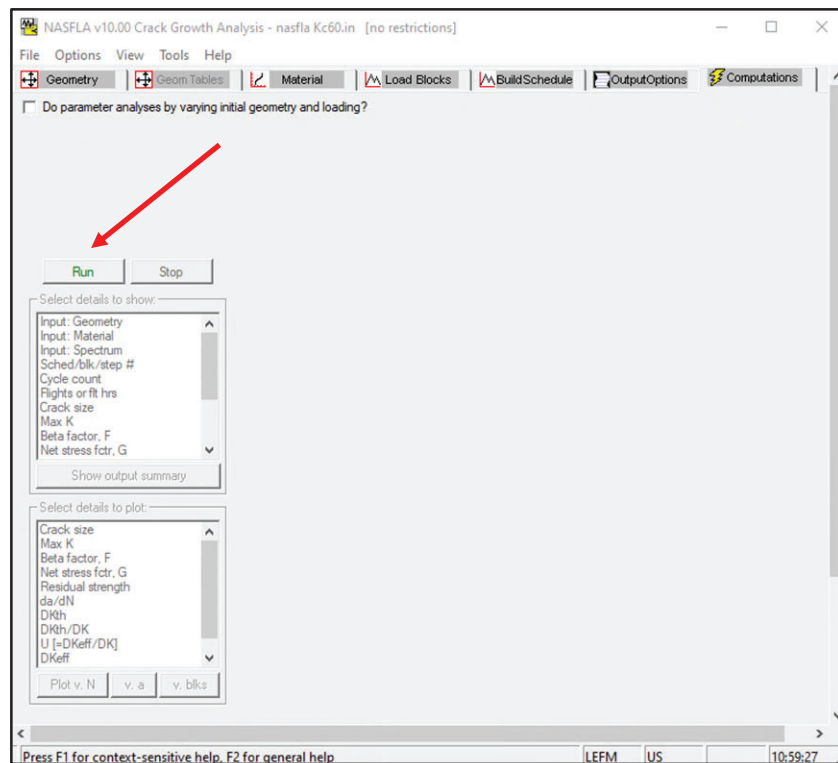


Figure 12.0-4. NASFLA Computations Screen Showing Run Button

## 12.1 NASFLA Output

The summary of the analysis results displayed in the center of the screen is very brief and primarily lists how the analysis terminated, the number of steps, blocks and cycles to that point, and the final crack sizes. Messages printed at the end of the calculation may include any of the following:

- Critical crack size has not been reached
- Unstable crack growth, max stress intensity exceeds critical value
- Net-section stress exceeds flow stress
- Computed FAD parameters (only if a FAD failure criterion is used)
- All stress intensities are below the fatigue threshold

The “Select details to show” GUI tool can be used to display text results for quantities listed in that window. Similarly, the “Select details to plot” GUI tool can be used to plot any of the quantities listed in that window. If the crack growth analysis was performed using a FAD failure criterion, then a “Plot FAD” button will appear below the “Select details to show” window.

In addition to being displayed on the screen, the NASFLA output is saved by default in text files named *nasfla.out1* and *nasfla.out2*. The *out1* file provides an echo of the input data for the analysis and the summary of results discussed above, including information on any crack shape transitions that may have occurred. The *out2* can be very large depending on the type of problem being analyzed and contains a list of all calculated quantities as a function of steps, cycles and crack size. It can be loaded into a spreadsheet from the GUI.

If a FAD failure criterion is chosen, the computed FAD parameters ( $K_r$ ,  $L_r$ ) as a function of crack size and cycles for each crack tip are also listed in the *out2* file. The data for the FAD are output in separate text files with extensions *l3ma* (for ASME/API 579 Level 3 Method A) or *l3mb* (for ASME/API 579 Level 3 Method B).

## 13 REPRESENTATIVE EXAMPLES

Four representative example analyses are presented in this section and are intended to illustrate the use of NASGRO for different FFS analyses of “real-world” pressure vessel applications. While these examples considered typical pressure vessel geometries and materials, they should only be treated as “notional” demonstrations of the NASGRO software capabilities and features. A brief description of each analysis is presented below, indicating the key NASGRO features that were used. All of the analyses used the API 579 Level 3, Method A, FAD failure criterion.

### *Section 13.1, LPV Outer Layer Surface Crack:*

- NASFLA crack growth analyses
- Axially oriented surface crack SIF (SC30)
- NASFLA AOS 1146a fatigue crack growth tabular data (E2FD12AB01)
- Two analyses using:
  - AOS 1146a material database toughness
  - API 579 lower bound toughness

### *Section 13.2, Nozzle Corner Crack*

- NASFLA crack growth analyses
- Two analyses using:
  - Nozzle corner crack SIF (CC27, API 579 KNCC1)
  - Nozzle corner crack weight function SIF (CC28)
- API 579 Barsom Paris equation for ferritic-pearlite steel
- API 579 lower bound toughness

### *Section 13.3, Internal Circumferential Surface Crack in a Pipe with Weld Residual Stress*

- Two NASFLA crack growth analyses (SC34)
- INSPECT crack growth analysis (KSCCE1)
- API 579 weld residual stress polynomial equation 9D.9
- Two NASFLA analyses using:
  - NASFLA A-106 Gr B steel tabular data (B1BB16AB01)
  - API 579 upper bound welded joint Paris equation
- INSPECT analysis using API 579 upper bound welded joint Paris equation
- API 579 lower bound toughness

### *Section 13.4, FAD Analysis of Embedded Cracks in a Sphere*

- FAD assessments for two cracks using:
  - NASFAD and weight function SIF EC05
  - INSPECT using API 579 SIF KSECCE
- API 579 lower bound toughness
- API 579 weld residual stress polynomial equation 9D7.1

### 13.1 LPV Outer Layer Surface Crack

This example considers an axially oriented shallow surface crack located in the base metal of the outer layer of a layered pressure vessel (LPV). The crack growth analyses were performed using the NASGRO surface crack in a plate weight function model SC30. The use of the surface crack in a plate model is appropriate because of the large diameter of the LPV. The applied membrane (tension) stress cycled from a minimum of 3.05 ksi to a maximum of 30.5 ksi and was uniform through the thickness of the plate.

The crack was assumed to be located in the center of a very wide plate (width,  $W = 50$  inches) having a thickness,  $t$ , of 0.269 inches. The initial crack depth was 0.20 inches and an aspect ratio ( $a/c$ ) of 0.3 was used, giving an initial half-surface crack length,  $c$ , of 0.6667 inches. Figure 13.1-1 shows the NASFLA input screen for this SC30 geometry.

The material model for this analysis was based on test data obtained at MSFC for the AOS 1146a wrapper steel [6]. In NASFLA, these data are represented by a 2-D table of  $da/dN$  vs  $\Delta K$  data with the material ID code E2FD12AB01. Figure 13.1-2 shows the NASFLA input screen for this material choice.

Two different crack growth analyses were performed. The first analysis used the fracture toughness contained in the NASFLA material database for the wrapper steel obtained in testing at MSFC (66.8 ksi $\sqrt{\text{in}}$ ). The second analysis used a lower bound toughness value calculated using the methodology specified by API 579 (see Section 7.3 of this report) at a temperature of 32°F. The GUI screen for computing the API lower bound toughness is shown in Figure 13.1-3 and results in a toughness of 40.1 ksi $\sqrt{\text{in}}$ . In each analysis, The API 579 Level 3 Method A FAD failure criterion is used, and the net section stress failure criterion is not used (as shown in Figures 13.1-2 and 13.1-3).

The crack growth curves and FAD for the analysis using the NASFLA database properties for the AOS wrapper steel are shown in Figures 13.1-4 and 5, respectively. The surface crack transitions to a through-thickness crack after 3,540 cycles when the crack depth reaches 95 percent of the thickness (0.256 inches). Since the SIF after transition is less than the fracture toughness of 66.8 ksi $\sqrt{\text{in}}$ , the crack then continues to grow as a through-crack (TC11) for an additional 8,848 cycles eventually failing by exceeding the FAD criterion at a total life of 12,388 cycles. The final crack size ( $2c$ ) is 2.88 inches. The FAD parameters ( $L_r$ ,  $K_r$ ) at failure were 0.42 and 0.97.

The second analysis was performed using the lower bound API 579 fracture toughness as computed in Figure 13.1-3. The crack growth curve for this analysis is identical to that for the first analysis up until the transition to a through crack at 3,450 cycles. However, in this case due to the much lower toughness (40.1 vs 66.8 ksi $\sqrt{\text{in}}$ ), the crack fails immediately after transition to a through crack with a computed  $K$  at failure of 45.18 ksi $\sqrt{\text{in}}$ . The final crack size ( $2c$ ) is 1.40 inches. The FAD parameters ( $L_r$ ,  $K_r$ ) at failure were 0.41 and 0.97 (Figure 13.1-6).

It is clear that using the API 579 lower bound toughness provides a much more conservative result when compared to the NASGRO material library toughness value for this wrapper steel material. This is not a surprising result given the large difference between the two fracture toughness values.

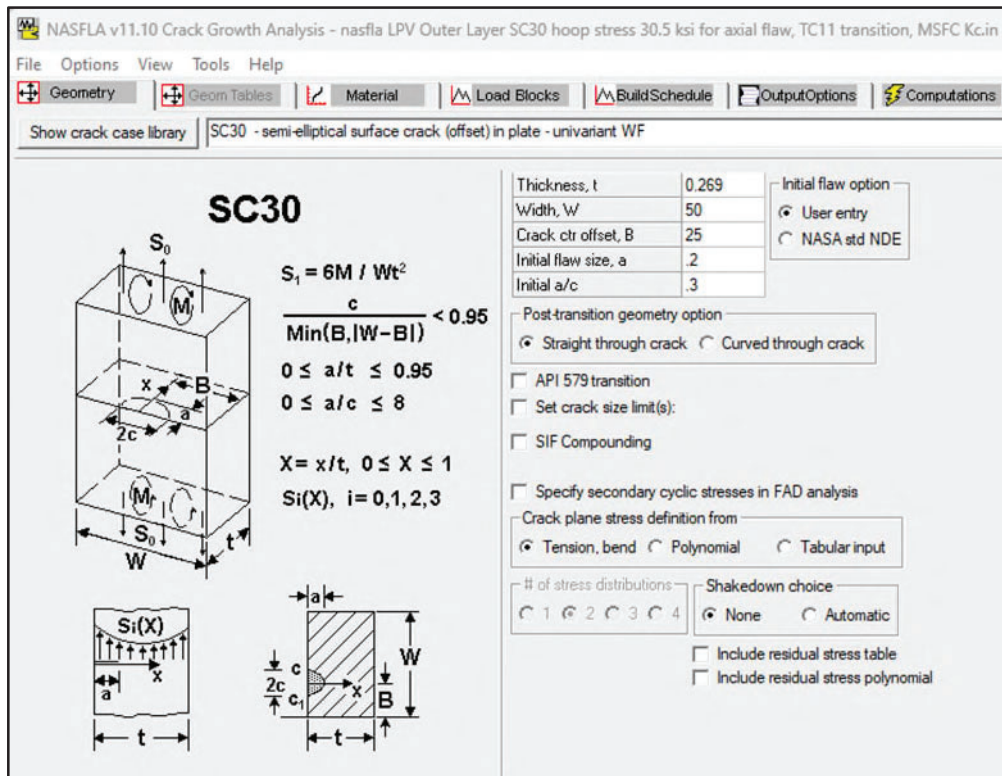


Figure 13.1-1. NASFLA Geometry Input Screen for Surface Crack in Plate (SC30)

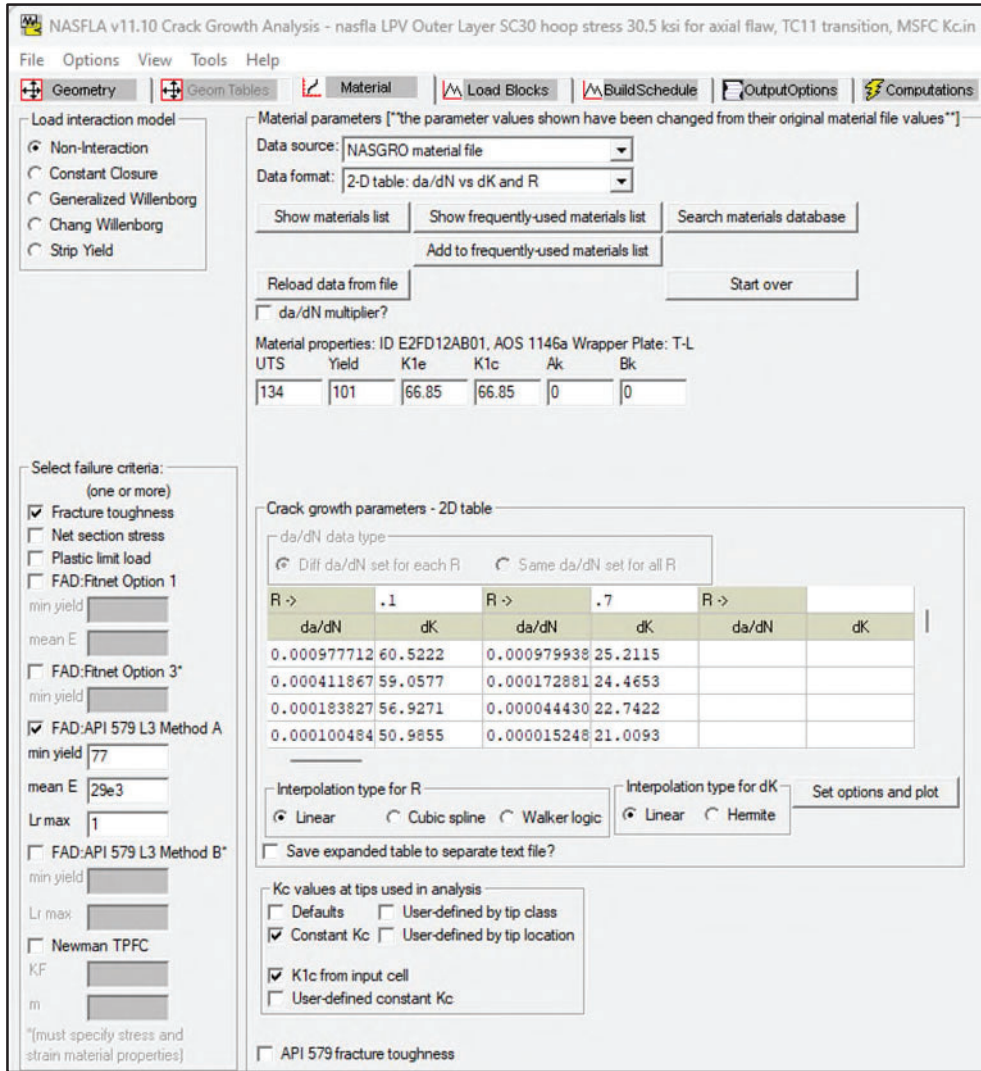


Figure 13.1-2. NASFLA Material Input Screen for AOS 1146a Wrapper Plate

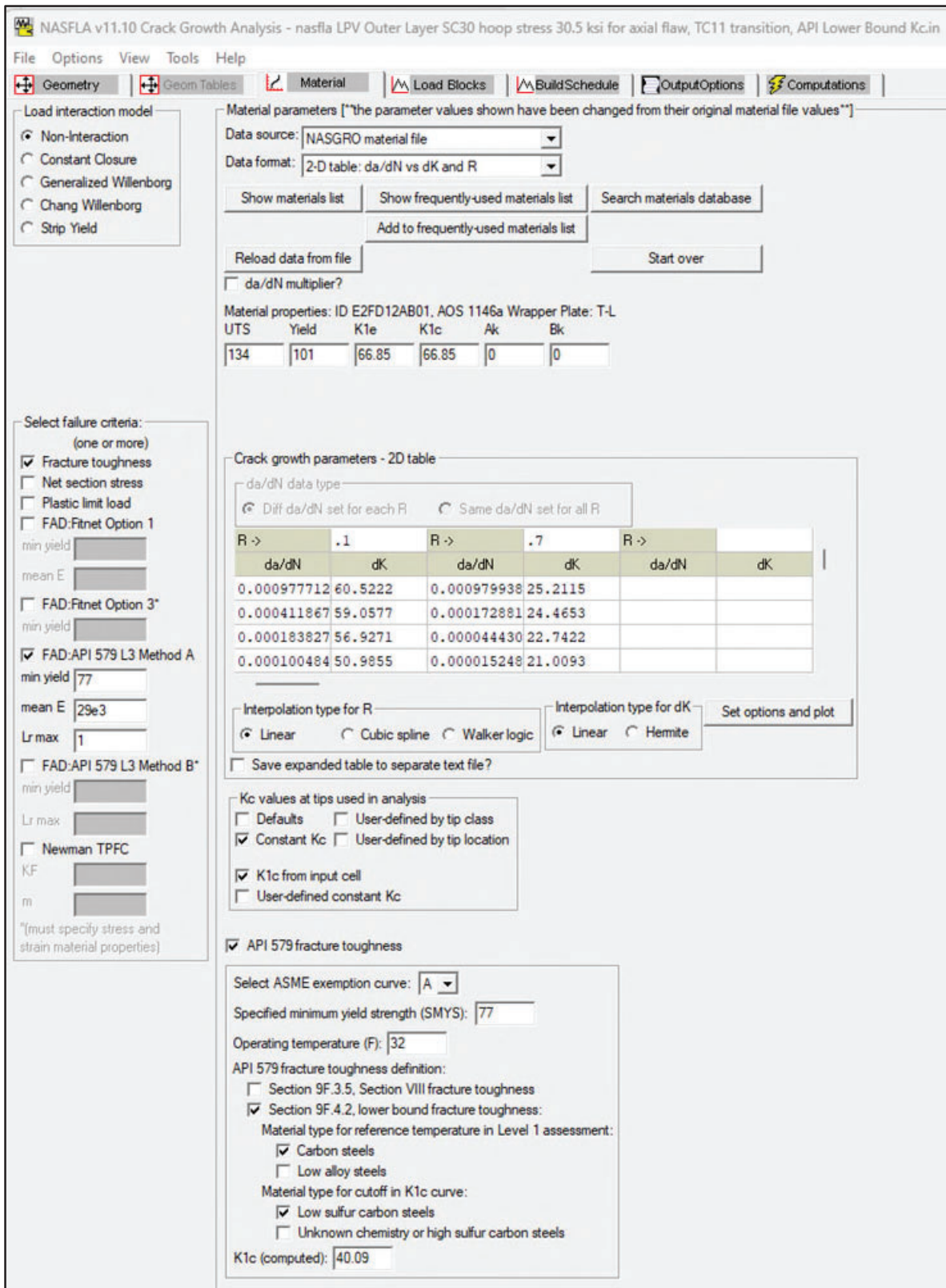
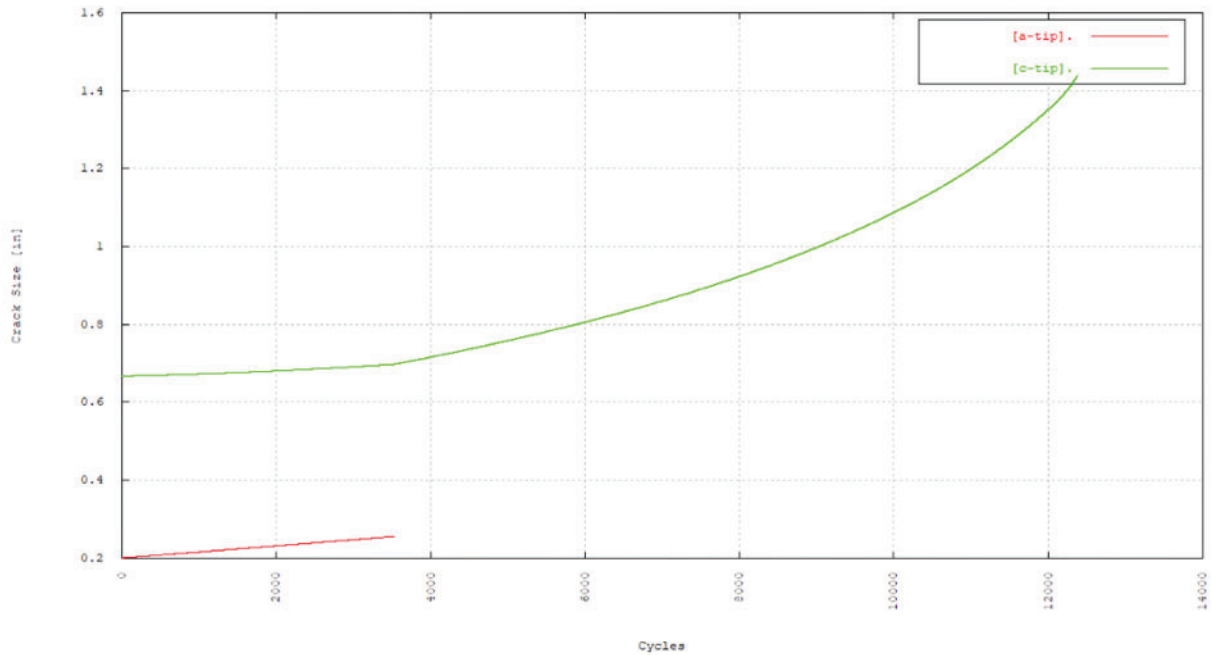
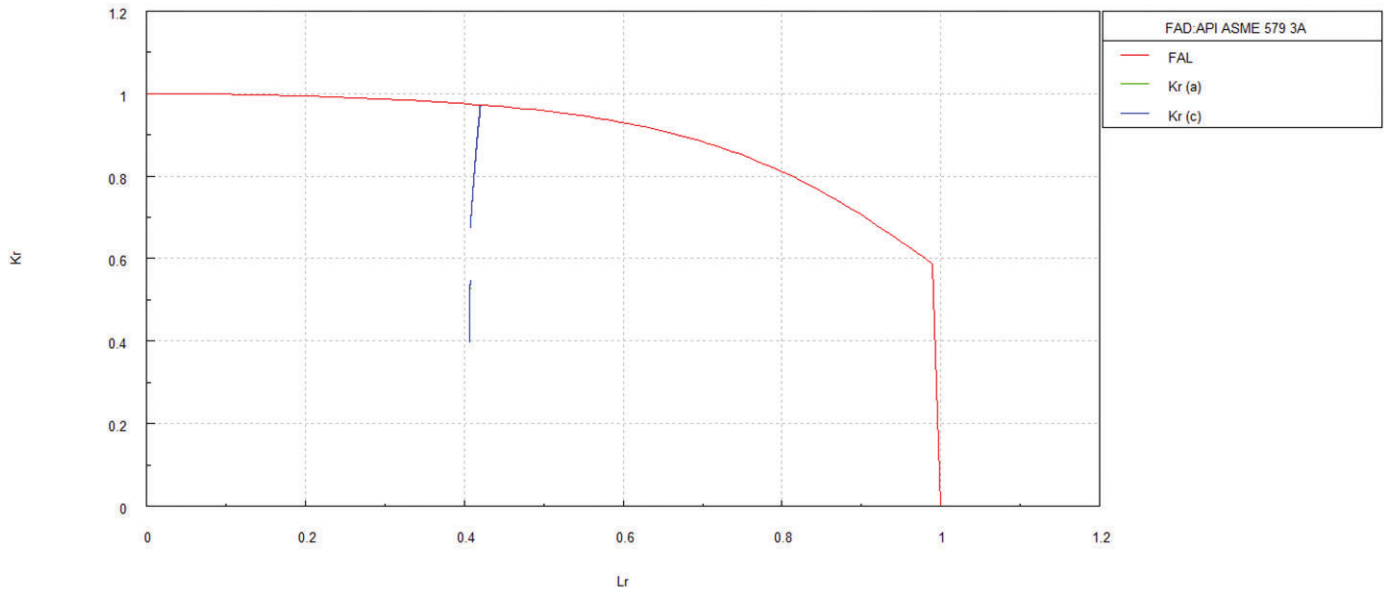


Figure 13.1-3. NASFLA Material Input Screen for AOS 1146a Wrapper Plate Showing Selection of API 579 Lower Bound Fracture Toughness



**Figure 13.1-4. Crack Growth Curves Showing Transition from Surface Crack to Through Crack using  $K_c = 66.8 \text{ ksi}\sqrt{\text{in}}$**



**Figure 13.1-5. Failure Assessment Diagram Showing Transition from Surface Crack to Through Crack using  $K_c = 66.8 \text{ ksi}\sqrt{\text{in}}$**

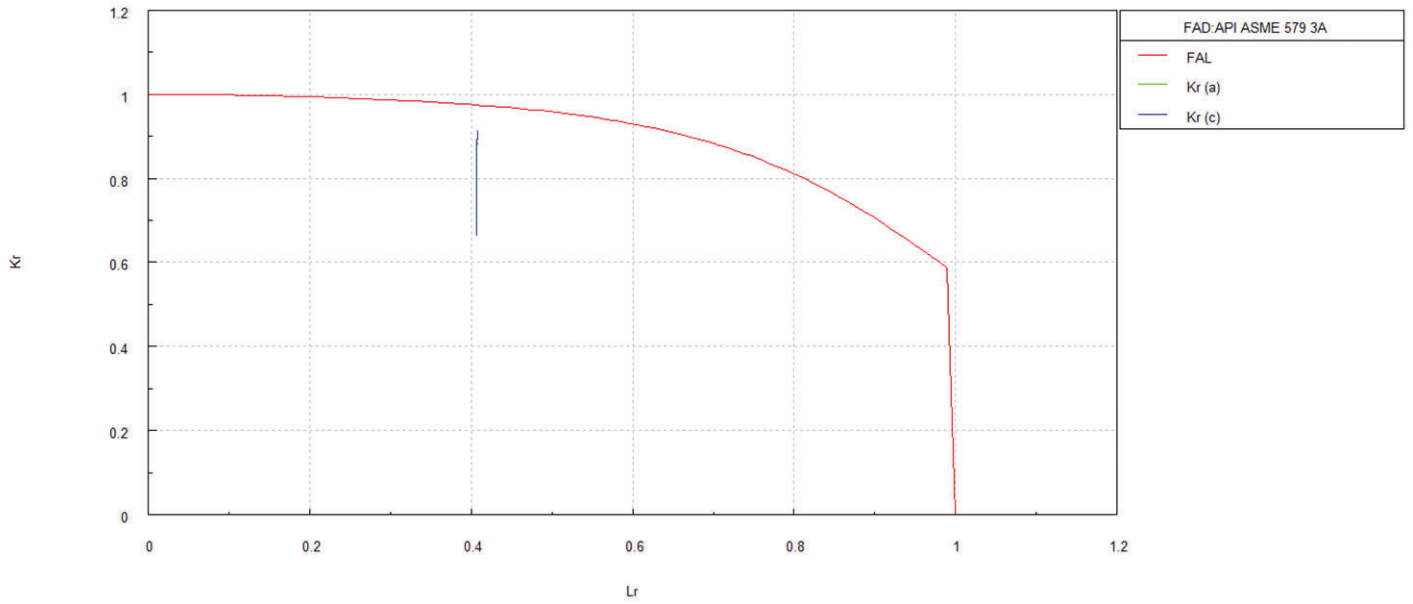


**Figure 13.1-6. Failure Assessment Diagram Using API 579 Lower Bound Toughness ( $Kc = 40.1 \text{ ksi}\sqrt{\text{in}}$ ) Without Transition**

## 13.2 Nozzle Corner Crack

NASGRO contains two SIF solutions for a corner crack at the interior corner of a nozzle in a pressure vessel, CC27 and CC28. The goal of this example is to compare the results of these two different solutions and to provide an overview of the differences in their individual modeling approaches and input data requirements. The example considers a 2-inch diameter nozzle attached to a vessel having a 2.635-inch thick vessel wall. The internal pressure cycles were defined in two steps: 250 cycles ranging from a minimum of 1.015 ksi to a maximum of 2.90 ksi, followed by two cycles ranging from zero to 2.90 ksi. With an outer diameter shell diameter of 65.27 inches, the hoop stress in the shell is 36 ksi.

The nozzle material was considered to be a ferritic-pearlite steel per API 579 and used the Barsom fatigue crack growth properties (Paris equation, API 579 Table 9F4.M) available in NASFLA in tabular form as a 1-D data table. For reference, the material ID is B1FPAPI2 and the material screen is shown in Figure 13.2-1. The option for the API 579 fracture toughness was used for both analyses resulting in a fracture toughness of 41.28 ksi $\sqrt{\text{in}}$  at 40°F. The API 579 Level 3 Method A FAD failure criterion was also used as shown in the figure.

The first analysis performed in this example uses NASGRO SIF solution CC27, corresponding to the API 579 corner crack at a nozzle solution KNCC1. This is a case of a quarter-circular corner crack in a nozzle attached to the shell. The crack is located at the corner of the connection where the inner surfaces of the shell and the nozzle meet at a 90 degree angle. The CC27 NASFLA geometry input screen for this example is shown in Figure 13.2-2. The CC27 SIF model is a relatively simple solution in that it considers only a quarter-circular corner crack throughout the life calculation, *i.e.*, it uses a constant aspect ratio of 1.0. An additional simplification is that a theoretical stress concentration factor (SCF) at the corner,  $k_{in}$ , is required input. As shown in Figure 13.2-2, the initial quarter-circular flaw size was 0.0625 inches and the SCF was 2.5.

The second analysis performed in this example uses NASGRO SIF solution CC28 which is a bivariate weight function solution for the corner crack at a nozzle. This is a much more advanced solution than CC27 in that it can accept a detailed two-dimensional hoop stress distribution computed from a finite element analysis (FEA). Although this analysis begins with the same quarter-circular initial crack size as the CC27 case with an aspect ratio of 1.0, CC28 allows for the crack to grow as a quarter-elliptical flaw. The CC28 NASFLA geometry input screen for this example is shown in Figure 13.2-3. The FEA stress distribution is input via a data file and is plotted (in normalized form) in Figure 13.2-4. Although CC28 can accept a 2-D hoop stress distribution, only a 1-D distribution was used in this case. The sharp discontinuity in the stress gradient shown in Figure 13.2-4 is due to the inclusion of the nozzle-to-shell weld geometry in the FEA. This FEA stress distribution was determined from analyses performed by NASA-MSFC [9].

The results of the two analyses are compared in Table 13.2-1. The CC28 analysis results in a computed cycles to failure more than ten times that computed using the CC27 solution. The crack growth curves and FADs are shown in Figures 13.2-5 and 6 for CC27 and in Figures 13.2-7 and 8 for CC28.

It is evident from this example that CC27 provides a much more conservative result on life than CC28. However, in the absence of a detailed stress analysis, CC27 can be used as an expedient.

CC28 is the preferred model to use for analyzing corner cracks in nozzles because of its capability to handle a much wider range of crack shape aspect ratios and its ability to accept input of user-specified stress gradients across the section computed from a FEM. And, although not used in this example, CC28 can also consider the presence of a residual stress distribution.

**Table 13.2-1. Comparison of Results for CC27 and CC28**

	<b>SIF Solution CC27</b>	<b>SIF Solution CC28</b>
<b>Initial Crack Size, a = c (in)</b>	0.0625	0.0625
<b>Final Crack Size, a (in)</b>	0.125	0.318
<b>Final Crack Size, c (in)</b>	0.125	0.337
<b>Final a/c</b>	1.00	0.94
<b>Cycles to Failure</b>	18,130	212,184
<b>FAD Parameters at Failure:</b>		
<b>Stress Intensity Fator, K (ksi√in)</b>	37.61	36.28
<b>Load Ratio, Lr</b>	0.648	0.708
<b>Toughness Ratio, Kr</b>	0.910	0.879

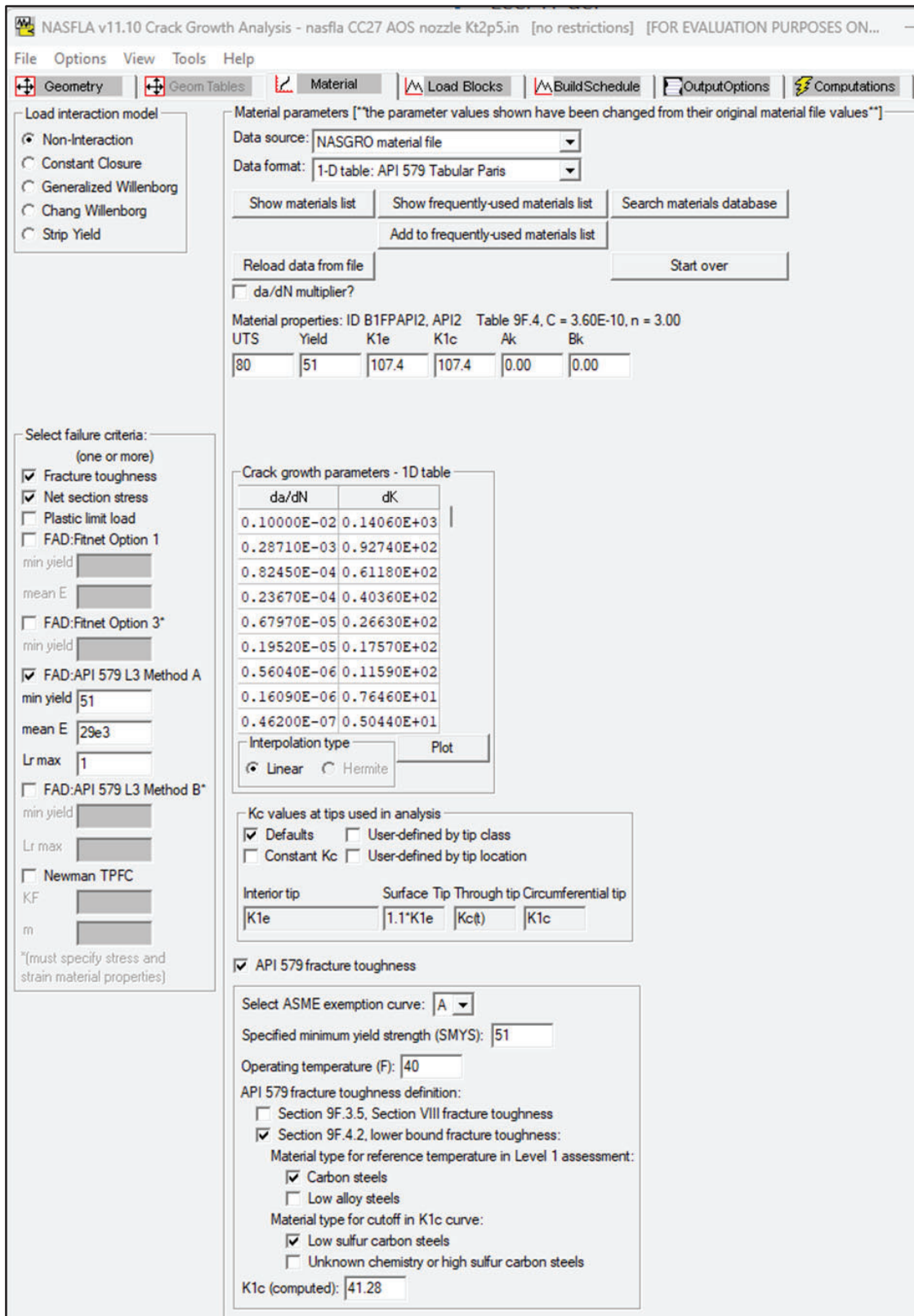


Figure 13.2-1. NASFLA Material Input Screen for API 579 Ferritic-Pearlite Steel

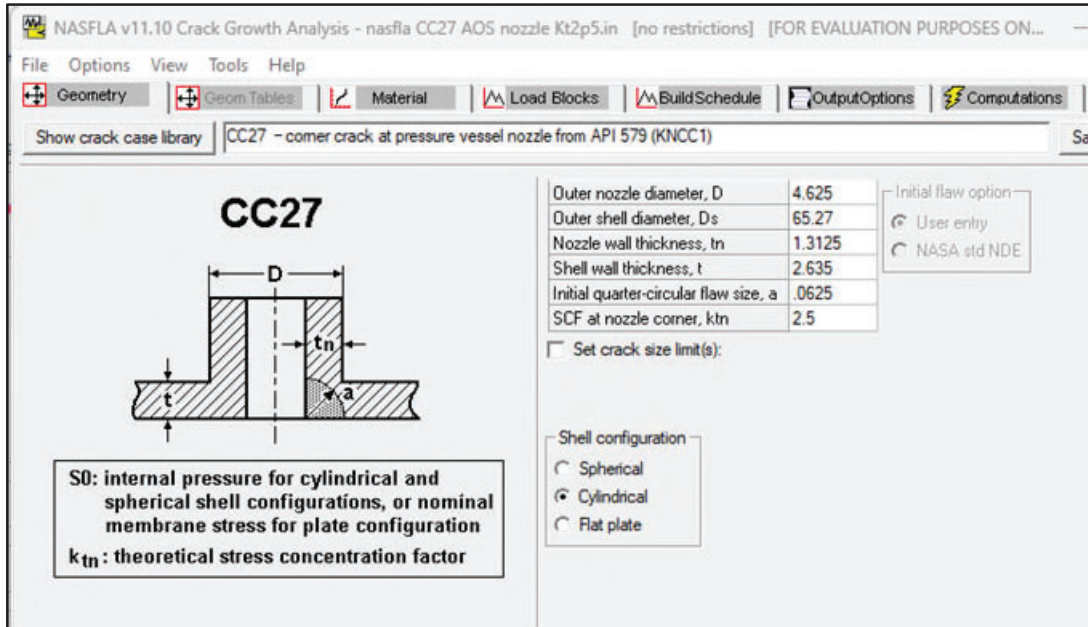


Figure 13.2-2. NASFLA Geometry Input Screen for Nozzle Corner Crack Using API 579 Solution KNCC1

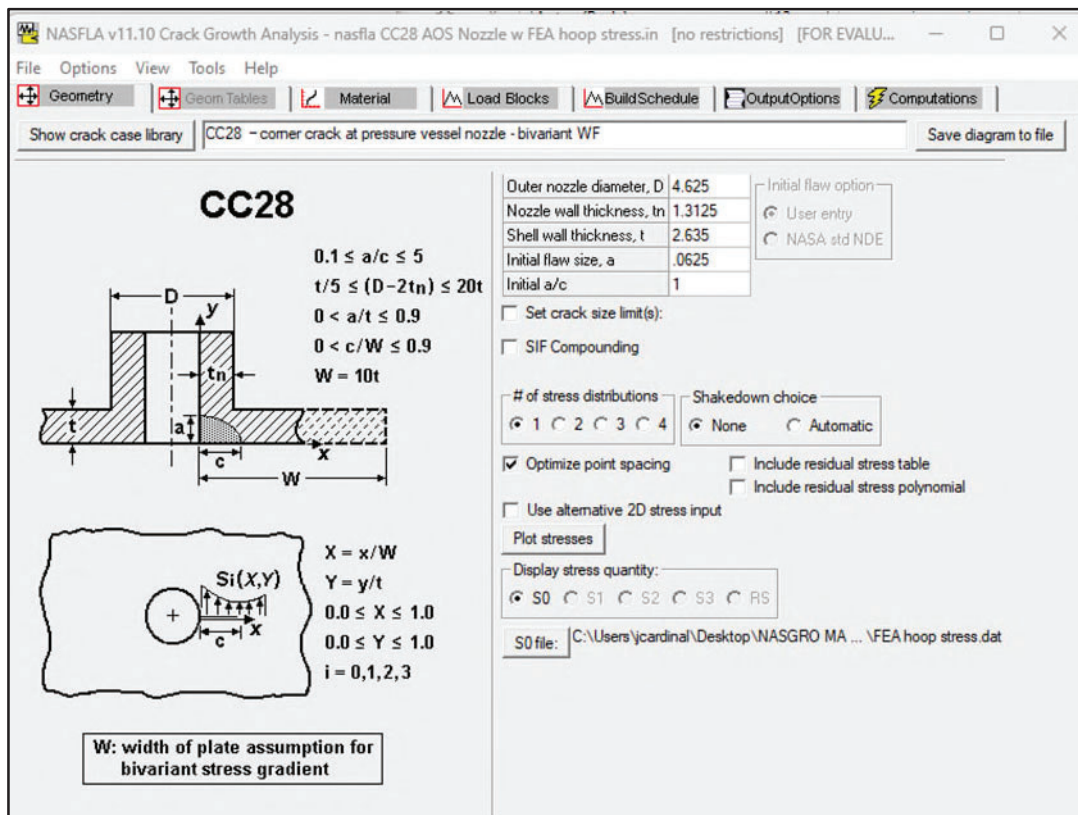
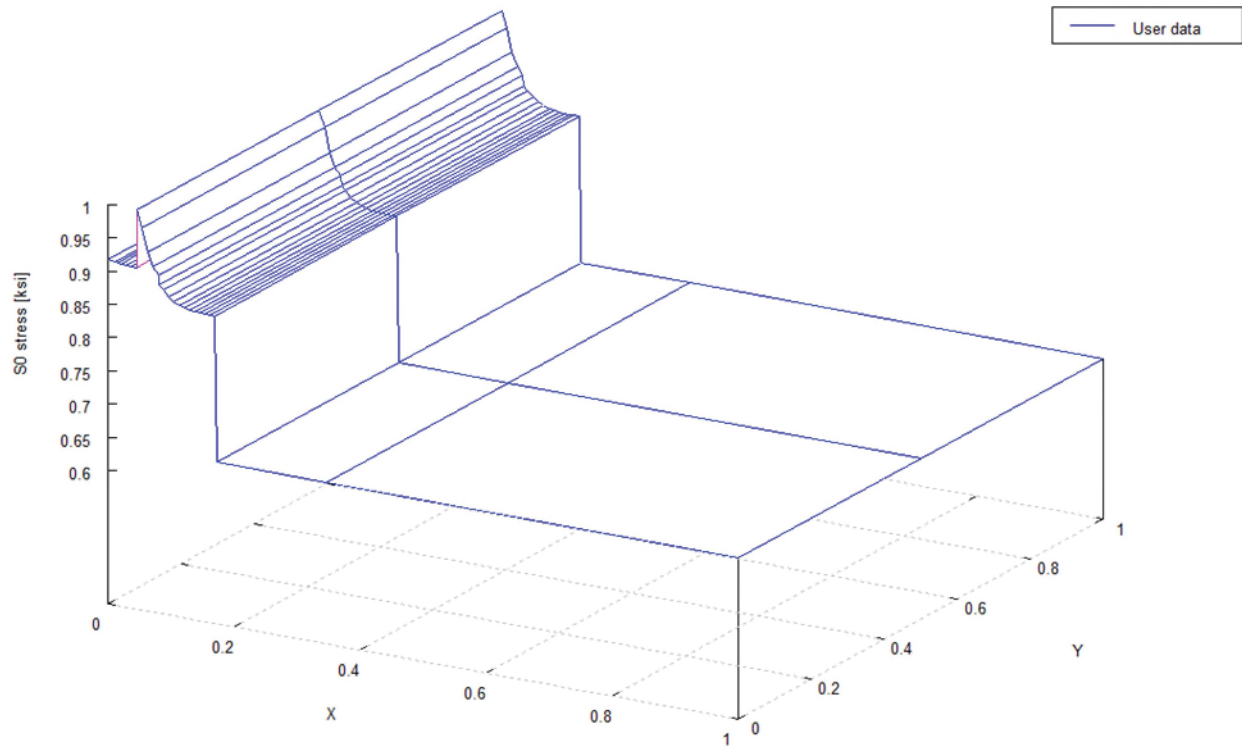
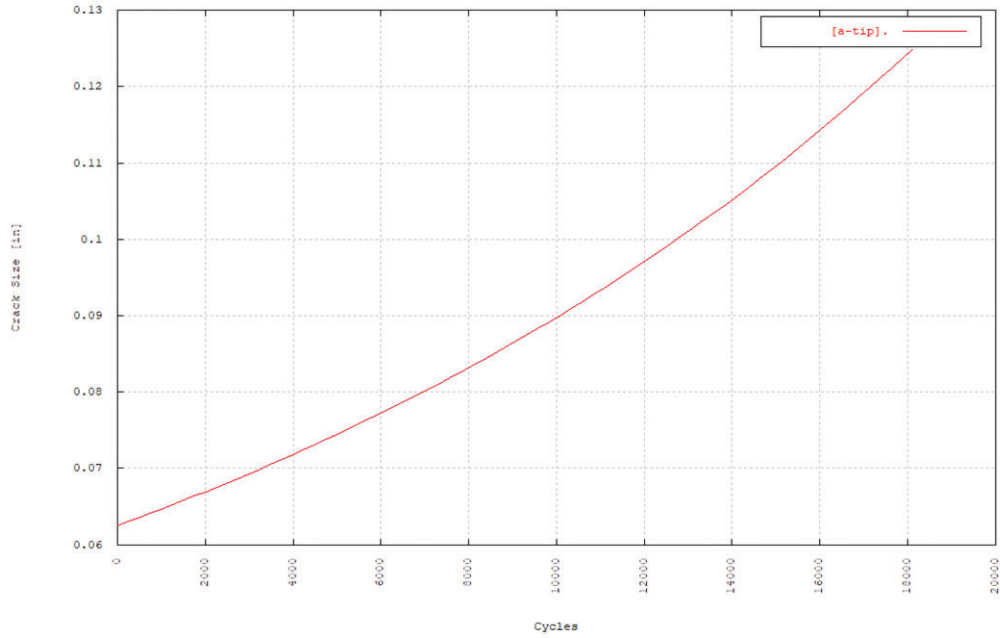


Figure 13.2-3. NASFLA Geometry Input Screen for Nozzle Corner Crack Using NASGRO Weight Function Model CC28



**Figure 13.2-4. Normalized Stress Distribution at Nozzle Corner from FEA for Input to CC28 Weight Function SIF Model**



**Figure 13.2-5. Nozzle Corner Crack Growth Curve for CC27 ( $a/c = 1$ )**

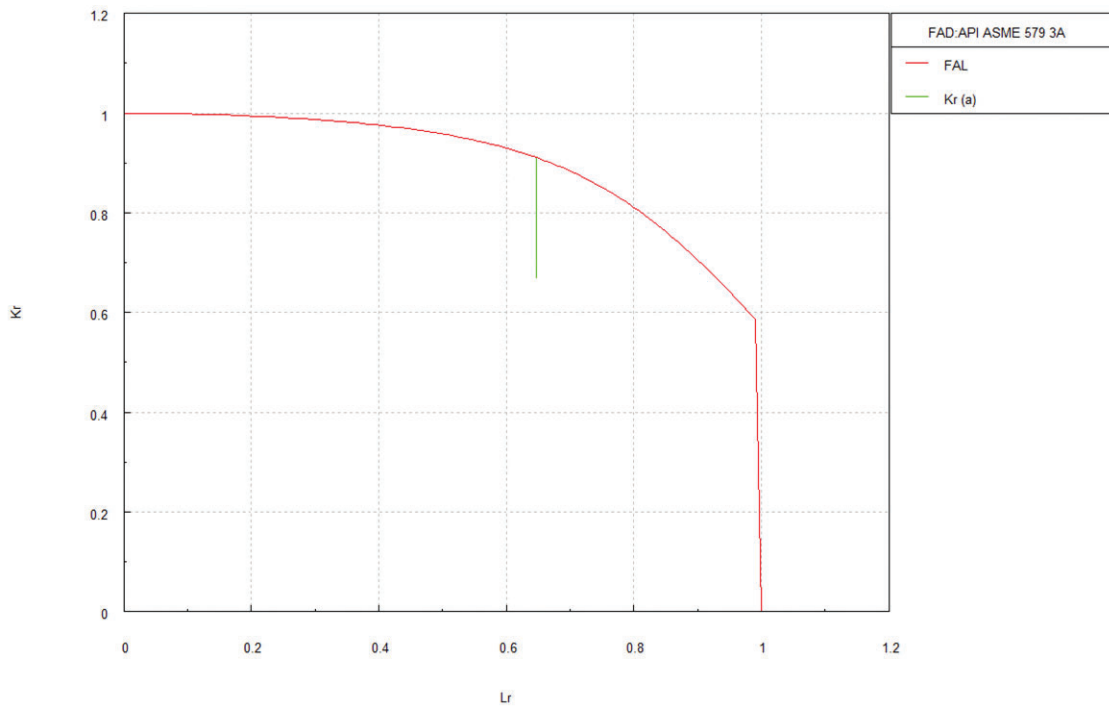


**Figure 13.2-6. Nozzle Corner Crack FAD for CC27**

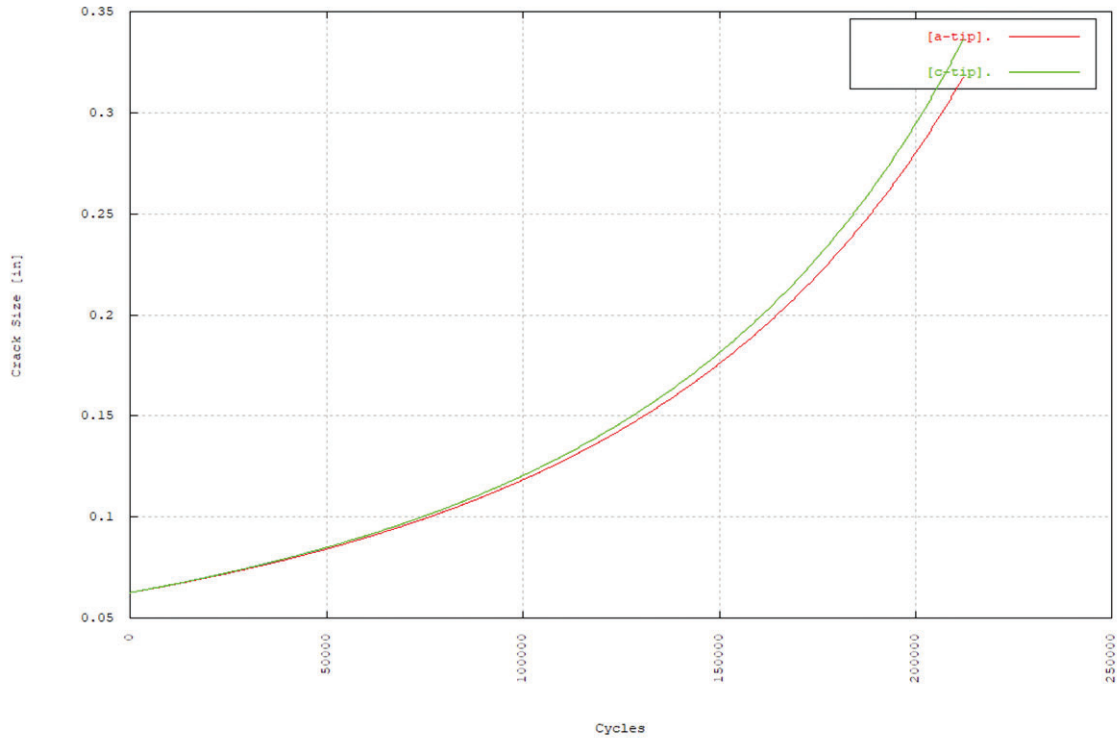


**Figure 13.2-7. Nozzle Corner Crack Growth Curves for CC28**

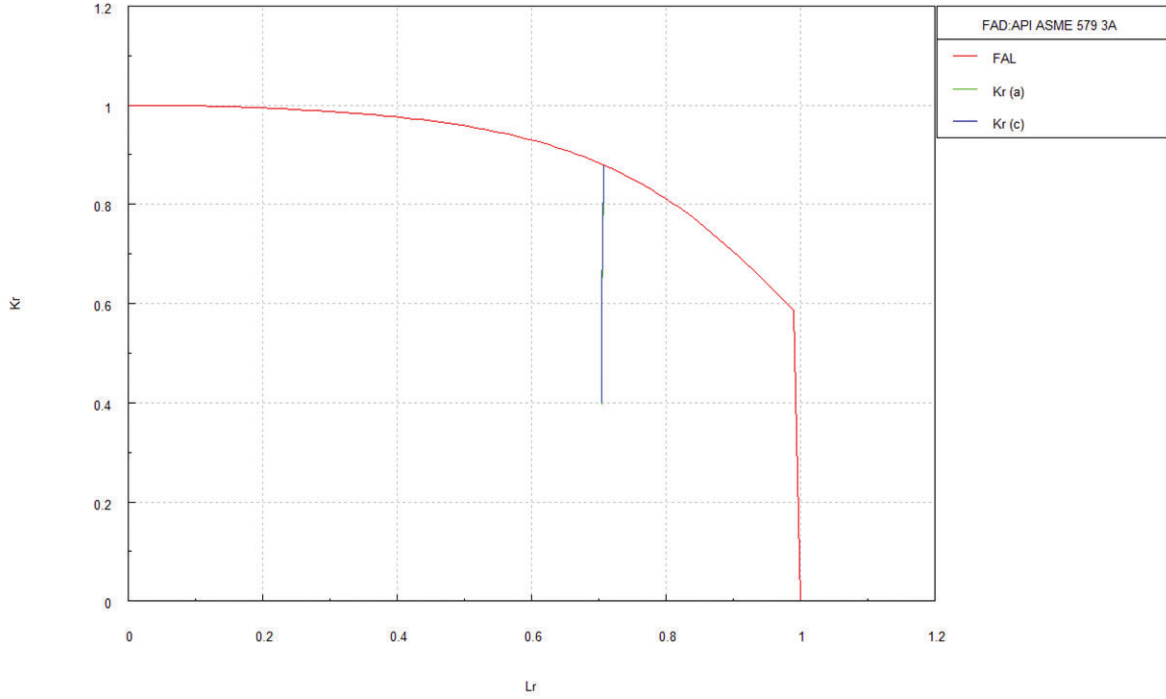


**Figure 13.2-8. Nozzle Corner Crack FAD for CC28**

### 13.3 Internal Circumferential Surface Crack in a Pipe with Weld Residual Stress

This example considers a circumferentially oriented shallow surface crack located in a weld on the interior of a pipe having an outer diameter of 8.625 inches and a wall thickness of 0.50 inches. The pipe material is A-106 Gr B steel. The internal pressure cycles from zero to 1.15 ksi combined with a remote bending stress cycling from zero to 5.0 ksi.

Two NASGRO crack growth analyses were performed using the SC34 circumferential surface crack in a cylinder weight function model for an internal crack. A separate, independent analysis of this geometry was also conducted by NASA-Ames using the INSPECT software [10]. This analysis used API 579 SIF solution KCSCCE1 [11].

The initial crack depth,  $a$ , was 0.155 inches and the initial half-surface crack length,  $c$ , was 0.5496 inches giving an aspect ratio ( $a/c$ ) of 0.282. Figure 13.3-1 shows the NASFLA input screen for this SC34 geometry. All three analyses used the API 579 weld residual stress polynomial equation 9D.9 from Section 9D.5.1 of API 579 for a full penetration circumferential weld in a cylinder. The inputs for this WRS choice for the NASFLA analyses are shown (in purple) in Figure 13.3-1 and the WRS polynomial is plotted in Figure 13.3-2.

Two different material models were used in these analyses. The first NASGRO analysis used a 1-D tabular representation of a Paris equation found in the literature for the A-106 Gr B steel [12], NASGRO material ID B1BB16AB01. The second NASGRO analysis and the INSPECT analysis each used the API 579 upper bound welded joint Paris equation from API 579 Table 9F.5. The NASGRO material ID for the 1-D tabular representation of this material choice is W1UPAPI4. The material screens for the two NASGRO analyses are shown in Figures 13.3-3 and 13.3-4, respectively.

All three analyses used the API 579 lower bound fracture toughness computed assuming ASME exemption curve B, a minimum yield strength of 35.0 ksi and an operating temperature of 32.0°F. These choices are shown in the lower portion of the NASFLA material screens in Figures 13.3-3 and 13.3-4 and result in a computed fracture toughness of 47.22 ksi $\sqrt{\text{in}}$ . The API 579 Level 3, Method A FAD failure criterion was used for each analysis with the minimum yield stress of 35.0 ksi.

The NASFLA Load Blocks screen is shown in Figure 13.3-5. The remotely applied bending stress (S1) is given as 5 ksi and the internal pressure (S2) is 1.15 ksi, both cycling from zero to the applied value. Note that when applying an internal pressure, the axial tension for a capped cylinder is automatically computed and included in the SC34 solution. The scale factors for S1 and S2 are 1.0. Since the WRS polynomial is normalized it must be scaled. This scale factor is usually taken to be the yield stress. API 579 Section 9D.3.3 recommends adding 10 ksi to the yield stress, so for this example a scale factor of 45 ksi is used (a yield stress of 35 ksi plus 10 ksi) as shown in Figure 13.3-5.

NASFLA v11.10 Crack Growth Analysis - SC34 A106B 1-D.in [no restrictions] [FOR EVALUATION PURPOSES ONLY]

File Options View Tools Help

Geometry Geom Tables Material Load Blocks BuildSchedule OutputOptions Computations

Show crack case library SC34 - semi-elliptical surface crack in a hollow cylinder - WF solution

### SC34

$X = x/t$   
 $0 \leq X \leq 1$   
 $D/t \geq 4$   
 $a/t \leq 0.9$   
 $c/R_1 \leq 0.6$   
 $\max\left(0.1, \frac{a/R_1}{a/R_1 + \Delta}\right) \leq a/c \leq 2$   
 $R_1 = 0.5 \times (D - 2t)$   
 $\Delta = 1 - \delta + \sqrt{\delta^2 - 1}$   
 $D_1 = D - 2t$   
 $R_1 = D_1/2$   
 $\delta = D/D_1$

**Notes:** Internal pressure (S2) implies that the cylinder is capped and generates an additional axial stress.

S3 and Residual stress, if entered, are axisymmetric stress gradients.

Thickness, t	0.5
Outer diameter, D	8.625
Initial flaw size, a	0.155
Initial a/c	0.282

Initial flaw option

User entry

NASA std NDE

Flaw location

Internal

External

Set crack size limit(s)

SIF Compounding

Specify secondary cyclic stresses in FAD analysis

Include crack plane stress S3

Optimize point spacing  Include residual stress table

Include residual stress polynomial

Input stresses from file

Plot stresses

Display stress quantity:

S0  S1  S2  S3  RS

	Coef 0	Coef 1	Coef 2	Coef 3	Coef 4	Coef 5	Coef 6
RS	1.00	-6.80	24.30	-28.68	11.18		

Select WRS API 579 polynomial equation (selected)

Section [9D.5.1] Full penetration circumferential welds in cylindrical shells

Equation [9D.9] Circumferential flaw; WRS perpendicular to weld

Low weld heat input; Ferritic and medium/low austenitic stainless steel welds

Clear selected WRS API 579 polynomial equation

Polynomial gradient direction:  (click to change)

**Figure 13.3-1. NASFLA Geometry Input Screen for Internal Circumferential Surface Crack in a Cylinder (SC34)**

The crack growth curves and FAD for the analysis using the NASFLA database properties for the A106 Gr B steel are shown in Figures 13.3-6 and 13.3-7, respectively. The crack growth curves and FAD for the analysis using the NASFLA database properties for the upper bound welded joint Paris equation from API 579 are shown in Figures 13.3-8 and 13.3-9, respectively. The results are compared in Table 13.3-1 with a dramatic difference noted in life between the two material models. This difference is attributed to the upper bound (conservative) nature of the API welded joint Paris equation. For comparison, the third column of Table 13.3-1 presents results from using the INSPECT software and the API 579 upper bound weld Paris equation.

It is clear that using the API 579 upper bound Paris equation provides a much more conservative result when compared to the NASGRO material library A106 Gr B Paris relationship. It is also noted that the  $L_r$  value computed by the INSPECT analysis is somewhat different than that computed by NASFLA. Additional investigation is required to identify the reason for this difference.

**Table 13.3-1. Comparison of Analysis Results for Circumferential Surface Crack in a Pipe**

	<b>NASGRO SC34 A-106 GrB 1-D Tabular B1BB16AB01</b>	<b>NASGRO SC34 API 579 Weld Paris W1UPAPI4</b>	<b>INSPECT KCSCCE1 API 579 Weld Paris</b>
<b>Initial Crack Size, a (in)</b>	0.1550	0.1550	0.1550
<b>Initial Crack Size, c (in)</b>	0.5496	0.5496	0.5496
<b>Initial a/c</b>	0.282	0.282	0.282
<b>Final Crack Size, a (in)</b>	0.323	0.317	0.312
<b>Final Crack Size, c (in)</b>	0.608	0.623	0.622
<b>Final a/c</b>	0.531	0.510	0.502
<b>Cycles to Failure</b>	2,496,100	310,700	273,500
<b>FAD Parameters at Failure:</b>			
<b>Stress Intensity Factor, K (ksi√in)</b>	41.99	41.99	41.58
<b>Load Ratio, Lr</b>	0.280	0.281	0.241
<b>Toughness Ratio, Kr</b>	0.989	0.989	0.837

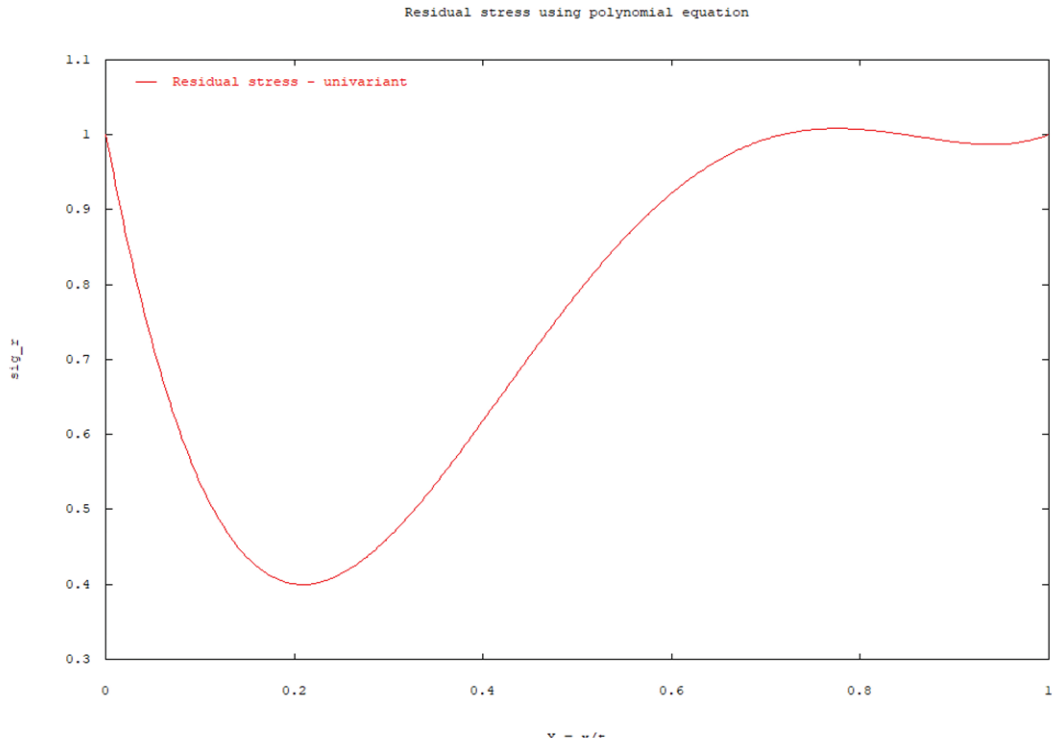


**Figure 13.3-2. NASFLA Plot of Weld Residual Stress Polynomial Equation 9D.9 from Section 9D.5.1 of API 579 for a Full Penetration Circumferential Weld in a Cylinder**

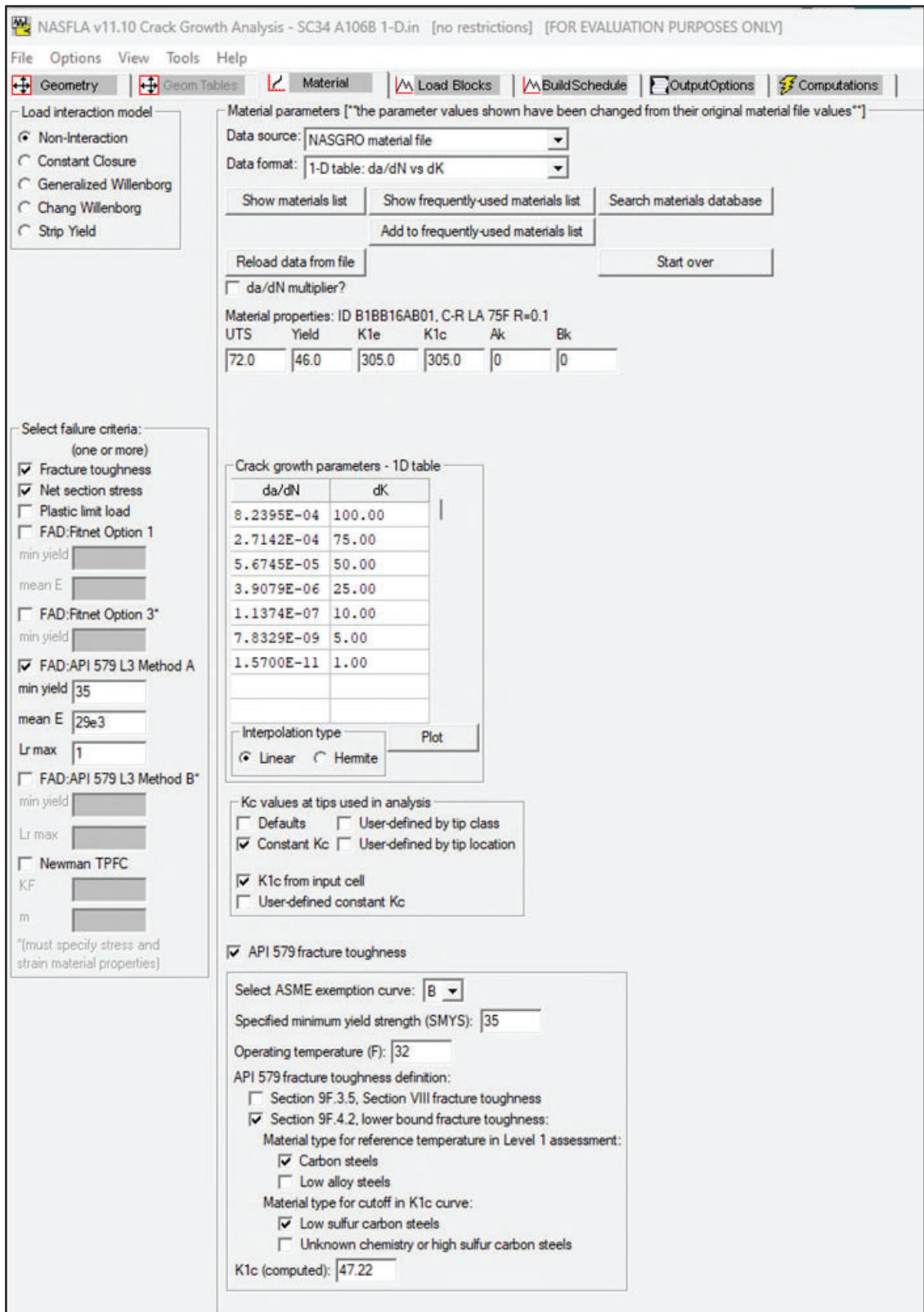


Figure 13.3-3. NASFLA Material Input Screen for Upper Bound Welded Joint Paris Equation from API 579 Table 9F.5

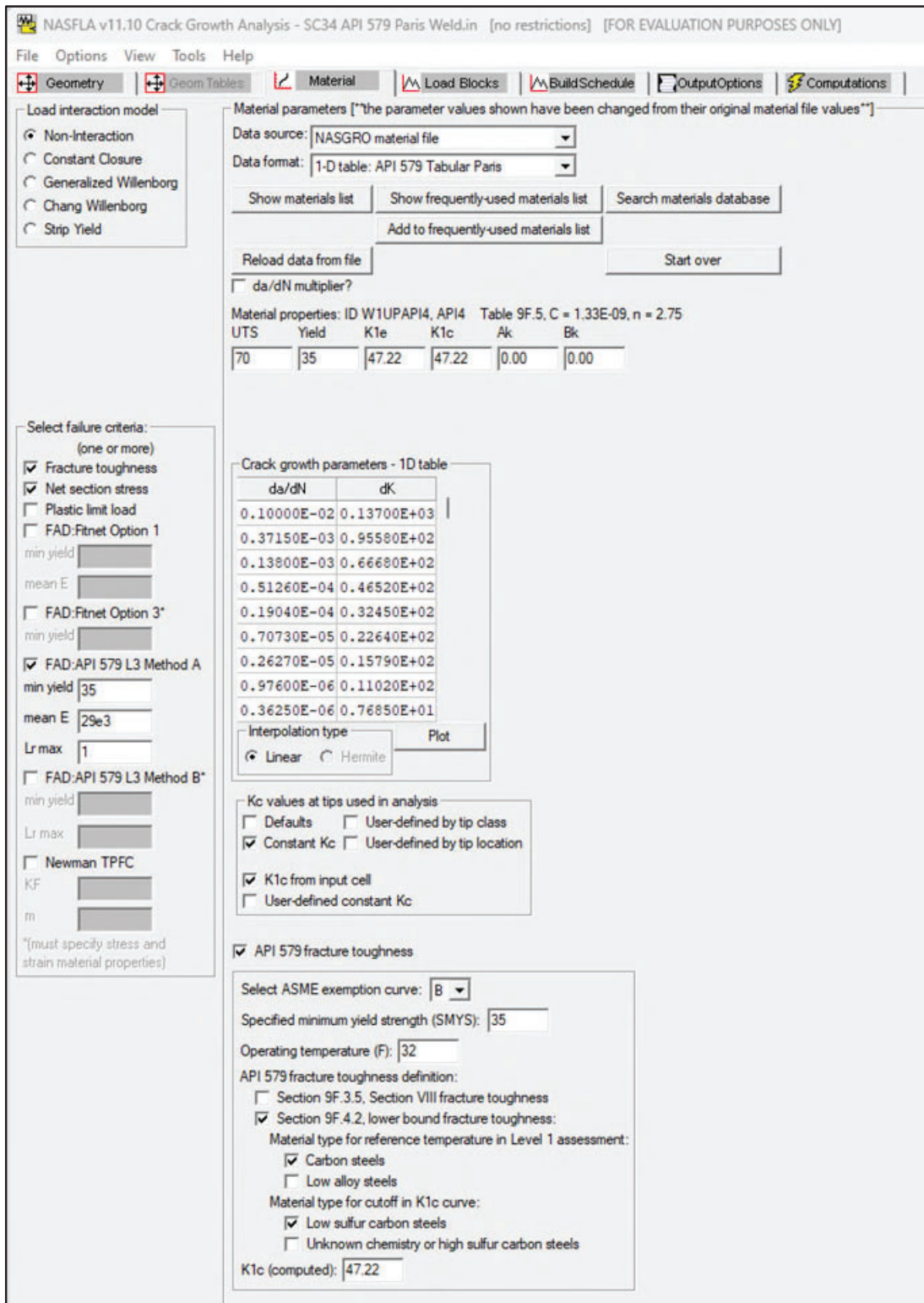


Figure 13.3-4. NASFLA Material Input Screen for Upper Bound Welded Joint Paris Equation from API 579 Table 9F.5

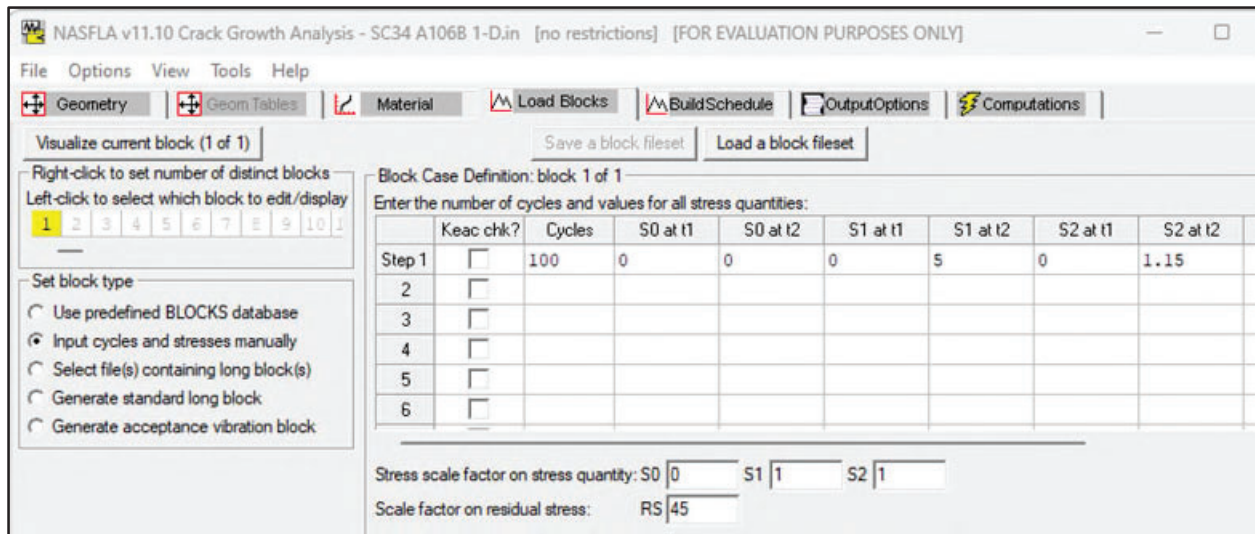
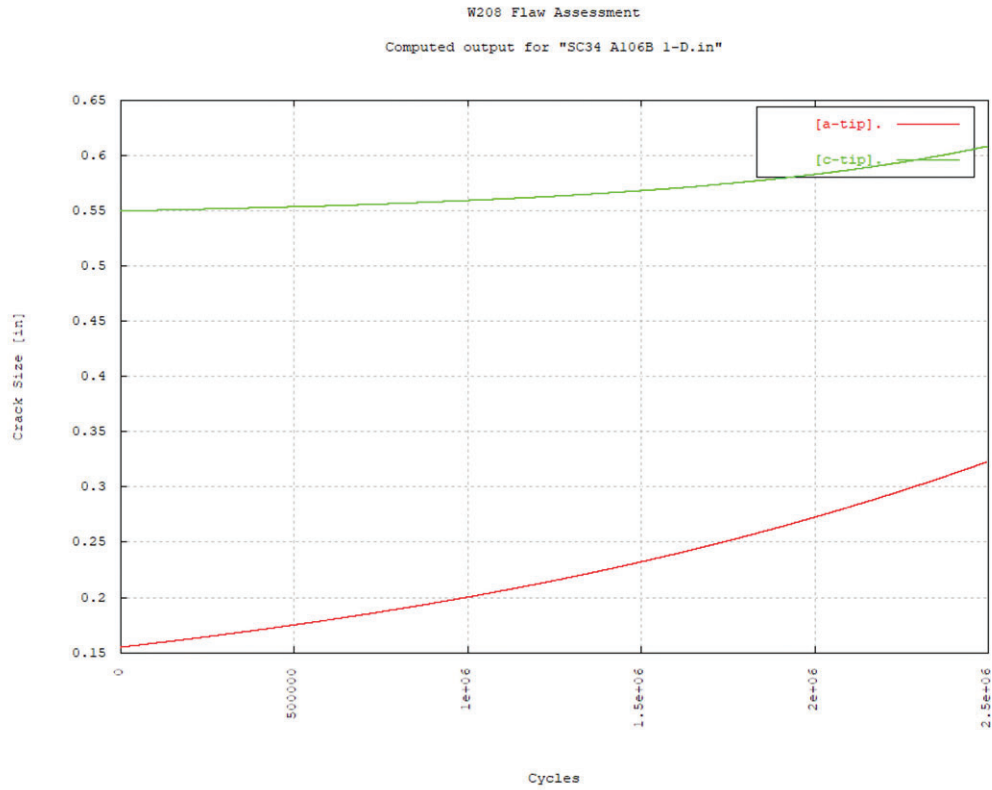
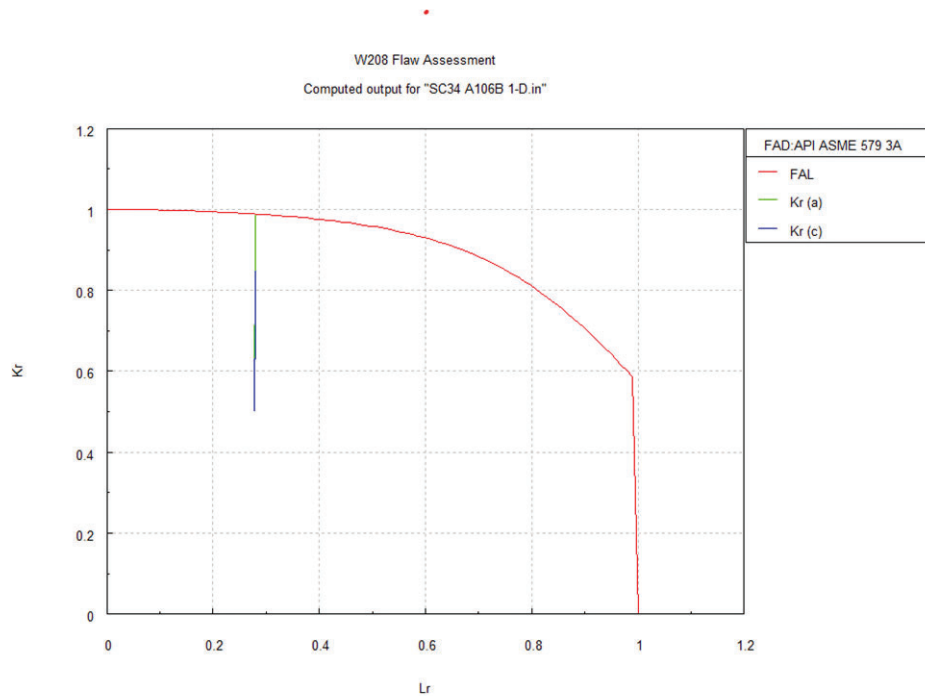


Figure 13.3-5. NASFLA Load Blocks Screen



**Figure 13.3-6. Crack Growth Curves for SC34 for A106 Gr B Steel Material**



**Figure 13.3-7. FAD for SC34 for A106 Gr B Steel Material**

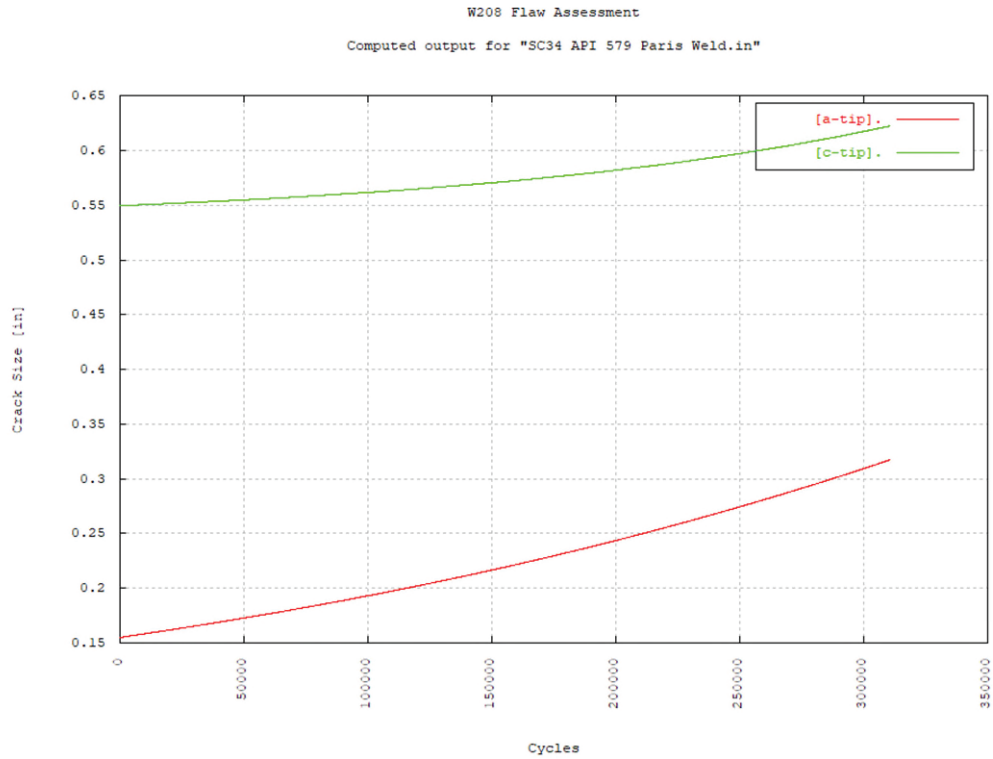


**Figure 13.3-8. Crack Growth Curves for SC34 for Upper Bound Weld Material**

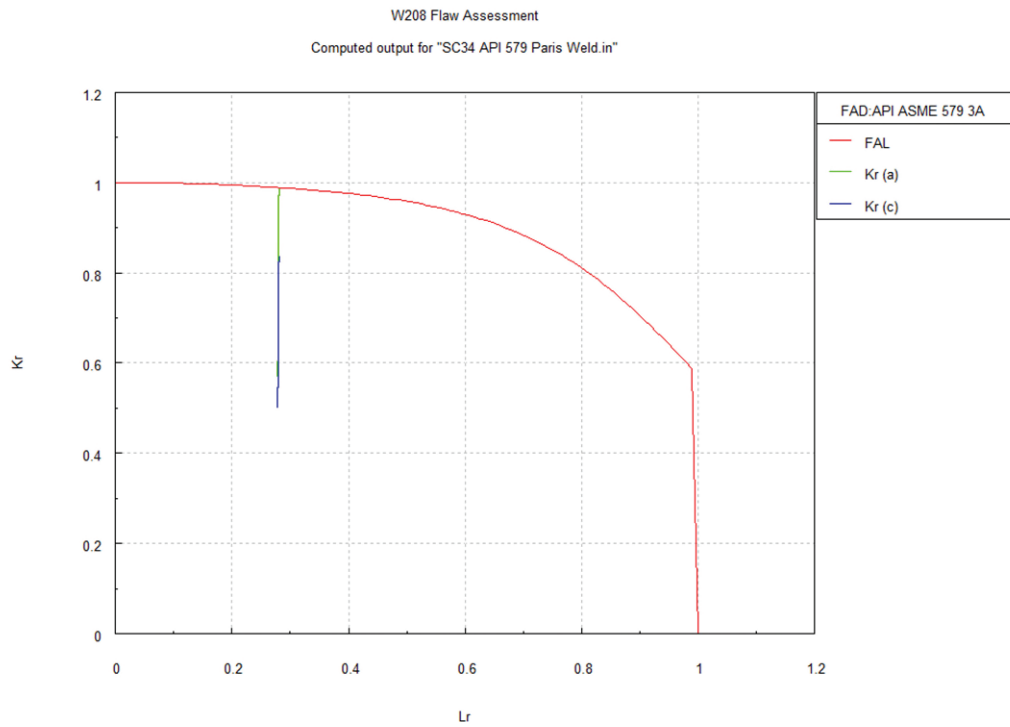


**Figure 13.3-9. FAD for SC34 for Upper Bound Weld Material**

### 13.4 FAD Analysis of Embedded Cracks in a Sphere

This example provides a FAD assessment of two different embedded elliptical cracks in a in a pressurized sphere meridional weld. The sphere has an outside diameter of 494.9 inches, a wall thickness of 1.45 inches and is subject to an internal pressure of 150 psi resulting in a membrane (hoop) stress of 11.96 ksi. FAD assessments were performed using both the NASFAD module of NASGRO and the INSPECT software [11] for comparison.

The INSPECT software uses API 579 solution KSECCE for an embedded crack in a sphere. However, it is noted that this solution is actually the same as the API 579 solution for an embedded crack in a flat plate (KPECE2). NASGRO does not have a SIF solution for embedded cracks in a sphere. However, because of the large radius of this sphere, the NASGRO univariant weight function model for an embedded crack in a plate (EC05) is deemed appropriate and is also similar to the API 579 plate model being used by the INSPECT software. Each analysis uses a very large plate width. Each analysis considers the presence of a weld residual stress distribution per API 579 Section 9D7.1 (Equation 9D.9).

The two elliptical crack sizes considered in the analyses are as follows:

Small crack (#1):  $a = 0.20$  inches,  $c = 0.50$  inches,  $a/c = 0.40$   
Large crack (#2):  $a = 0.3905$  inches,  $c = 1.485$  inches,  $a/c = 0.263$

In each case, the crack was offset from the center of the plate with a distance from the plate surface of 0.693 inches.

The NASFAD geometry input screen is shown in Figure 13.4-1 and includes the display of the API 579 weld residual stress polynomial coefficients. The same WRS distribution is used by both NASFLA and INSPECT and is plotted in Figure 13.4-2, normalized as a function of distance through the thickness. The insert in Figure 13.4-1 shows the tabular input of the membrane stress (S0).

Figure 13.4-3 displays the NASFAD material screen for these analyses using representative properties of an A200 series steel. Neither NASGRO nor INSPECT had data for the actual steel (A201B) and each analysis used the properties shown in the figure. The API 579 lower bound fracture toughness option was used resulting in a computed toughness of 40.83 ksi $\sqrt{\text{in}}$ . The FAD calculations were performed using API 579 Level 3, Method A as listed in the sidebar of the material screen with a minimum yield stress of 32.0 ksi.

The NASFAD Options screen is shown in Figure 13.4-4 indicating that a FAD Assessment is being performed and provides the crack size and shape input data for the small and large cracks. The scale factor for S0 is 1.0 since the tabular membrane stress was entered with the actual value of hoop stress (see Figure 13.4-1). Since the WRS polynomial is normalized it must be scaled. This scale factor is usually taken to be the yield stress. API 579 Section 9D.3.3 recommends adding 10 ksi to the yield stress, so for this example a scale factor of 42.0 ksi is used (a yield stress of 32 ksi plus 10 ksi) as shown in Figure 13.4-4.

The FAD for each of the cracks is plotted in Figure 13.4-5. It is easily seen that the large crack (Crack #2, blue squares) lies outside the FAD curve and is unsafe by a large margin for the *a*-tip. The assessment points for the small crack (Crack #1, green stars) lie within the FAD curve indicating a safe condition; however, the *a*-tip is quite close to the failure criterion.

Table 13.4-1 below compares the NASFAD results for these two cracks with the corresponding results obtained from the INSPECT software. While every effort was made to ensure that there was an apples-to-apples consistency between the two analysis approaches, there existed some uncertainty in the interpretation of the INSPECT results. Nevertheless, the bottom-line results are consistent: the small crack is within the safe zone of the FAD and the large crack far exceeds the FAD failure criterion.

For the small crack, the stress intensity factors agree quite well between the two analyses; however, for the large crack the INSPECT SIFs are about five to ten percent higher than those computed by EC05. The cause of this difference is unknown and needs to be investigated. Additionally, it is seen that the Load Ratios computed using INSPECT are much higher than those computed by NASFAD and EC05. A preliminary investigation into this difference indicates that  $L_r$  computed by INSPECT for this example is a local value while the  $L_r$  computed by EC05 is a global value (for the plate model). While NASFAD computes the local value, it is not currently output (by NASFAD or NASFLA). Further investigation is needed here also including assessing the possibility of outputting both the global and local  $L_r$  values from NASGRO.

**Table 13.4-1. Comparison of Analysis Results for Two Embedded Cracks in a Sphere**

	Small Crack (#1)	Large Crack (#2)
<b>Crack Sizes:</b>		
Crack Depth, <i>a</i> (in)	0.20	0.3905
Crack Length, <i>c</i> (in)	0.50	1.4850
Aspect Ratio, <i>a/c</i>	0.40	0.2630
<b>FAD Parameters (NASFAD EC05):</b>		
Stress Intensity Factor, <i>K</i> @ <i>a</i> -tip (ksi√in)	38.2100	68.3176
Stress Intensity Factor, <i>K</i> @ <i>c</i> -tip (ksi√in)	20.9024	26.2022
Toughness Ratio, <i>K<sub>r</sub></i> @ <i>a</i> -tip	0.9358	1.6730
Toughness Ratio, <i>K<sub>r</sub></i> @ <i>c</i> -tip	0.5120	0.6419
Load Ratio, <i>L<sub>r</sub></i>	0.3760	0.3868
<b>FAD Parameters (INSPECT):</b>		
Stress Intensity Factor, <i>K</i> @ <i>a</i> -tip (ksi√in)	38.4330	71.6010
Stress Intensity Factor, <i>K</i> @ <i>c</i> -tip (ksi√in)	20.8560	29.1630
Toughness Ratio, <i>K<sub>r</sub></i> @ <i>a</i> -tip	0.9424	1.7557
Toughness Ratio, <i>K<sub>r</sub></i> @ <i>c</i> -tip	0.5114	0.7151
Load Ratio, <i>L<sub>r</sub></i>	0.4375	0.6240

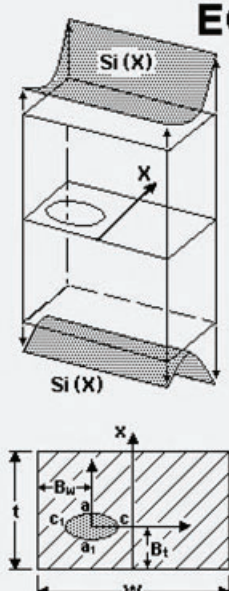
NASFAD v11.01 Failure Assessment Diagram - nasfad sphere EC05.in [no restrictions]

File Options View Tools Help

Geometry Geom Tables Material FAD Options Computations

Show crack case library EC05 - elliptical embedded crack (offset) in plate - univariant WF

### EC05



$S_0 = S_0(X) = 1$   
 $S_1 = 6M_1 / Wt^2$   
 $S_1(X) = S_1(1 - 2X/t)$   
 $S_i^{WF} = S_i(X)$   
 $S_i^{POLY} = \sum C_i(X/t)^i$

$0 \leq a / \text{Min}(B_t, t - B_t) \leq 0.99$   
 $0 \leq c / \text{Min}(B_w, W - B_w) \leq 0.99$   
 $0.01 \leq a/c \leq 10$   
 $0.0 \leq X \leq 1.0$

Thickness, t	1.45
Width, W	50.0

SIF Compounding

Specify secondary cyclic stresses in FAD analysis

Crack plane stress definition from:

Tension, bend  Polynomial  Tabular input

# of stress distributions:  1  2  3  4

Shakedown choice:  None  Monotonic

Optimize point spacing  Include residual stress table

Include residual stress polynomial

Input stresses from file

Plot stresses

Display stress quantity:

S0  S1  S2  S3  RS

	Coef 0	Coef 1	Coef 2	Coef 3	Coef 4	Coef 5	Coef 6
RS	1.00	-6.80	24.30	-28.68	11.18		

Select WRS API 579 polynomial equation (selected)

Section [9D.7.1] Full penetration circumferential welds in spheres and heads

Equation [9D.9] Circumferential flaw; WRS parallel to weld

Low weld heat input; ferritic and medium/low austenitic stainless steel welds

Clear selected WRS API 579 polynomial equation

Polynomial gradient direction:  (click to change)

Figure 13.4-1. NASFAD Geometry Screen for EC05 Showing Choice of API 579 WRS Equation

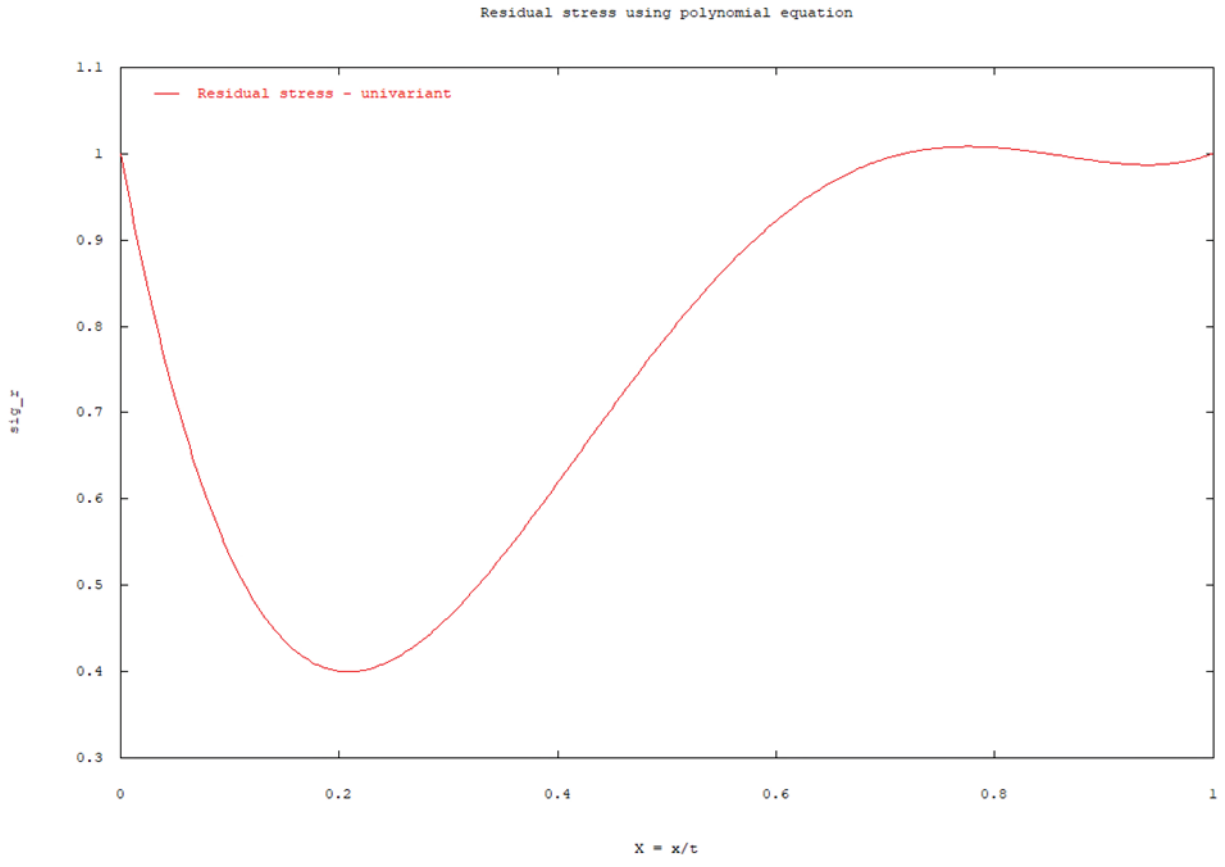


**Figure 13.4-2. NASFAD Plot of Weld Residual Stress Polynomial Equation 9D.9 from Section 9D7.1 of API 579 for Full Penetration Circumferential Weld in a Sphere**

NASFAD v11.01 Failure Assessment Diagram - nasfad sphere EC05.in [no restrictions]

File Options View Tools Help

Geometry | **Geom Tables** | Material | FAD Options | Computations

Material parameters

Data source: New data  
Data format: NASGRO equation constants

Show materials list  
Save data to user file

1-char category code: B description: ASTM SPEC. GRADE STL  
1-char group code: 2 description: A200 series  
2-character alloy code: description:  
4-6 char form/orient/env code: description:

Through crack toughness computed from K<sub>c</sub> 50.0  
 value entered directly  K1c, Ak, Bk equation  Kc v. thickness table

Material properties: ID code = B2...  
 UTS Yield K1e  
 60.0 32.0 50.0

FAD Option (select one)

FAD:Fitnet Option 1  
 min yield  
 mean E

FAD:Fitnet Option 3\*  
 min yield

FAD:API 579 L3 Method A  
 min yield 32.0  
 mean E 29560  
 Lr max 1.25

FAD:API 579 L3 Method B\*  
 min yield  
 Lr max

\*(must specify stress and strain material properties)

K<sub>c</sub> values at tips used in analysis  
 Defaults  User-defined by tip class  
 Constant K<sub>c</sub>  User-defined by tip location  
 Interior tip Surface Tip Through tip Circumferential tip  
 K1e 1.1\*K1e Kc(t) K1c

API 579 fracture toughness

Select ASME exemption curve: A  
 Specified minimum yield strength (SMYS): 32.0  
 Operating temperature (F): 40.0

API 579 fracture toughness definition:  
 Section 9F.3.5, Section VIII fracture toughness  
 Section 9F.4.2, lower bound fracture toughness:  
 Material type for reference temperature in Level 1 assessment:  
 Carbon steels  
 Low alloy steels  
 Material type for cutoff in K1c curve:  
 Low sulfur carbon steels  
 Unknown chemistry or high sulfur carbon steels  
 K1c (computed): 40.83

Figure 13.4-3. NASFAD Material Property Screen for a Representative A200 Series Steel

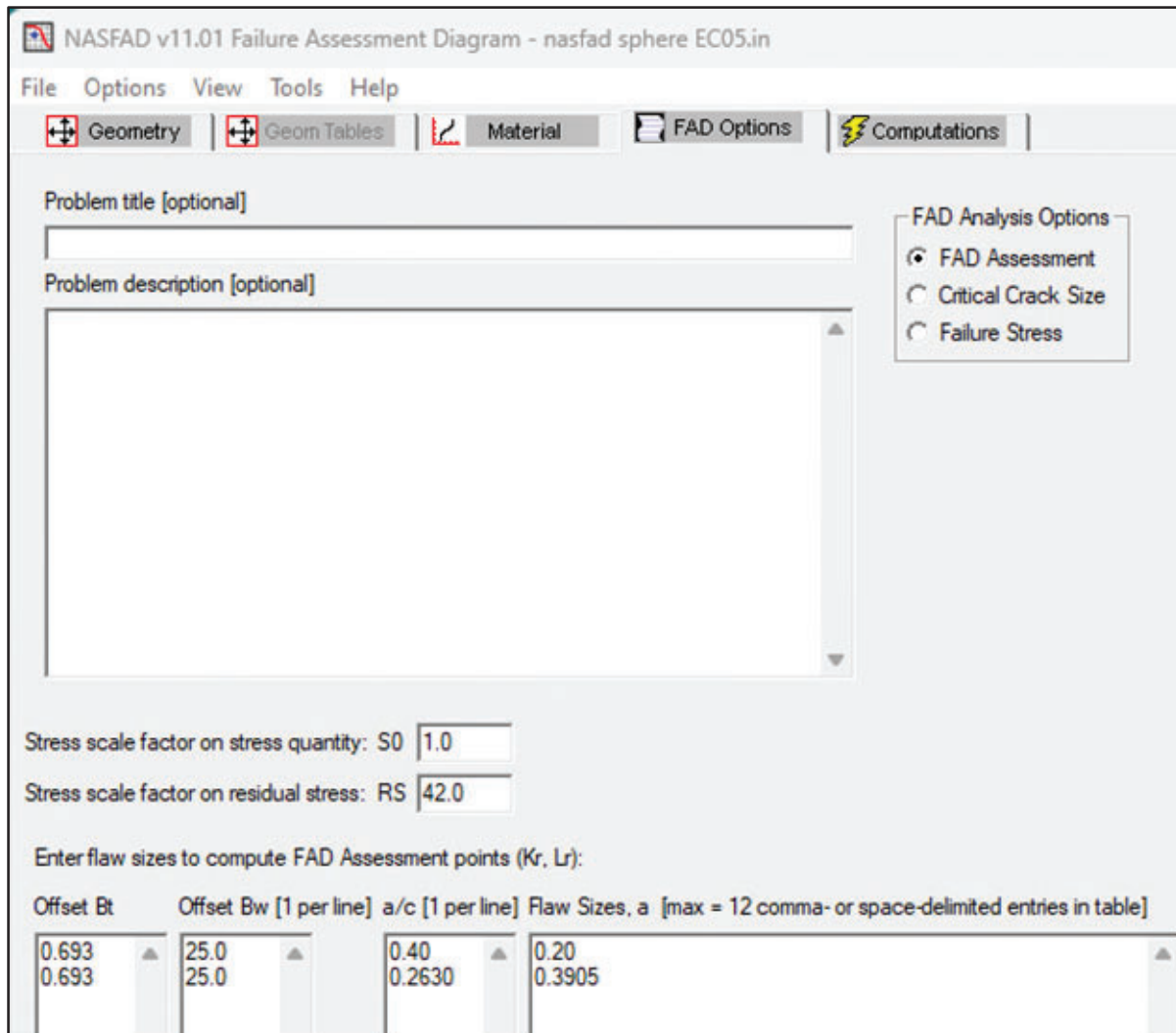


**Figure 13.4-4. NASFAD Options Screen Showing Crack Sizes and WRS Scale Factor**

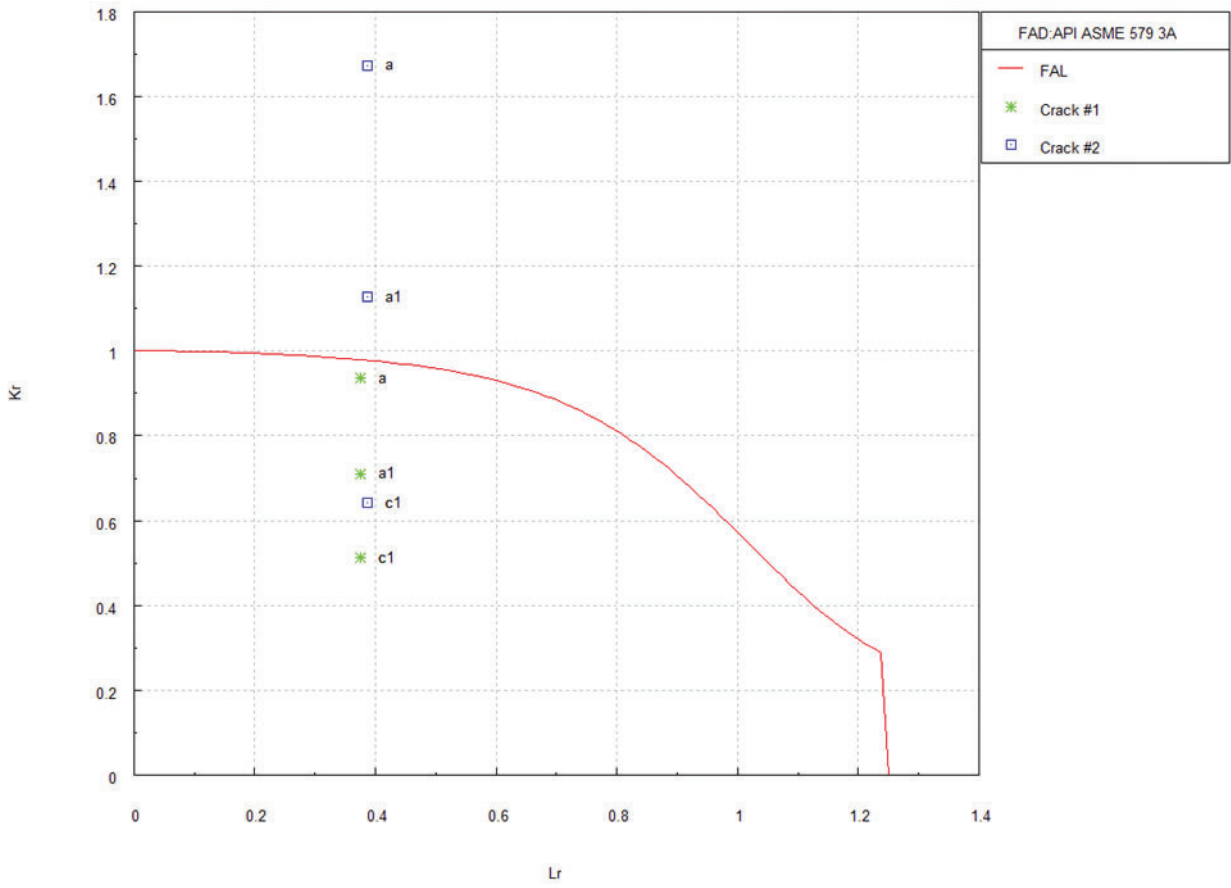


**Figure 13.4-5. NASFAD Plot of FAD for Two Cracks**

## 14 SUMMARY AND RECOMMENDATIONS

The work presented in this report provides guidance in the use of the NASGRO fracture mechanics and fatigue crack growth analysis software to perform fitness-for-service assessments of crack-like flaws in typical pressure system components in accordance with procedures outlined in Part 9 of API 579-1/ASME FFS-1. NASGRO has recently been enhanced to perform FFS analyses of safety-critical ground-based steel pressure vessels and other non-flight structures using approaches contained in the API and ASME standards. The guidelines for performing FFS assessment procedures for crack-like flaws outlined in this report are based on the well-known Failure Assessment Diagram (FAD). The objective of this report was to provide guidance in the use of NASGRO and the FAD to perform FFS assessments and fatigue crack growth analyses.

Following an overview of the general FFS analysis approaches, a summary of the NASGRO analysis modules and material property databases relevant to FFS analyses was presented. To assist analysts who may be familiar with API 579 SIF solutions but not with NASGRO SIF solutions (and *vice versa*), a comparison matrix (table) was developed to cross-reference API 579 SIF solutions with corresponding NASGRO SIF solutions. This matrix was provided in Tables 4.4-1 through 4.4-5. It is recommended that this matrix be studied by analysts when choosing a SIF model to use in their FFS analysis,

Summaries of the input data process (using GUI screen shots) for the three key NASGRO analysis modules (NASCCS, NASFAD, and NASFLA) were provided. New features implemented in NASGRO v11.0 and v11.1 were reviewed and included:

- Option to use the API 579 criteria for surface and embedded crack transitions in lieu of the NASGRO default transition criteria
- Implementation of a GUI menu to choose API 579 polynomial weld residual stress distributions (in lieu of directly entering polynomial coefficients)
- Option to compute and use API 579 fracture toughness values:
  - API 579 Section 9F.3.5 (uses ASME Section VIII fracture toughness)
  - API 579 Section 9F.4.2 (lower bound fracture toughness)
- Implementation of API 579 and ASME Paris crack growth equations in tabular form:
  - API 579 Barsom Paris equations (1-D tables)
  - API 579 welded joint Paris equations (1-D tables)
  - ASME Section VIII, Div. 3 Paris equations (2-D tables)
- Addition of material data for A-106 Gr B steel (1-D tabular da/dN)
- Access to material property database from NASCCS

Four representative example analyses were presented in Section 13.0 and were intended to illustrate the use of NASGRO for different FFS analyses of “real-world” pressure vessel applications. While these examples considered typical pressure vessel geometries and materials,

they should only be treated as “notional” demonstrations of the NASGRO software capabilities and features.

A key aspect of the examples presented herein is the use of different choices for material properties such as the fatigue crack growth relationship and the fracture toughness. In general, it was shown that the API 579 material property choices produce results that are conservative relative to the NASGRO database materials. It is recommended that analysts be aware of these differences when setting up an analysis.

Comparisons between results obtained with NASGRO and the INSPECT software were made for two of the examples. These benchmark comparisons produced reasonably good agreement between the SIFs and final crack sizes; however key differences were noted between the value of  $L_r$  used in the FAD. As previously stated, these differences are most likely due to the difference between a local and global failure computation used by the two programs. NASGRO is currently lacking in providing output of a number of quantities to resolve these discrepancies. Therefore, it is recommended that future NASGRO enhancements include the output of the reference stress and  $L_r$  values for both the local and global failure conditions, with an option for the analyst to choose which one to use for the FAD.

Lastly, additional benchmark analyses are recommended between NASGRO and other FFS software programs to identify and understand differences such as those noted above.

## 15 REFERENCES

1. “NASGRO<sup>®</sup> Fracture Mechanics and Fatigue Crack Growth Analysis Software,” v11.1, Southwest Research Institute and NASA Johnson Space Center, September 2025. ([www.nasgro.swri.org](http://www.nasgro.swri.org))
2. *Fitness-For-Service*, API-579-1/ASME FFS-1, December 2021.
3. *FITNET Fitness-For-Service (FFS) Procedure*, M. Koçak, S. Webster, J. J. Janosch, R. A. Ainsworth, and R. Koers, Editors, 2008.
4. “Guide to Methods for Assessing the Acceptability of Flaws in Metallic Structures,” BS 7910:2013+A1:2015, BSI Standards Ltd., 2016.
5. Anderson, T. L., *Fracture Mechanics, Fundamentals and Applications*, Fourth Edition, CRC Press, 2017.
6. Shelton, R. Levi, NASA Ground-Based Layered Pressure Vessels Materials Report, NASA/TM-20210019043. NASA Marshall Space Flight Center, Huntsville, AL, 35805, September 2021.
7. ASME Boiler and Pressure Vessel Code, Section VIII, Division 3: Alternative Rules for Construction of High Pressure Vessels, 2023 ed., ASME July 1, 2023.
8. ASME Boiler and Pressure Vessel Code, Section XI, 2023.
9. Fraser, D. (NASA Ames Research Center) and Stoltz, B. (NASA Marshall Space Flight Center), Personal communication, June 2025.
10. Fraser, D. (NASA ARC), Personal communication, June 2025.
11. INSPECT API 579-1 FFS Software, 2025 Build 8510, Codeware, Inc.
12. Liaw, P.K., Saxena, A, and Perrin, J., “Life Extension Technology for Steam Pipe Systems – I. Development of Material Properties,” *Engineering Fracture Mechanics*, Vol. 45, No. 6, pp. 759-786, 1993.